

University of Windsor

## Scholarship at UWindsor

---

Electronic Theses and Dissertations

Theses, Dissertations, and Major Papers

---

1993

### Sedimentology and dolomitization in the upper Mississippian Turner Valley carbonates, Quirk Creek, Alberta, Canada.

Feng-Hu Lu  
*University of Windsor*

Follow this and additional works at: <https://scholar.uwindsor.ca/etd>

---

#### Recommended Citation

Lu, Feng-Hu, "Sedimentology and dolomitization in the upper Mississippian Turner Valley carbonates, Quirk Creek, Alberta, Canada." (1993). *Electronic Theses and Dissertations*. 3397.  
<https://scholar.uwindsor.ca/etd/3397>

This online database contains the full-text of PhD dissertations and Masters' theses of University of Windsor students from 1954 forward. These documents are made available for personal study and research purposes only, in accordance with the Canadian Copyright Act and the Creative Commons license—CC BY-NC-ND (Attribution, Non-Commercial, No Derivative Works). Under this license, works must always be attributed to the copyright holder (original author), cannot be used for any commercial purposes, and may not be altered. Any other use would require the permission of the copyright holder. Students may inquire about withdrawing their dissertation and/or thesis from this database. For additional inquiries, please contact the repository administrator via email ([scholarship@uwindsor.ca](mailto:scholarship@uwindsor.ca)) or by telephone at 519-253-3000ext. 3208.



National Library  
of Canada

Acquisitions and  
Bibliographic Services Branch

395 Wellington Street  
Ottawa, Ontario  
K1A 0N4

Bibliothèque nationale  
du Canada

Direction des acquisitions et  
des services bibliographiques

395, rue Wellington  
Ottawa (Ontario)  
K1A 0N4

*Your file* *Votre référence*

*Our file* *Notre référence*

## NOTICE

The quality of this microform is heavily dependent upon the quality of the original thesis submitted for microfilming. Every effort has been made to ensure the highest quality of reproduction possible.

If pages are missing, contact the university which granted the degree.

Some pages may have indistinct print especially if the original pages were typed with a poor typewriter ribbon or if the university sent us an inferior photocopy.

Reproduction in full or in part of this microform is governed by the Canadian Copyright Act, R.S.C. 1970, c. C-30, and subsequent amendments.

## AVIS

La qualité de cette microforme dépend grandement de la qualité de la thèse soumise au microfilmage. Nous avons tout fait pour assurer une qualité supérieure de reproduction.

S'il manque des pages, veuillez communiquer avec l'université qui a conféré le grade.

La qualité d'impression de certaines pages peut laisser à désirer, surtout si les pages originales ont été dactylographiées à l'aide d'un ruban usé ou si l'université nous a fait parvenir une photocopie de qualité inférieure.

La reproduction, même partielle, de cette microforme est soumise à la Loi canadienne sur le droit d'auteur, SRC 1970, c. C-30, et ses amendements subséquents.

**Canada**

**SEDIMENTOLOGY AND DOLOMITIZATION IN THE UPPER  
MISSISSIPPIAN TURNER VALLEY CARBONATES,  
QUIRK CREEK, ALBERTA, CANADA**

**by  
Feng-Hu Lu**

**A Thesis submitted to the  
Faculty of Graduate Studies and Research  
through the Department of Geology in Partial Fulfillment  
of the requirements for the Degree  
of Master of Science at the  
University of Windsor**

**Windsor, Ontario, Canada**

**1993**



National Library  
of Canada

Acquisitions and  
Bibliographic Services Branch

395 Wellington Street  
Ottawa, Ontario  
K1A 0N4

Bibliothèque nationale  
du Canada

Direction des acquisitions et  
des services bibliographiques

395, rue Wellington  
Ottawa (Ontario)  
K1A 0N4

*Your file* *Votre référence*

*Our file* *Notre référence*

**The author has granted an irrevocable non-exclusive licence allowing the National Library of Canada to reproduce, loan, distribute or sell copies of his/her thesis by any means and in any form or format, making this thesis available to interested persons.**

**L'auteur a accordé une licence irrévocable et non exclusive permettant à la Bibliothèque nationale du Canada de reproduire, prêter, distribuer ou vendre des copies de sa thèse de quelque manière et sous quelque forme que ce soit pour mettre des exemplaires de cette thèse à la disposition des personnes intéressées.**

**The author retains ownership of the copyright in his/her thesis. Neither the thesis nor substantial extracts from it may be printed or otherwise reproduced without his/her permission.**

**L'auteur conserve la propriété du droit d'auteur qui protège sa thèse. Ni la thèse ni des extraits substantiels de celle-ci ne doivent être imprimés ou autrement reproduits sans son autorisation.**

ISBN 0-315-83028-X

**Canada**

Name Feng-Hu Lu

Dissertation Abstracts International is arranged by broad, general subject categories. Please select the one subject which most directly describes the content of your dissertation. Enter the corresponding four-digit code in the spaces provided.

Sedimentology and Geochemistry  
SUBJECT TERM

0372  
SUBJECT CODE

U·M·I

**Subject Categories**

**THE HUMANITIES AND SOCIAL SCIENCES**

**COMMUNICATIONS AND THE ARTS**

Architecture	0729
Art History	0377
Cinema	0900
Dance	0378
Fine Arts	0357
Information Science	0723
Journalism	0391
Library Science	0399
Mass Communications	0708
Music	0413
Speech Communication	0459
Theater	0465

**EDUCATION**

General	0515
Administration	0514
Adult and Continuing	0516
Agricultural	0517
Art	0273
Bilingual and Multicultural	0282
Business	0688
Community College	0275
Curriculum and Instruction	0727
Early Childhood	0518
Elementary	0524
Finance	0277
Guidance and Counseling	0519
Health	0680
Higher	0745
History of	0520
Home Economics	0278
Industrial	0521
Language and Literature	0279
Mathematics	0280
Music	0522
Philosophy of	0998
Physical	0523

Psychology	0525
Reading	0535
Religious	0527
Sciences	0714
Secondary	0533
Social Sciences	0534
Sociology of	0340
Special	0529
Teacher Training	0530
Technology	0710
Tests and Measurements	0288
Vocational	0747

**LANGUAGE, LITERATURE AND LINGUISTICS**

Language	
General	0679
Ancient	0289
Linguistics	0290
Modern	0291
Literature	
General	0401
Classical	0294
Comparative	0295
Medieval	0297
Modern	0298
African	0316
American	0591
Asian	0305
Canadian (English)	0352
Canadian (French)	0355
English	0593
Germanic	0311
Latin American	0312
Middle Eastern	0315
Romance	0313
Slavic and East European	0314

**PHILOSOPHY, RELIGION AND THEOLOGY**

Philosophy	0422
Religion	
General	0318
Biblical Studies	0321
Clergy	0319
History of	0320
Philosophy of	0322
Theology	0469

**SOCIAL SCIENCES**

American Studies	0323
Anthropology	
Archaeology	0324
Cultural	0326
Physical	0327
Business Administration	
General	0310
Accounting	0272
Banking	0770
Management	0454
Marketing	0338
Canadian Studies	0385
Economics	
General	0501
Agricultural	0503
Commerce-Business	0505
Finance	0508
History	0509
Labor	0510
Theory	0511
Folklore	0358
Geography	0366
Gerontology	0351
History	
General	0578

Ancient	0579
Medieval	0581
Modern	0582
Black	0328
African	0331
Asia, Australia and Oceania	0332
Canadian	0334
European	0335
Latin American	0336
Middle Eastern	0333
United States	0337
History of Science	0585
Law	0398
Political Science	
General	0615
International Law and Relations	0616
Public Administration	0617
Recreation	0814
Social Work	0452
Sociology	
General	0626
Criminology and Penology	0627
Demography	0938
Ethnic and Racial Studies	0631
Individual and Family Studies	0628
Industrial and Labor Relations	0629
Public and Social Welfare	0630
Social Structure and Development	0700
Theory and Methods	0344
Transportation	0709
Urban and Regional Planning	0999
Women's Studies	0453

**THE SCIENCES AND ENGINEERING**

**BIOLOGICAL SCIENCES**

Agriculture	
General	0473
Agronomy	0285
Animal Culture and Nutrition	0475
Animal Pathology	0476
Food Science and Technology	0359
Forestry and Wildlife	0478
Plant Culture	0479
Plant Pathology	0480
Plant Physiology	0817
Range Management	0777
Wood Technology	0746

**Biology**

General	0306
Anatomy	0287
Biostatistics	0308
Botany	0309
Cell	0379
Ecology	0329
Entomology	0353
Genetics	0369
Limnology	0793
Microbiology	0410
Molecular	0307
Neuroscience	0317
Oceanography	0416
Physiology	0433
Radiation	0821
Veterinary Science	0778
Zoology	0472

**Biophysics**

General	0786
Medical	0760

**EARTH SCIENCES**

Biogeochemistry	0425
Geochemistry	0996

Geodesy	0370
Geology	0372
Geophysics	0373
Hydrology	0388
Mineralogy	0411
Paleobotany	0345
Paleoecology	0426
Paleontology	0418
Paleozoology	0985
Palynology	0427
Physical Geography	0368
Physical Oceanography	0415

**HEALTH AND ENVIRONMENTAL SCIENCES**

Environmental Sciences	0768
Health Sciences	
General	0566
Audiology	0360
Chemotherapy	0992
Dentistry	0567
Education	0350
Hospital Management	0769
Human Development	0758
Immunology	0982
Medicine and Surgery	0564
Mental Health	0347
Nursing	0569
Nutrition	0570
Obstetrics and Gynecology	0380
Occupational Health and Therapy	0354
Ophthalmology	0381
Pathology	0571
Pharmacology	0419
Pharmacy	0572
Physical Therapy	0382
Public Health	0573
Radiology	0574
Recreation	0575

Speech Pathology	0460
Toxicology	0383
Home Economics	0386

**PHYSICAL SCIENCES**

**Pure Sciences**

Chemistry	
General	0485
Agricultural	0749
Analytical	0486
Biochemistry	0487
Inorganic	0488
Nuclear	0738
Organic	0490
Pharmaceutical	0491
Physical	0494
Polymer	0495
Radiation	0754
Mathematics	0405

**Physics**

General	0605
Acoustics	0986
Astronomy and Astrophysics	0606
Atmospheric Science	0608
Atomic	0607
Electronics and Electricity	0607
Elementary Particles and High Energy	0798
Fluid and Plasma	0759
Molecular	0609
Nuclear	0610
Optics	0752
Radiation	0756
Solid State	0611
Statistics	0463

**Applied Sciences**

Applied Mechanics	0346
Computer Science	0984

**Engineering**

General	0537
Aerospace	0538
Agricultural	0539
Automotive	0540
Biomedical	0541
Chemical	0542
Civil	0543
Electronics and Electrical	0544
Heat and Thermodynamics	0348
Hydraulic	0545
Industrial	0546
Marine	0547
Materials Science	0794
Mechanical	0548
Metallurgy	0743
Mining	0551
Nuclear	0552
Packaging	0549
Petroleum	0765
Sanitary and Municipal	0554
System Science	0790
Geotechnology	0428
Operations Research	0796
Plastics Technology	0795
Textile Technology	0994

**PSYCHOLOGY**

General	0621
Behavioral	0384
Clinical	0622
Developmental	0620
Experimental	0623
Industrial	0624
Personality	0625
Physiological	0989
Psychobiology	0349
Psychometrics	0632
Social	0451



©Feng-Hu Lu 1993

**APPROVED BY:**

Iain M. Samson

Dr. I. M. Samson (Internal Examiner)

Keith Taylor

Dr. K. E. Taylor (External Examiner)

I. S. Al-Aasm

Dr. I. S. Al-Aasm (Advisor)

## ABSTRACT

The Mississippian Turner Valley Formation at the Quirk Creek field is composed of a shallowing-upward sequence of shallow platform to restricted lagoon and sabkha carbonates with a thickness of 115 m. Carbonates of the Turner Valley Formation have undergone a complex diagenetic history. Major diagenetic events include: cementation, compaction, silicification, anhydritization, and dolomitization. Various mechanical and chemical compaction fabrics are present and formed during different diagenetic stages. All calcite cementation occurred during early diagenetic stages. Silicification occurred as replacements and cements in chert nodules. Cherts may have formed during relatively early stages after calcite cementation and before massive dolomitization. Burial anhydrite usually coexists with massive dolomite, and they may have similar origins.

The most important of all diagenetic events involves a continuous spectrum of early to late dolomitization. Four types or generations of dolomite are identified: microdolomite, patchy dolomite, pervasive matrix dolomite and coarse dolomite. Microdolomite (4-10  $\mu\text{m}$ ) is dense, and locally occurs only in sabkha lithofacies. It is characterized by its high Sr, Na concentrations and relatively heavy  $\delta^{18}\text{O}$  values (0 to -2.22 per mil PDB). These parameters suggest a sabkha evaporative dolomitization origin. However, its perfect crystal shape, overgrowth rims and variable values of  $^{87}\text{Sr}/^{86}\text{Sr}$  (0.70773 to 0.70874) may represent recrystallization during late stages of dolomitization. Patchy dolomite (20 to 200  $\mu\text{m}$ ) floats between skeletal grains, and is distributed along dissolution seams and early stylolites ( $\delta^{18}\text{O}$ , -0.79 to -3.52 per mil PDB). This type of dolomite is interpreted to have formed during early chemical compaction, and it also underwent some modification during late dolomitization events. Pervasive matrix dolomite or massive dolomite (20 to 300  $\mu\text{m}$ ) is the most abundant type of dolomite with predominantly reservoir porosity. It has modified and/or obliterated most earlier diagenetic fabrics. Since pervasive matrix dolomite has the lowest trace-element (e.g. Sr, Na) concentrations, slightly radiogenic Sr isotopes (0.70834 to 0.70848), slightly depleted  $\delta^{18}\text{O}$  (-1.11 to -5.46 per mil PDB), and widely coexists with secondary anhydrite, a



mixing zone associated with a regional groundwater system beneath the Mississippian/Pennsylvanian unconformity is envisaged here for its formation. The fluids resulted from flushing the overlying evaporites by meteoric water and mixing it with seawater could have been the source of secondary anhydrite as well as massive dolomite. Megadolomite (0.5 to 2 mm) consists of coarse, euhedral rhombs and moldic-dolomite. It replaces massive dolomite and crosscuts late stylolites. Megadolomite has higher Fe, Mn, and radiogenic Sr (0.70836 to 0.70875) and lowest  $\delta^{18}\text{O}$  (-2.12 to -6.47 per mil PDB), suggesting formation in a later and deeper burial environment.

The reservoir porosity of the Turner Valley Formation is mainly controlled by the degree of dolomitization. The most abundant porosity is presented in carbonates with a dolomite component of 70% to 95%. The potential reserves could be found in these carbonates.

**This work is dedicated to my mother: A great woman.**

## ACKNOWLEDGEMENTS

This work should be attributed to many people. First of all, I would extend my sincere thanks to my supervisor, Dr. I.S. Al-Aasm, his advice, encouragement, and financial aids are highly appreciated.

Thanks are extended to Dr. I.M. Samson for his help on the study of fluid inclusions and his helpful and constructive comments; to Dr. K.E. Taylor for his helpful and constructive reading, to Dr. Jeff Packard for suggesting this project and helpful information. Thanks are also extend to Mr. A. Knitl for his help in thin section preparation, to Mrs. T. Pare for her help in trace element analysis, and to my friend Scott Durocher, who served as a consulting grammarian.

Thanks are also extended to ESSO, Resource Canada Ltd., which provided samples and some financial aids; to the Faculty of Graduate Studies, University of Windsor for the Scholarship during my study.

I would like to thank my parents, brothers , and sisters for their understanding, love, and encouragement.

Finally, a special thank to my wife, Yinghui, for her love, patience, and encouragement without which this work could not have been completed.

## TABLE OF CONTENTS

<b>ABSTRACT</b> .....	iv
<b>DEDICATION</b> .....	vi
<b>ACKNOWLEDGEMENTS</b> .....	vii
<b>LIST OF FIGURES</b> .....	xii
<b>LIST OF PLATES</b> .....	xiv
<b>LIST OF TABLES</b> .....	xvi
<b>CHAPTER I INTRODUCTION</b> .....	1
1.1 PREAMBLE .....	1
1.2 PREVIOUS WORK .....	1
1.3 OBJECTIVES OF STUDY .....	3
1.4 METHODS OF STUDY .....	4
<b>CHAPTER II SEDIMENTOLOGY AND STRATIGRAPHY</b> .....	6
2.1 REGIONAL SETTING .....	6
2.2 REGIONAL STRUCTURAL SETTING .....	6
2.3 REGIONAL STRATIGRAPHY .....	7
2.4 STRATIGRAPHY OF THE TURNER VALLEY FORMATION ...	9
2.5 LITHOFACIES OF THE TURNER VALLEY FORMATION .....	11
2.5.1 Grainstone Facies .....	11
2.5.2 Packstone Facies .....	14

2.5.3 Wackestone and Mudstone Facies . . . . .	14
2.5.4 Sabkha Mudstone Facies . . . . .	14
2.6 ENVIRONMENTAL INTERPRETATION . . . . .	17

**CHAPTER III DIAGENESIS AND GEOCHEMISTRY OF THE TURNER**

<b>VALLEY FORMATION . . . . .</b>	<b>19</b>
3.1 INTRODUCTION . . . . .	19
3.2 MICRITIZATION . . . . .	19
3.3 COMPACTION . . . . .	20
3.3.1 Mechanical (physical) Compaction . . . . .	20
3.3.2 Chemical Compaction . . . . .	20
3.4 CEMENTATION . . . . .	24
3.4.1 Syntaxial Overgrowth Rim . . . . .	24
3.4.2 Vein Calcite Cement . . . . .	24
3.4.3 Bladed Prismatic Calcite . . . . .	25
3.4.4 Blocky Calcite Cement . . . . .	25
3.4.5 Coarse Calcite Spar . . . . .	25
3.4.6 Poikilotopic Calcite Cement . . . . .	26
3.5 SILICIFICATION . . . . .	26
3.5.1 Petrography of Silicification . . . . .	26
3.5.2 Source of Silica . . . . .	30
3.5.3 Timing of Silicification . . . . .	32
3.6 ANHYDRITIZATION . . . . .	32
3.6.1 Primary Anhydritization . . . . .	33
3.6.2 Secondary Anhydrite . . . . .	33
3.6.3 Source and Timing of Secondary Anhydrite . . . . .	35
3.7 DOLOMITIZATION . . . . .	36
3.7.1 Petrography . . . . .	36
3.7.2 Spatial Distribution of Dolomite . . . . .	40
3.8 FRACTURING . . . . .	40

3.9 DISSOLUTION . . . . .	42
3.10 GEOCHEMISTRY OF THE TURNER VALLEY FORMATION . .	42
3.10.1 Fluid Inclusions . . . . .	43
3.10.2 Cathodoluminescence (CL) Petrography . . . . .	45
3.10.3 Fluorescence Stratigraphy . . . . .	46
3.10.4 Major, Minor, and Trace Elements . . . . .	47
3.10.4.1 Introduction . . . . .	47
3.10.4.2 Calcium and Magnesium . . . . .	48
3.10.4.3 Sodium . . . . .	49
3.10.4.4 Strontium . . . . .	50
3.10.4.5 Manganese . . . . .	53
3.10.4.6 Iron . . . . .	53
3.10.4.7 Analytical Results of Microprobe . . . . .	53
3.10.4.8 Summary of Major, Minor and Trace Elements . .	56
3.10.5 Isotopes . . . . .	57
3.10.5.1 Oxygen and Carbon Isotopes . . . . .	57
3.10.5.2 Sulfur Isotopes . . . . .	63
3.10.5.3 Strontium Isotopes . . . . .	64
3.10.5.4 Summary of Isotopic Studies . . . . .	66
3.11 SUMMARY OF DIAGENESIS . . . . .	67
<b>CHAPTER IV ORIGINS AND MODELS OF DOLOMITIZATION . . . . .</b>	<b>70</b>
4.1 FACIES AND MASSIVE DOLOMITIZATION . . . . .	70
4.2 DISTRIBUTION OF DOLOMITE IN LIMESTONES . . . . .	70
4.3 DOLOMITIZATION AND OTHER DIAGENETIC EVENTS . . . . .	73
4.4 ORIGINS AND MODELS OF DOLOMITIZATION . . . . .	75
4.4.1 Microdolomite . . . . .	76
4.4.2 Patchy Dolomite . . . . .	78
4.4.3 Pervasive Matrix Dolomite . . . . .	78
4.4.4 Megadolomite . . . . .	85

4.5 SUMMARY .....	86
<b>CHAPTER V POROSITY AND POROSITY EVOLUTION .....</b>	<b>89</b>
5.1 INTRODUCTION .....	89
5.2 PRIMARY POROSITY .....	89
5.3 SECONDARY (DIAGENETIC) POROSITY .....	90
5.4 POROSITY EVOLUTION DURING DIAGENESIS .....	92
5.5 SUMMARY .....	98
<b>CHAPTER VI CONCLUSIONS AND REMARKS .....</b>	<b>100</b>
6.1 CONCLUSIONS .....	100
6.2 REMARKS .....	102
<b>REFERENCES .....</b>	<b>103</b>
<b>APPENDIX I .....</b>	<b>110</b>
<b>APPENDIX II .....</b>	<b>115</b>
<b>VITA AUCTORIS .....</b>	<b>120</b>

## LIST OF FIGURES

### Figure

1.1. Location Map of study area. . . . .	2
1.2. Field well locations of studied cores. . . . .	2
2.1. Mississippian regional structural profile of south Alberta. . . . .	8
2.2. Diagrammatic interpretation of the Turner Valley deposition. . . . .	18
3.1. Na vs. Sr for all calcite and dolomite components. . . . .	51
3.2. Sr-Depth relationship for massive dolomite. . . . .	51
3.3. Na-Depth relationship for massive dolomite. . . . .	54
3.4. Sr-Depth relationship for calcitic crinoidal fragments. . . . .	54
3.5. Scatter diagram of Mn vs. Fe for dolomites. . . . .	55
3.6. Scatter diagram of Fe and Sr for dolomites. . . . .	55
3.7. Oxygen and Carbon isotopes of calcitic crinoids and cements. . . . .	59
3.8. Oxygen and Carbon isotopes of various types of dolomite. . . . .	59
3.9. Burial history curve of the Turner Valley Carbonates. . . . .	62



3.10. $^{87}\text{Sr}/^{86}\text{Sr}$ values of dolomites. . . . .	65
4.1. Relationship between dolomite percentage and crystal size. . . . .	72
4.2. Relationship between the amount of insoluble materials and dolomite percentage	72
4.3. Schematic diagram of the Turner Valley massive dolomitization. . . . .	83
4.4. Evolution of dolomitization fluids. . . . .	87
4.5. Simplified origin and evolution of various types of dolomite. . . . .	87
5.1. Porosity and various diagenetic events. . . . .	93
5.2. Plot of porosity and dolomite percentage. . . . .	96
5.3. Plot of porosity and depth of the Turner Valley carbonates. . . . .	99

## LIST OF PLATES

### Plate

2.1. Core photography of grainstones. . . . .	10
2.2. Echinoderm Grainstone Subfacies. . . . .	13
2.3. Echinoderm-bryozoan grainstone Facies. . . . .	13
2.4. Oolitic Grainstone Subfacies and micrite envelope. . . . .	15
2.5. Packstone Facies. . . . .	15
2.6. Wackestone facies. . . . .	16
2.7. Sabkha mudstone Facies. . . . .	16
3.1. A broken micrite envelope. . . . .	21
3.2. Vein calcite cement is crosscut by stylolites. . . . .	21
3.3. Dissolution seams and crystals of patchy dolomite. . . . .	23
3.4. Core photography of chert nodules and bands. . . . .	23
3.5. Megaquartz replaces coarse calcite spars. . . . .	28
3.6. Microquartz replaces skeletal grains . . . . .	28

3.7. Massive dolomite crosscuts microquartz. . . . .	29
3.8. Length-fast chalcedony and microquartz. . . . .	29
3.9. Core photography of microdolomite and anhydrite. . . . .	31
3.10. Core photography of burial anhydrite nodules. . . . .	31
3.11. Burial anhydrites are distributed along fractures. . . . .	34
3.12. Back-scattered electron micrography of microdolomite. . . . .	34
3.13. Back-scattered micrography of an enlarged-grain. . . . .	38
3.14. Overgrowth rims of patchy dolomite. . . . .	38
3.15. Massive dolomite with subhedral to euhedral crystals. . . . .	41
3.16. Megadolomite replaces burial anhydrite (red ones). . . . .	41
5.1. Core photography of moldic porosity. . . . .	91
5.2. Core photography of vuggy porosity. . . . .	91

## LIST OF TABLES

### Table

2.1. Correlation of Mississippian strata. . . . .	8
3.1. Fluid inclusions and homogenization temperatures. . . . .	44
3.2. Trace element concentrations of dolomites. . . . .	49
3.3. Paragenetic sequence of Turner Valley carbonates. . . . .	69
4.1. Temperatures and $\delta^{18}\text{O}$ values of dolomites. . . . .	86

# CHAPTER I

## INTRODUCTION

### 1.1 PREAMBLE

Mississippian carbonates of the Western Canada Basin are extremely important hydrocarbon hosts. They collectively yield 20.8% of the basin's marketable gas reserves and 14.4% of recoverable oil reserves (GSC Maps 1558A, 1559A). Remaining undiscovered gas potential is considerable but no published figures are available. Approximately  $340 \times 10^3$  m<sup>3</sup> of known reserves of recoverable light and medium oils occur in Carboniferous strata in the Western Canada Basin and there remains an estimated further potential of  $43 \times 10^3$  m<sup>3</sup> of undiscovered oil (Conn and Christie, 1988). These major reserves are trapped in the Turner Valley Formation and its lateral equivalents in thrust-faulted anticlinal structures of the Foothills and Plains of southwestern Alberta (Stein, 1977). The Turner Valley Formation has been recognized as a highly prospective horizon ever since the discovery of the Turner Valley field in 1924. Subsequent discovery of condensate and sulphur-rich gas accumulations in the general area, at Jumping Pound (1947), Sarcee (1954), Wildcat Hills (1958), Jumping Pound West (1961), Quick Creek (1967), and so on, have proven that the Turner Valley Formation contains substantial hydrocarbon reserves (Rupp, 1969).

Quirk Creek, one of Foothills fields, lies approximately 40 km southwest of Calgary, Alberta (Fig.1.1). Typical reservoir rock consists of partially to completely dolomitized packstone and wackestone distributed in the top and base (?) of the Turner Valley Formation. All limestones in the Turner Valley Formation have been variably dolomitized with a dolomite component ranging from 10 to 100 per cent.

### 1.2 PREVIOUS WORK

Douglas (1958, 1959 in Bamber et al., 1981) first described the lithology and stratigraphy of Mississippian exposures in the Foothills and Southern Rocky Mountains and called them the "Rundle Group"; we now know them as Livingstone (Pekisko,

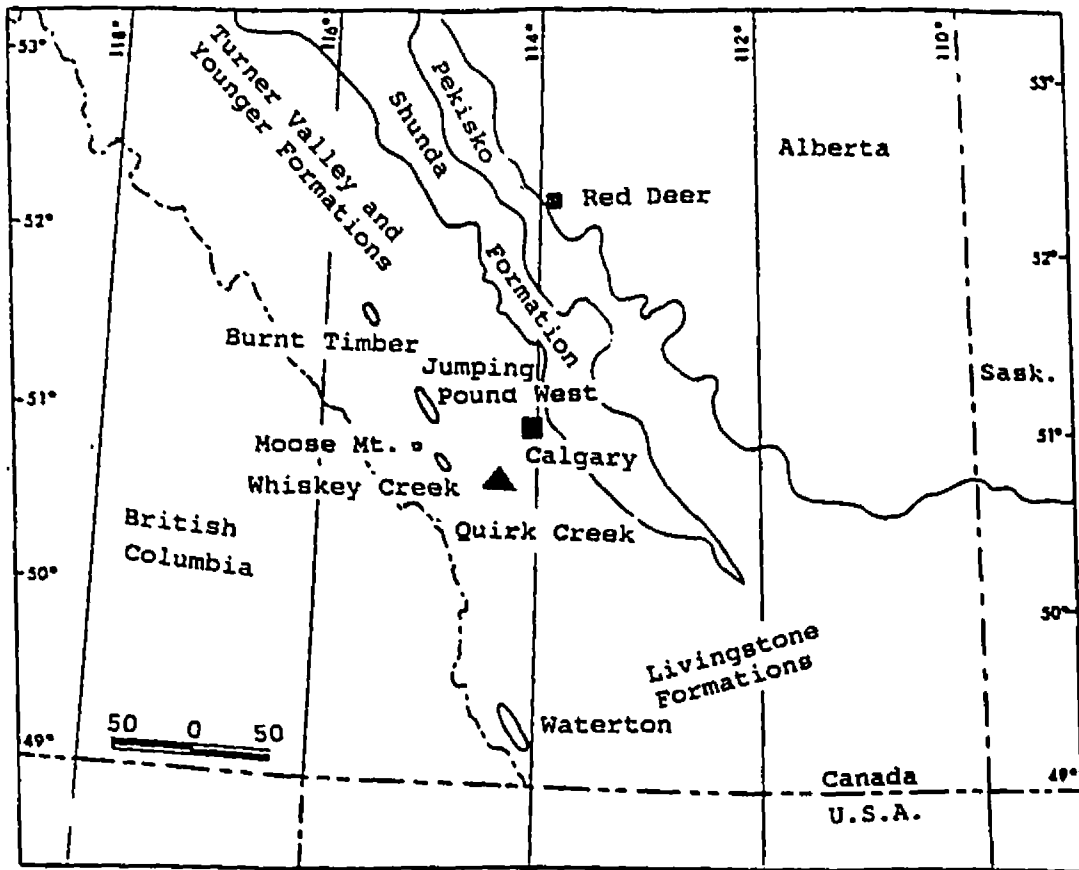


Fig.1.1. Location map of study area (after Stein, 1977).

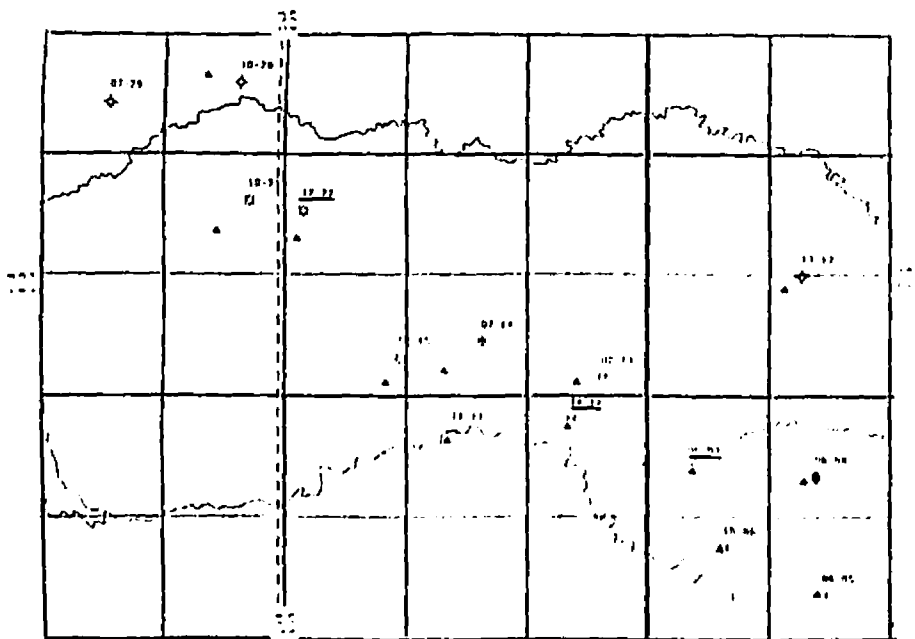


Fig.1.2. Field well locations of studied cores.

Shunda, and Turner Valley), Mount Head, and Etherington Formations. Illing (1959) provided a detailed account of the Mississippian sequence at the Moose Mountain culmination, and sketched the oscillation of sedimentary environments very clearly. Units recognized by Illing include the Banff, Pekisko, Shunda, and Turner Valley Formations, as they are used today. Moreover, Illing (1959) studied dolomitization of the Turner Valley Formation, and first proposed the burial compaction model of dolomitization.

Middleton (1963, in Bamber et al., 1981) studied sedimentary facies variations within the Moose Mountain culmination. Macqueen and Bamber (1967, 1981) correlated the lithology and stratigraphy of the Banff, Pekisko, Shunda, Turner Valley Formations in a regional study. Murray and Lucia (1967) studied dolomitization of the lower parts of the Turner Valley Formation in Moose Mountain and proposed that the most completely dolomitized parts of the formation were originally composed mainly of lime mud; limestones with less than 15% dolomite were deposited as mud-free skeletal limestones. Ng and Jones (1989) also studied the stratigraphy, depositional environments and diagenesis of Upper Mississippian to Lower Permian strata in Talbert Lake area, Jasper National Park, Alberta. All these studies mentioned above dealt mainly with the stratigraphy, lithofacies, sedimentary environments and some aspects of diagenesis of the Turner Valley Formation. Their conclusions were not supported by any geochemical data.

### **1.3 OBJECTIVES OF STUDY**

This study is the first to adopt geochemical techniques such as isotopic analyses, major and minor elemental analyses and cathodoluminescence observations, in addition to detailed petrographic observations, to examine and analyze the carbonates and its diagenesis in the Turner Valley Formation of the Quirk Creek field. The objectives of this research are: (1) to determine the various lithofacies, their distribution and sedimentary environments; (2) to determine the type, distribution and features of various diagenetic event, and a paragenetic sequence; (3) to interpret different types of dolomite, and to establish models of dolomitization; (4) to evaluate the nature and development of porosity related to diagenesis.

#### 1.4 METHODS OF STUDY

The field work was conducted in the summer of 1991. Carbonate rocks of the Turner Valley and those around the contacts between the Turner Valley Formation and the underlying Shunda and overlying Mount Head Formations were selectively sampled in the vertical succession at obvious changes in lithology from three wells in the Quirk Creek field. The three wells are 12-22, 14-12, 6-7 (Fig. 1.2). Approximately 100 thin sections were examined under a standard petrographic microscope. All thin sections were stained with a mixture of Alizarin Red-S and Potassium Ferricyanide according to the procedure outlined by Dickson (1965). Seventy thin sections were dyed with a blue fluorescent dye for the recognition of microporosity using an epoxy resin and blue fluorescent dye mixture following the method by Yanguas and Dravis (1985). All thin sections were examined under a Cathodoluminescence (CL) device, using a Technosyn Model 8200 MKII and a Luminoscope. Operating conditions for cathodoluminescence were a beam of 12 to 15 kv range and a current intensity of about 0.42-0.43 mA. Fluorescence was also studied using a Nikon EPI Fluorescence attached to a microscope. Eight doubly polished thin sections were prepared for the study of fluid inclusions of the Turner Valley carbonates and impurities, being operated on a Linkam TH600 stage. Ten slightly polished slabs were etched with 50% acetic acid for two minutes, and coated with carbon, were examined under a NANOLAB scanning electron microscope (SEM) to study diagenetic textures and microporosity present. Four uncovered, polished thin sections were analyzed under an electron microprobe for trace elements. Each thin section was then covered by a thin layer of carbon and analyzed using a Cameca Camebax SX50 equipped with three crystal spectrometers and a back-scattered electron detector (BSE). The operating conditions during analysis were an acceleration voltage of 15 kV, a measured beam current of 6 nA, and a beam diameter between 1 and 10  $\mu\text{m}$ . The standards used were wollastonite (Ca), MgO (Mg), MnTiO<sub>3</sub> (Mn), hematite (Fe), strontianite (Sr), and albite (Na). Triplicate analyses of Mg and Ca revealed a precision better than 0.5 mol%.

Forty-four samples from calcite and dolomite components were chemically analyzed using an atomic absorption spectrometer for major and minor elements. A microscope-



mounted drill assembly was used to sample crinoids, calcite cements, as well as various types of dolomite. Powdered dolomite and calcite samples were put into an oven at 115°C for at least two hours. After weighing the dry powder, it was dissolved in solutions of 20 ml of 6% and 8% (v/v) HCl for calcite and dolomite, respectively, for four hours (e.g. Brand and Veizer, 1980). Six elements, Ca, Mg, Na, Sr, Fe and Mn were analyzed on a Varian Spectra AA300 Spectrometer. KCl (2000 ppm K) was added to sample and standard rock solutions for Sr analysis. Insoluble residues were subtracted in chemical calculations. The standard was prepared from the Standard Reference Material 88b (National Bureau of Standards, dolomitic limestone). Systematic error in percentage is reported in decreasing order: Na (5.2), Mn (4.8), Mg (2.8), Sr (1.1), Ca (0.3), and Fe (0.3). O, C, S and Sr isotopes of carbonates and sulfates were studied. Calcite and dolomite components were obtained using a microscope mounted drill assembly. Each sample was then reacted with 100% phosphoric acid at 25°C for calcite and at 50°C for dolomite. Samples containing both calcite and dolomite were subjected to chemical separation techniques described by Al-Aasm et al. (1990). All extractions of O, C, S were done at the Stable Isotope Lab, University of Windsor. The evolved CO<sub>2</sub> and SO<sub>2</sub> gases were analysed for C, O and S isotopes using a SIRA-12 mass spectrometer at the University of Ottawa. The δ<sup>18</sup>O and δ<sup>13</sup>C were reported relative to PDB. Precision is better than 0.1 per mil. Sr isotopes were analyzed at the University of Bochum in Germany. Sample analysis was performed on a Finnigan MAT 262 with 5 fixed collectors. <sup>87</sup>Sr/<sup>86</sup>Sr ratios were normalized to <sup>88</sup>Sr/<sup>86</sup>Sr=8.375209. NBS and ocean water were used as standard references. Precision was better than 0.00010.

## **CHAPTER II**

### **SEDIMENTOLOGY AND STRATIGRAPHY**

#### **2.1 REGIONAL SETTING**

In western Canada, the Mississippian succession consists of an eastern belt of thick platform carbonates and detrital clastics that grade laterally into a western belt of thin basinal shales across a transitional carbonate platform margin with a very low depositional slope. These two sinuous lithofacies belts extend from southern Alberta and British Columbia northwestward to the northern Yukon Territory (Bamber et al., 1980).

In general, the Mississippian succession is grossly regressive upward commencing with open marine shales of the Banff Formation. A similar lateral sequence, but far less pronounced, produces more restricted beds to the east in any one "time" unit. Superimposed on the gross cycle are minor episodes of transgression and regression. In the early Mississippian sequence, prolific and geologically unique echinoderms were developed. The Osagian and early Meramecian were characterized by the development of carbonate banks and shoals over much of southern Alberta. Enormous volumes of echinoderm and bryozoan limestones accumulated in the Pekisko, Turner Valley, and Livingstone formations; peritidal carbonates and evaporites (Shunda and Mount Head Formations) accumulated to the east of the banks during late Osagian time (Stein, 1977).

#### **2.2 REGIONAL STRUCTURAL SETTING**

Surface exposures of Rundle Group strata in the vicinity of Moose Mountain outline the core of a large doubly plunging, faulted anticline, loosely referred to as "Moose Dome". Quirk Creek is located at the southeast end of "Moose Dome". Moose Mountain is one of a series of structural highs, or culminations, that occur at intervals along the regional northwest to southeast strike within the Foothills. Many of these culminations bring inliers of Palaeozoic rocks to the surface to form small mountains of carbonate rock above the more widespread, but less resistant, Mesozoic shale and sandstone (Bamber et al., 1988). Hydrocarbon reservoirs are common in culminations within the

Foothills, typically at considerable depth. The structure surrounding the Moose Mountain culmination consists of a series of folds and imbricated, west dipping thrusts, the latter separating discrete "plates" of strata. At depth, a few gently dipping thrusts, or sole faults, of large displacement, separate large fault plates. The sole faults splay upwards to form more numerous plates and high-angle thrusts of small to moderate displacement at the surface of the Moose Mountain culmination. The orientation and displacement of structures indicate a major southwest-northeast direction of compression, with crustal shorting and translation toward the northeast (Fig 2.1).

### **2.3 REGIONAL STRATIGRAPHY**

In southwest Alberta, Mississippian stratigraphy is characterized by a lower, micritic and argillaceous Banff Formation and an upper, resistant Rundle Group. Table 2.1 shows the regional variations of the Mississippian succession.

Within the platform carbonates of the overlying Lower Rundle Group, Macqueen and Bamber (1967) recognized an eastern peritidal lithofacies and a western open marine lithofacies. The eastern lithofacies is distributed in the central Foothills, Rocky Mountains and Southern Alberta Plains and consists of four formations in ascending order: Banff, Pekisko, Shunda and Turner Valley Formations (Fig. 1.1). The Pekisko and Turner Valley Formations are predominantly echinoderm-rich limestones and dolomites, and the intervening Shunda Formation is dominated by wackestones, mudstones with evaporite solution breccia and dolomite assemblages (Macqueen et al., 1967). The western lithofacies, which is distributed in the Rocky Mountains near Banff and in southeast Alberta, consists of the Banff and Livingstone Formations, which are predominantly clean echinodermal limestones and their dolomite equivalents. Therefore, Macqueen and Bamber (1967) suggested that the Livingstone Formation is the lateral equivalent of the Pekisko, Shunda and Turner Valley Formations. The upper Rundle group is composed of the Mount Head Formation, which consists predominantly of shallow marine limestone with supratidal carbonates and the Etherington Formation with various facies. The Mississippian succession is regionally overlain unconformably by Pennsylvanian strata.

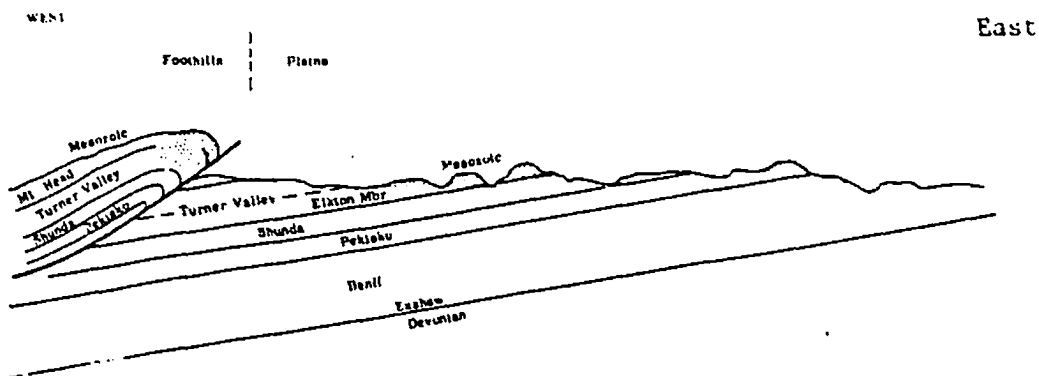


**Fig.2.1.** Mississippian regional structural profile of southwestern Alberta without scale (After Procter et al., 1968).

**Table 2.1.** Correlation of Mississippian Formations of southwestern Alberta. (modified from Macqueen et al., 1967; Bamber et al., 1981).

Banff-Jasper Front Ranges		Bow Valley Front Ranges		Moore Mt. Area	Mount Head Area	Rundle Group
		upper	Etherington		Etherington	
		middle				
		lower				
Mount Head				Mount Head	Mount Head	
Turner Valley	Livingstone			Turner Valley	Turner Valley	
Shunda				Shunda	Shunda	
Pekisko				Pekisko	Pekisko	
Banff						

## **2.4 STRATIGRAPHY OF THE TURNER VALLEY FORMATION**

In the subsurface of southwestern Alberta, the Turner Valley Formation consists of widespread shallow marine carbonates dominated by echinoderm and bryozoan debris and carbonate muds. The Turner Valley Formation has a thickness of about 115 m in Quirk Creek and, regionally, is underlain unconformably by dark micritic carbonates of the Shunda Formation, and overlain unconformably by peritidal micritic limestones and dolomites of the Mount Head Formation (Bamber et al., 1981).

The fivefold-subdivision of Rupp (1969) for the Turner Valley Formation in the subsurface of the Jumping Pound Field are somewhat parochial and not widely used today. However, three informally (industry influenced) named members, "Lower Porous" (Elkton), "Middle Dense", and "Upper Porous", are often applied and are also adopted in this thesis.

The "Lower Porous" (or Elkton) member is the lower part of the Turner Valley Formation. In Quirk Creek, it is about 43 meters thick. The base of the Elkton consists predominantly of an alternation of echinoderm or echinoderm-bryozoan grainstones and packstones. In Quirk Creek, the Elkton was terminated by a minor regressive phase which resulted in the deposition of tight wackestone and even mudstone. In many grainstones or packstones, the calcitic component of skeletal grains is still retained, although some have been completely dolomitized. Some skeletal limestones show cross-bedded depositional structures (Plate 2.1). Anhydrite often replaces some matrix materials and calcite cements. Primary porosity (intergranular) is very low, usually occluded by calcite cements, anhydrite and patchy dolomite, but locally leached fragments become significant, especially in packstones and wackestones.

The "Middle Dense" member is variable in thickness with a range from 20 to 30 meters, and consists predominantly of wackestones and mudstones containing some scattered clastic quartz grains. The major part of this member is composed of nearly completely dolomitized limestones. Secondary porosity is intercrystalline and fossil moldic. The deposition of this member represents the most regressive phase, from restricted lagoon to sabkha deposition, within the Turner Valley Formation (Rupp, 1969).

The "Upper Porous" Member represents a return to more normal marine circulation,

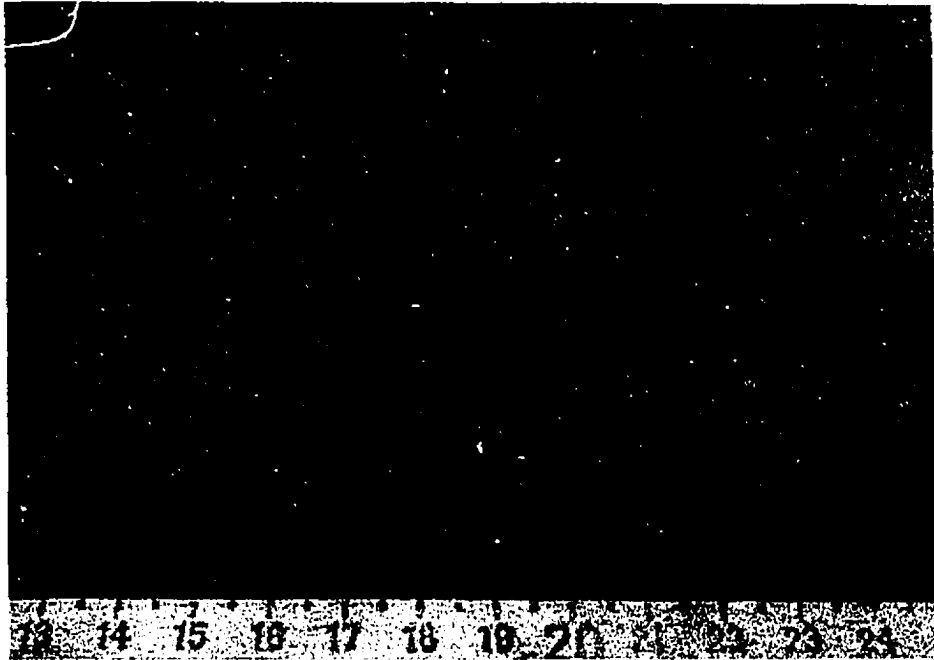


**Plate 2.1.** Core photography of cross-bedded, fine- to medium-grained, crinoidal grainstone. Scale in cm. Core 14-12, depth 2118 m.

and is characterized by the deposition of echinoderm and echinoderm-bryozoan bearing grainstones, packstones and wackestones to mudstones. Grain size is generally smaller than that of the Elkton, changing vertically upward from coarse to fine. Besides minor primary intergranular porosity, much fossil moldic and intercrystalline pores are present, sometimes lined with solid hydrocarbons. This member is about 47 meters thick at Quirk Creek.

## **2.5 LITHOFACIES OF THE TURNER VALLEY FORMATION**

The sediments in the Turner Valley Formation are typically medium to thickly bedded limestones which were deposited in the Mississippian Period in Quirk Creek. They are somewhat similar to those described by Macqueen (1966), Murray and Lucia (1967), and Bamber et al. (1981) in the Moose Mountain and Canyon Creek areas.

The limestone and dolomitic limestone in the Turner Valley Formation in Quirk Creek are composed predominantly of crinoids, bryozoan, and other skeletal particles; smaller in volume, including brachiopods, corals, foraminiferas and calcareous algae. The amount of lime mud varies in different depositional environments.

All Turner Valley limestones are regionally dolomitized (Illing, 1959; Bamber et al., 1981). In spite of the fact that some indication of pre-diagenetic fabrics is often evident, or even clear in some phases, completely dolomitized limestone fabrics are so obliterated that they can be described only by their crystallization texture. Based on the generalized classification of Dunham (1962), five major lithofacies are identified: grainstone, packstone, wackestone, mudstone and sabkha mudstone, and some subfacies are also described in this thesis.

### **2.5.1 Grainstone Facies**

Grainstones are easily recognizable in both hand sample and under the microscope. They generally appear grey or brownish grey in colour. Most grainstones in Turner Valley are calcarenites, calcirudites and their dolomitized equivalents, with varying proportions of coarse echinoderm and bryozoan fragments. Most of the remains of crinoids are columinals and plates, and less crinoid spines are present. Bryozoans are

present mostly as complete fronds and fenestrate forms. Axial canals of both echinoderm columnals and bryozoan zooecia are sometimes filled with some micrite.

Grainstones still consisting of calcite components commonly have little porosity due to compaction and tight cementation by syntaxial overgrowth cement, and poikilotopic cement. Secondary anhydrite and patchy dolomite also fill some pores. However, in highly dolomitized grainstones, much secondary porosity developed (details in Chapter V). Three subfacies can be recognized in this facies: echinoderm grainstones, echinoderm-bryozoan grainstones and oolitic grainstones.

**Echinoderm Grainstone:** In Quirk Creek, Turner valley grainstones are predominantly composed of echinoderm skeletal grains. In crinoid grainstone lithofacies, 90% is crinoid skeletal constituents (Plate 2.2). Crinoid grainstones are characterized by a coarse to very coarse grain size (1-20 mm). Sorting is moderate. Grains often have close packing with extensive grain interpenetration. Large and small crinoid fragments characteristically show typical single-crystal extinction, still retain single-crystal structure, but microtexture is obliterated. Some of these single-crystal fragments and their overgrowths are in optical continuity. Twin zones or/and cleavages of calcite crystals are continuous from grain to cement. Varying amounts of dolomite and anhydrite are present as replacements of calcite cements and skeletal fragments.

**Echinoderm-Bryozoan Grainstone:** some of the Turner valley grainstones in Quirk Creek consist of closely packed, medium to coarse grained accumulations of echinoderm and bryozoan remains (Plate 2.3). This lithofacies shows considerable variations in grain size and sorting.

**Oolitic Grainstone:** oolitic grainstones of the Turner Valley formation in Quirk Creek are very rare, occurring only at the upper parts of well 6-7 and the bases of well 12-22 and well 14-12. They consist of concentric layers of microcrystalline calcite surrounding nuclei of echinoderm and bryozoan fragments (Plate 2.4). Oolites coexist with superficial oolites, which have thin concentric coatings, and also coexist with asymmetric oolites, suggesting formation in agitated waters (Wilson, 1975). Individual oolites vary from 0.5 to 2 mm with an average diameter around 1.5 mm.



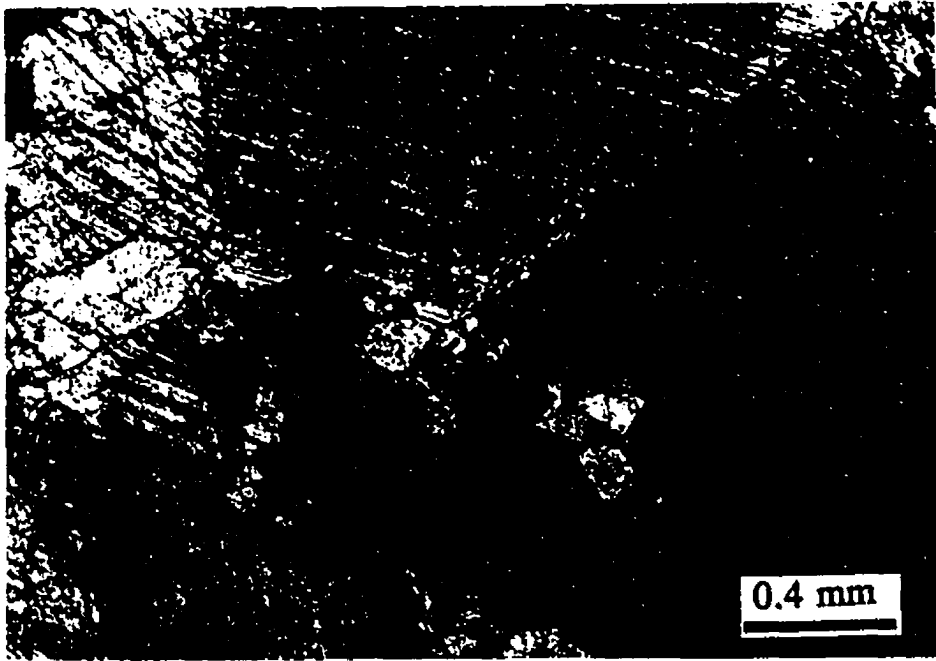


**Plate 2.2.** Echinoderm grainstone subfacies. Grains are crinoids, patchy dolomitic rhombs are distributed between crinoids. Note crinoid columnals and their accompanying rims exhibit continuous, well-developed twinning.

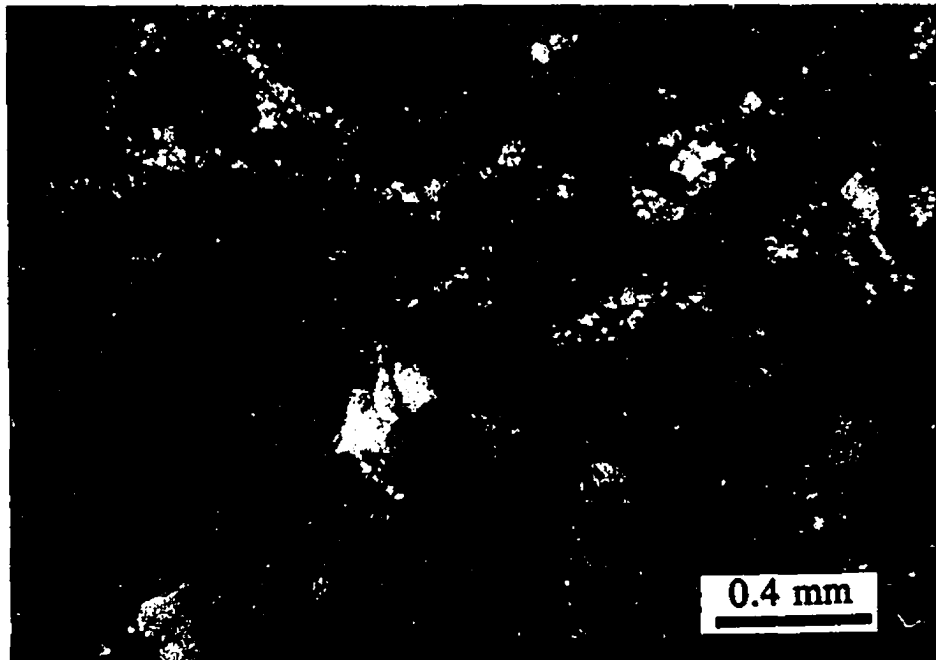


**Plate 2.3.** Echinoderm-bryozoan grainstone facies. Note rhombs of patchy dolomite are only presented in bryozoans.

### **2.5.2 Packstone Facies**

In hand samples, packstones are similar to grainstone. They are grey and brownish grey in colour. Packstones of the Turner Valley Formation consist of calcarenites and calcirudites of echinoderm and bryozoan fragments or dolomite equivalents. Packstones have been strongly dolomitized, with the proportion of dolomite varying between 20 and 80%, which has obliterated the primary matrix texture. Two packstone subfacies are recognized in the Turner Valley Formation: Echinoderm packstone and echinoderm-bryozoan packstone (Plate 2.5). They are similar in grain size and texture, but the difference is the type of skeletal components.

### **2.5.3 Wackestone and Mudstone Facies**

Wackestones and mudstones are discussed together here, because they have several characteristics in common such as their occurrence as discrete units interbedded with packstones, and are vertically and horizontally gradational with each other, and both formed thin to thick beds. The skeletal debris is predominantly crinoids with little bryozoan and other detritus (Plate 2.6). The debris occurs randomly throughout the matrix, although they occur also grouped together on pods and occasionally as discrete layers. Most calcitic wackestones have been highly dolomitized from 50 to 100%. Mudstones usually do not have skeletal fragments, or are very rare if any. Mudstones have almost completely dolomitized.

### **2.5.4 Sabkha Mudstone Facies**

This lithofacies rarely occurs in the Turner Valley Formation of the Quirk Creek field. The rock is composed of uniform grey to dark brown microcrystalline dolomite (Plate 2.7). Primary anhydrite is present in the lithofacies, and has typical chicken-wire texture. In some thin sections, solution breccia structure is observed, probably resulting from the dissolution of primary sulfate. This lithofacies is very thin, usually thinner than 2 meters, and occurs locally in the middle and upper parts of the Turner Valley Formation, and is absent at one (14-12) of the three wells in the Quirk Creek field.



**Plate 2.4.** Oolitic grainstone subfacies and micrite envelope.

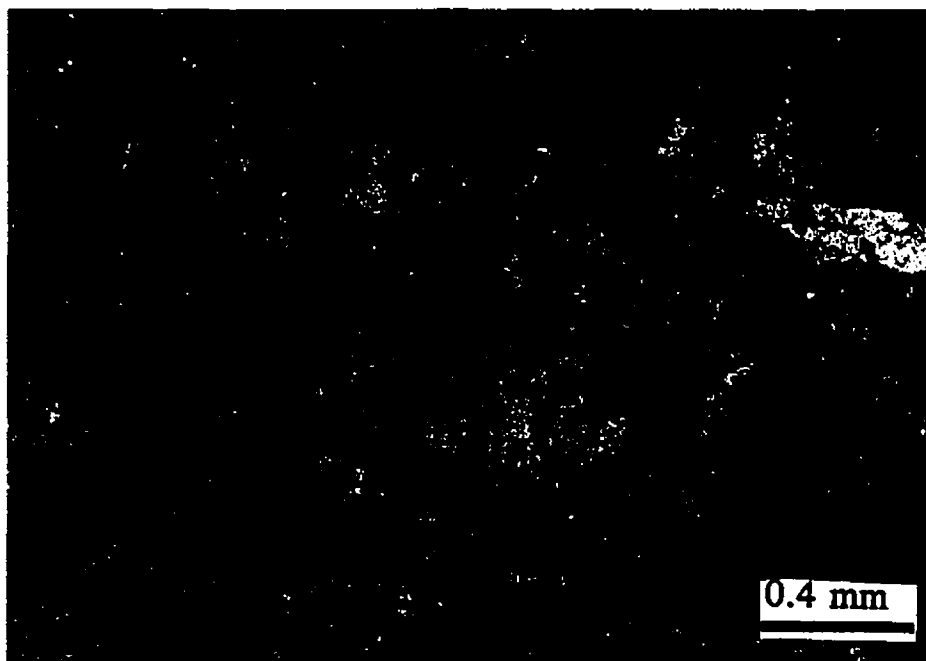


**Plate 2.5.** Packstone facies. Some skeletal grains retains calcite mineralogy, whereas matrix have been dolomitized.



**Plate 2.6.** Wackstone facies. Skeletal crinoids are still calcite mineralogy. Matrix have been completely dolomitized.



**Plate 2.7.** Sabkha mudstone facies. Microdolomite has replaced all precursor micrite. White colour minerals are megaquartz grains.

## **2.6 ENVIRONMENTAL INTERPRETATION**

The abundant normal marine fauna of echinoderms and bryozoans, and cross-bedded skeletal carbonates suggest that they were deposited in a broad, stable, slowly subsiding shallow marine carbonate platform adjacent to the emergent, low relief craton (Bamber et al., 1981). A model showing the relationship between environment, sediment type and rock type is illustrated in **Fig. 2.2** (modified from Bamber et al., 1981). Four general lithologic assemblages, corresponding to environments A to D, are recognized, and several energy levels of sedimentation are indicated. This model can be applied to Turner Valley carbonates in Quirk Creek as follows: (1) Medium- to very coarse-grained, oolitic and skeletal grainstone (environment B)-high energy level, accumulating in barrier shoals and tidal flats close to sea level where wave and current action are the strongest (the base of the Elkton and the base of the "Upper Porous" Member). (2) Fine to coarse grained skeletal grainstones and packstones (environment A)-moderate to high energy level, reworking of debris from echinoderm and bryozoan banks by moderate to strong currents (the upper parts of the Elkton and the "Upper Porous" Member). (3) Wackestones, mudstones, and microcrystalline dolomite with primary sulfate (environment C and D)-low energy level, accumulating within shallow saline lagoon and tidal flats grading to supratidal sabkha. All these environments vertically occur in cycles from high energy to low energy within the sedimentary sequence of the Turner Valley carbonates.

The Elkton member has the most abundant and very coarse skeletal grains of the echinoderm and echinoderm-bryozoan, with minor oolites, suggesting that they were deposited in a shallow shoal (B) within the zone of wave agitation. Some packstones and even wackestones are present in the Elkton member, represent the intervening of relatively low energy (A). The large amount of wackestones and mudstones in the "Middle Dense" member represents deposition in a restricted lagoon and even sabkha environment (from C to D). In the "Upper Porous" member, smaller amounts of coarse grained grainstones and packstones grade upward to larger amounts of wackestones and mudstones, suggesting that the depositional environments became shallow and energy level gradually decreased (from A to C and D).

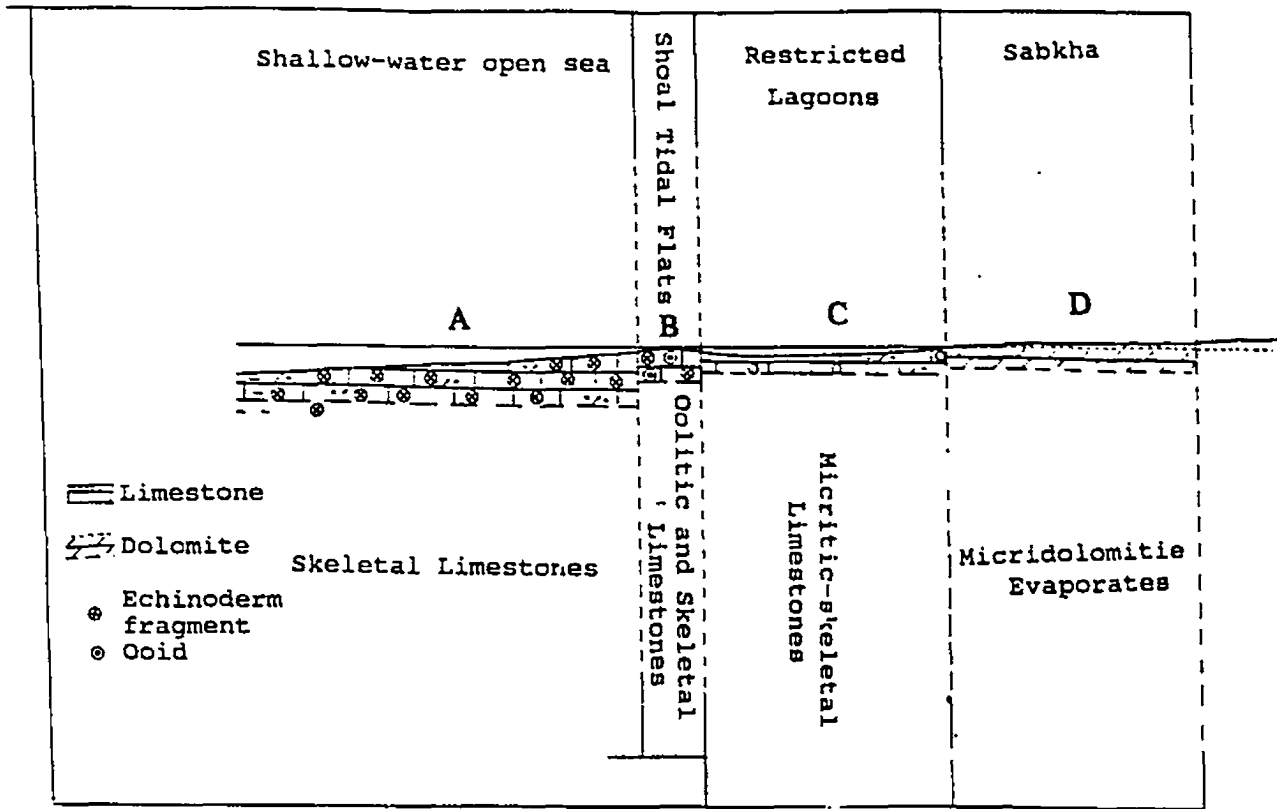


**Fig.2.2.** Diagrammatic interpretation of the Turner Valley depositional environments, southwestern Alberta (modified from Bamber et al., 1981).

# **CHAPTER III**

## **DIAGENESIS AND GEOCHEMISTRY**

### **OF THE TURNER VALLEY FORMATION**

#### **3.1 INTRODUCTION**

The diagenesis of carbonate sediments encompasses all those natural processes which occur and affect the sediments or sedimentary rocks after deposition until the realms of incipient metamorphism at elevated temperature and pressure (Tucker and Wright, 1990). The Turner Valley Formation has a complex diagenetic history with diverse spatially and temporally distributed features. Early diagenetic fabrics have been modified, even obliterated by later diagenetic events; meanwhile, later diagenesis has been affected, and even controlled, by earlier fabrics.

A detailed paragenetic sequence is listed in Table 3.3 (section 3.11). Major diagenetic events including cementation, compaction, silicification, anhydritization and dolomitization, are discussed using petrographic observations and geochemical results, according to the types and temporal order of diagenetic events.

#### **3.2 MICRITIZATION**

This process is one where bioclasts are altered on the seafloor, or just below, by endolithic algae, fungi and bacteria (Tucker et al., 1990). Therefore, it is the initial phase of diagenesis of carbonate sediments occurring while still in the marine environment. The skeletal grains were bored around the margins, and the holes filled with fine-grained sediments or cements. These borings later formed rims or envelopes during diagenesis. When the metastable aragonite or high Mg calcite of skeletal grains came into contact with undersaturated fluids, it was dissolved out with the micritic envelope remaining to define the original shell outline. The molds were filled with sparry calcite cement (Plate 2.4). Micritization is not widely observed in the Turner Valley Formation, only on the periphery of crinoid grains, and also prevented the growth of syntaxial cement on those grains.

### **3.3 COMPACTION**

After deposition of carbonate sediments, various compactional textures and fabrics were developed sooner or later due to the overburden stresses. Compaction processes and products are generally classified into two categories: mechanical (or physical) and chemical compaction. The first begins soon after deposition probably just one meter deep, while the second probably requires several hundred meters of burial (Choquette and James, 1986). There exists abundant evidence that the Turner Valley carbonate sediments underwent strong mechanical and chemical compaction during burial.

#### **3.3.1 Mechanical Compaction**

Mechanical compaction of the Turner Valley carbonate sediments not only resulted in closer grain packing and dewatering, especially in lime muds, but also porosity loss and considerable reduction in sediment thickness, as well as a preferred orientation of elongate bioclasts in grain sediments. It also contributed significantly to the production of fractures and the ductile deformation of grains. Some skeletal fragments broke with fracture surfaces and broken envelopes can be observed (Plate 3.1). Most pressure-welded grains are in direct contact, suggesting no significant cementation before mechanical compaction.

Early fractures developed widely in the Turner Valley Formation, probably resulting from mechanical compaction or/and structural movement. Fractures are usually filled by calcite cement (veins)(Plate 3.2). Generally, the number and size of fractures (veins) decrease with increasing depth possibly due to the brittle property of sediments during shallow burial.

#### **3.3.2 Chemical Compaction**

Chemical compaction is more commonly observed in carbonate sediments of the Turner Valley Formation. Various dissolution textures are present. There are numerous classifications of chemical-compaction fabrics (Wanless, 1979; Buxton and Sibley, 1981; Bathurst, 1987). Three types of pressure dissolution features are identified: (1) fitted fabrics; (2) dissolution seams and (3) stylolites.





**Plate 3.1.** A broken micrite envelope and interpenetration of crinoid grains.



**Plate 3.2.** Vein calcite cement is crosscut by stylolites (filled by black bitumen).

**Fitted Fabrics:** They are observed in grainstone lithofacies. Fitted fabrics were created by the pressure dissolution of grain-grain contact, and resulted in slight saturated to curved to planar contacts between the surfaces of grains. No significant cementation, except syntaxial overgrowth in the matrix, had occurred before the development of fitted fabrics due to the prevention of cements for pressure dissolution (Bathurst, 1987).

**Dissolution Seams:** They are observed in only some wackestones and algal mudstones. They are smooth, undulose seams of insoluble residue without distinctive sutures of stylolite, and they usually pass around grains instead of crosscutting through them (**Plate 3.3**). Dissolution seams possibly formed contemporaneously with fitted fabrics, during the same compaction stage, but distributed in different lithofacies. Both of them were truncated by later stylolite (II), and another similarity is that both of them have a by-product of patchy dolomite, which is restricted to the areas of pressure dissolution (Wanless, 1979). Patchy dolomite is the earliest dolomitization occurring in the burial environment (section 3.7).

**Stylolites:** They are widely distributed in carbonates of the Turner Valley Formation. Stylolites are usually irregular interpenetrating surfaces of two rock units with a sutured contact morphology from quite smooth to jagged to pillar and socket in cross-section. The amplitude of the suture varies from less than 1 mm to decimeters, and is much larger than the diameters of the sediment grains (**Plates 2.5 and 3.2**).

Most stylolites in the Turner Valley carbonates are parallel to or at moderate angles to sedimentary layers, suggesting that stylolites predominately resulted from lithostatic stress (Wanless, 1979) or from the effective stress perpendicular to primary layers. Stylolites are present in any lithofacies from grainstones to mudstones, more commonly between two different lithofacies. The amplitude of stylolite in finer grained lithofacies is smaller than in coarse grained lithofacies. The highest amplitude of stylolite usually occurs in grainstone lithofacies and between grainstone and packstone lithofacies. Two generations of stylolite are observed. Early stylolites (I), with much lower amplitude, were cut through and separated by late stylolites (II) (**Plate 2.5**). Stylolite I is rarely present and is accompanied by patchy dolomite, and probably formed with dissolution seams and

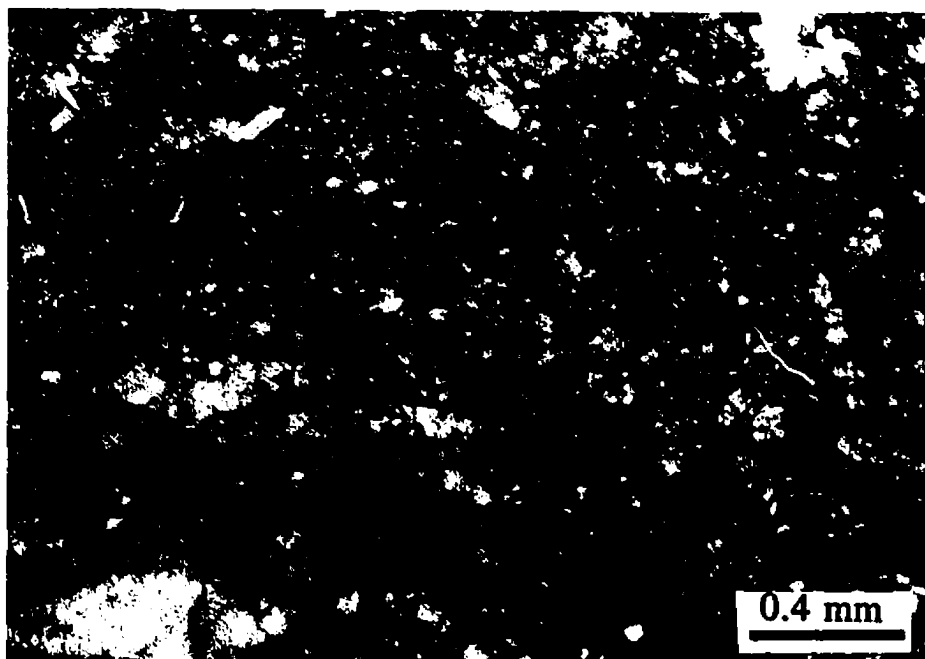


**Plate 3.3.** Dark dissolution seams and accompanying rhombs of patchy dolomite. Coarse grains are calcite skeletal fragments.

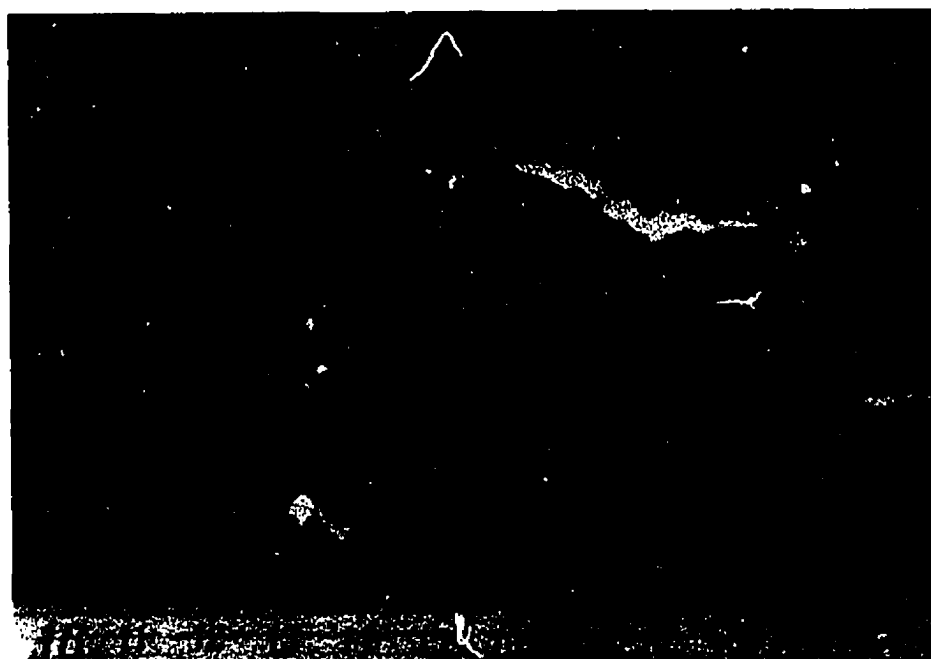


**Plate 3.4.** Core photography of chert nodules and bands. Note the primary laminations are still preserved, and are continuous from chert nodules to mudstone facies. Scale in cm. Core 12-22, depth 1954 m.

fitted fabrics at the same time. Stylolite I and stylolite II transect skeletal grains, sedimentary fabrics and many diagenetic fabrics. Stylolite II crosscuts massive dolomite. Stylolite II is also usually filled with brown-grey, dark insoluble materials (clays?) and organic matter, and is crosscut by megadolomite and late fractures.

### **3.4 CEMENTATION**

Though cementation is a very important diagenetic process, cements in the Turner Valley Formation are not widely distributed, temporally and spatially. Six types of cement were observed in the Turner Valley carbonates from early to late stage: (1) syntaxial overgrowth rim, (2) bladed prismatic calcite cement, (3) blocky calcite cement, (4) equant calcite cement, (5) coarse mosaic calcite spar, and (6) poikilotopic calcite cement. All these calcite cements formed during relatively early diagenetic stages, either in a marine environment or in early burial stages. All of them have been replaced partially by dolomites, diagenetic cherts and anhydrite. All types of cement are non-ferroan and composed entirely of diagenetic low-Mg calcite. Types (1) and (6) are usually observed in calcite grainstones; whereas types (2) to (5) are usually distributed in strongly dolomitized limestones, including microdolomite and massive dolomite.

#### **3.4.1 Syntaxial Overgrowth Rim**

This type of cement is usually a monocrystalline syntaxial overgrowth on echinoderm fragments (Plate 2.2). The syntaxial overgrowth rim and its host grain have a unit extinction. Rim crystals tend to be large and poikilotopically engulf surrounding grains. This type of cement is predominately developed on crinoid grains and also on other skeletal grains (e.g., bryozoans), but does not occur around those grains displaying peripheral micrite rims (envelopes). Well-developed cleavage planes and twin zones are of optical continuity from host grains to rim cement. The presence of syntaxial overgrowth rims prevented mechanical compaction.

#### **3.4.2 Vein Calcite Cement**

Volumetrically, vein calcite cement is the most abundant cement type in the Turner

Valley Formation. It is a characteristic fracture-filling cement (Plate 3.2), where the fractures probably developed as a result of early compaction and/or structural stress due to basin sedimentary tilting and rising (Mundy et al., 1992). These fractures are now filled with calcite crystals, forming veins. Vein cement consists entirely of non-ferroan, equant calcite, and has a typical drusy fabric of increasing crystal size towards the center of the pore (Plate 3.2). Most calcite veins usually occur in strongly dolomitized carbonates and are absent in limestones. Stratigraphically, they are usually present in the upper parts of the formation, decreasing in abundance with increasing depth.

#### **3.4.3 Bladed Prismatic Calcite**

This type of cement consists of medium, elongate, scalenohedral crystals, observed growing directly on carbonate groundmass (e.g., microdolomite crystals) in cavities. Calcite crystals have various sizes, varying from 50 to 300  $\mu\text{m}$  long with prismatic terminations. Bladed prismatic calcite crystals are succeeded by coarse calcite spar toward the center of the cavity. Such calcite could be an early burial cement (Choquette and James, 1987); some workers have proposed that its origin is associated with the mixing zone of freshwater and seawater (e.g., Saller, 1985).

#### **3.4.4 Blocky Calcite Cement**

This cement has crystals of about 0.5 to 1 mm in size. It usually fills the pores left by the dissolution of skeletal grains in strongly dolomitized wackestones and packstones. Its crystals are usually clean and inclusion-free; euhedral pyrite crystals are often present around the cement. Blocky calcite cement is crosscut by equant calcite cement veins.

#### **3.4.5 Coarse Calcite Spar**

This type of cement usually consists of coarse, plane-sided equant crystals ranging from 0.5 to 3 mm in size. Coarse calcite spar usually succeeds bladed prismatic calcite cement in the cavities of microdolomite and dolomitized packstones or grainstones with a mosaic texture. It shows a drusy texture of increasing crystal size toward the center of the cavity.

### **3.4.6 Poikilotopic Calcite Cement**

This type of cement occurs in grainstone and packstone facies. It is composed of coarse crystals, up to a few mm in diameter, and usually engulfs several skeletal grains. It has tightly cemented skeletal grains and their fragments. This type of cement probably formed after syntaxial rim cement, and simultaneously with equant calcite and coarse mosaic spar cements. Its presence might have prevented some later diagenetic events because well-developed poikilotopic calcite cement in grainstones and oolites, anhydrite and dolomite are rarely present.

## **3.5 SILICIFICATION**

Multiple stages of silicification occur widely in carbonates of the Turner Valley Formation, though small in volume. Cherts are present as nodules, irregular masses, elongate parallel to bedding and as nodule bands parallel to bedding with various thickness (Plate 3.4). Silicification occurs as both cementation and replacement from mudstone facies to grainstone facies.

### **3.5.1 Petrography of Silicification**

Four petrographic types of chert have been identified: (1) length-slow chalcedony, (2) megaquartz, (3) microquartz, and (4) length-fast chalcedony and macroquartz.

#### **Length-slow Chalcedony**

Length-slow chalcedony is present as a fibrous fabric. Bundles of fibres (or quartz crystals) commonly grew radiating from a single point or crystal. This fabric occurs in chert nodules replacing primary evaporites (anhydrite), and coexists with megaquartz. Length-slow chalcedony has been used as evidence of "vanished evaporites" (e.g., Folk and Pittman, 1971). In the Turner Valley Formation, primary evaporites (e.g., anhydrite) are present, only partially replaced by cherts.

#### **Megaquartz**

This type of silica usually occurs in the voids of algal mudstone-microcrystalline

dolomite (Plate 3.5). Its crystal size ranges from 0.2 to 2 mm and most crystals are around 0.5 mm. Single megaquartz crystals often show uniform extinction with euhedral termination. Megaquartz has a replacive origin, usually occurring along the boundaries between microdolomite and primary anhydrite (or poikilotopic calcite cement), and replaces anhydrite and calcite cement. It always contains anhydrite and/or calcite inclusions. Some crystals of megaquartz were dissolved later, but the pores still retain their molds.

### **Microquartz**

Volumetrically, microquartz is the most abundant type of chert in the Turner Valley Formation. It occurs most commonly in beds of packstones and grainstones as a variety of grey, brown, or white nodules, lenses, and stringes. In some thin sections, microquartz crystals present tightly together in nodules and parallel to the sedimentary bedding, providing the rocks with a distinctive banded appearance.

Microquartz consists of equant, anhedral microcrystals (5-20  $\mu\text{m}$ ) with undolose extinction. Although it occurs mostly as a replacement of bioclasts, it is also occasionally present as a replacement of fine matrix. Sometimes, microquartz occurs as isopachous rims of megaquartz (Plate 3.5), and often grades to length-fast chalcedony. Microquartz has a typical replacive fabric. It usually partially and selectively replaces skeletal fragments, whereas the primary sedimentary fabrics, such as cross-bedding, fine laminations and even the internal skeletal textures, are fairly well preserved (Plate 3.6). Patchy rhombic dolomite is often floating in chert nodules as a relict of chert replacement, suggesting patchy dolomite formed before microquartz. However, microquartz was replaced or/and crosscut by massive dolomite (Plate 3.7).

### **Length-fast Chalcedony and Macroquartz**

Length-fast chalcedony is also one of fibrous fabrics. This type of chert usually coexists with microquartz, but is present as a cement in cavities. It often occurs as well-arranged spherulitic structures of length-fast fabrics (usually 0.1-0.3 mm in length), perpendicular

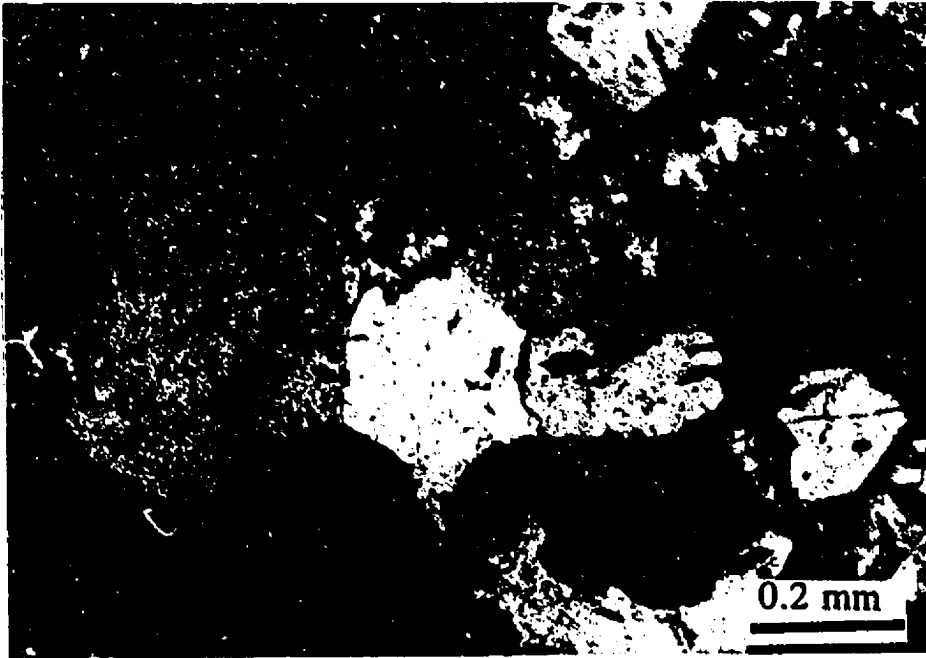


**Plate 3.5.** Megaquartz (grey) replaces coarse calcite spars (dark red) and microdolomite (fine grains). Note microquartz crystals are growing around megaquartz crystals.

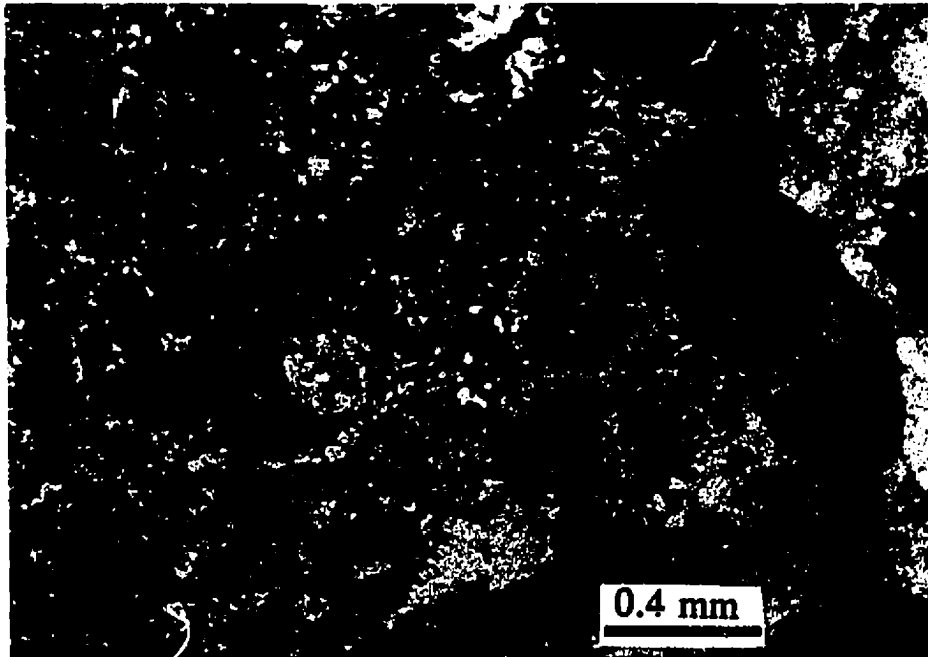


**Plate 3.6.** Microquartz replaces skeletal grains. The internal textures of grains are still partially preserved. A stylolite goes around the chert nodule.



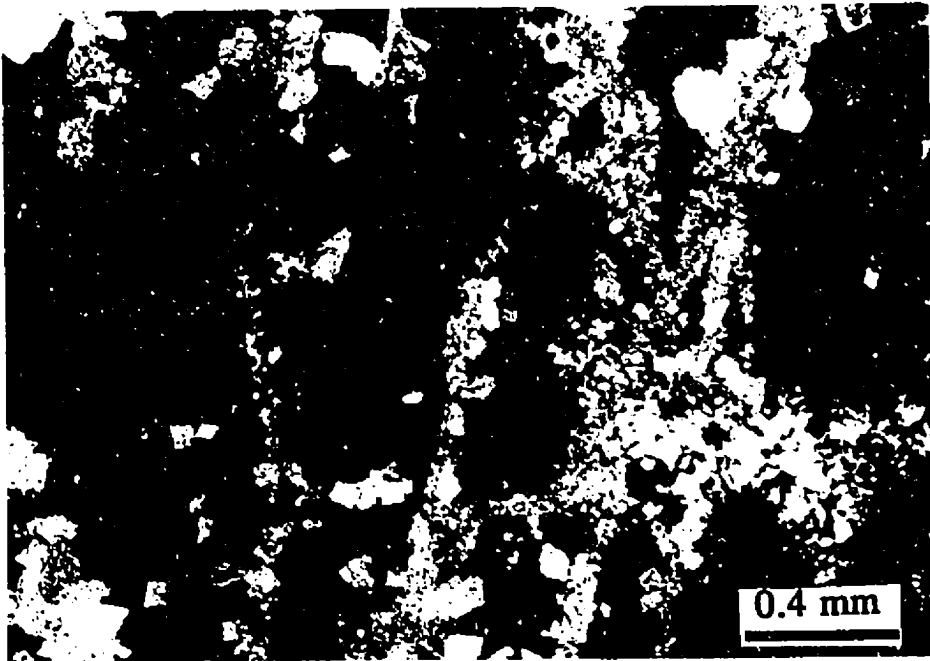


**Plate 3.7.** Massive dolomite replaces and crosscuts microquartz.

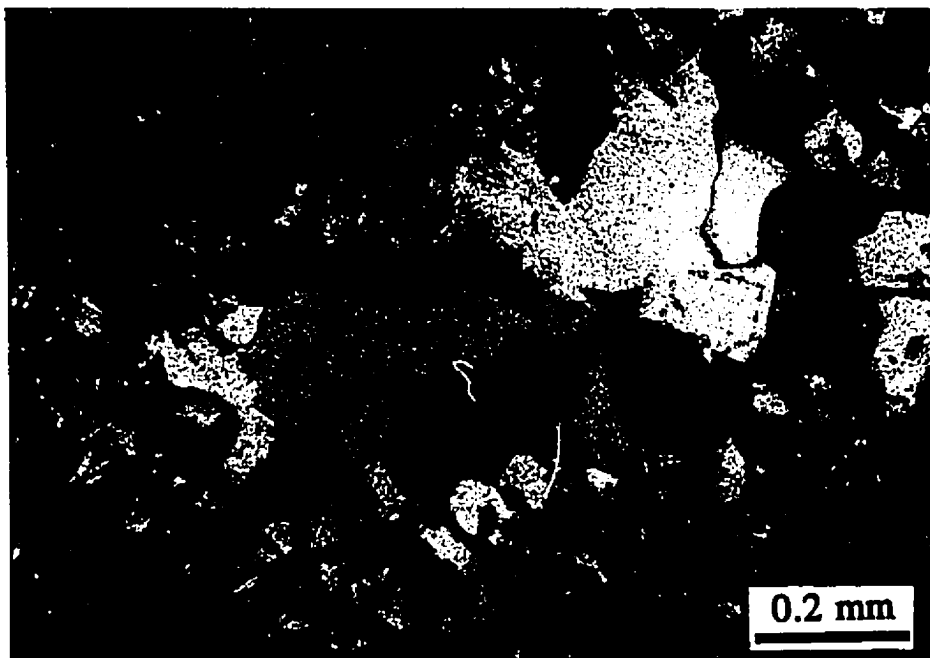


**Plate 3.8.** Length-fast chalcedony (at the rims of cavity) and macroquartz (center), and microquartz (massground).

to cavity walls. Bundles of fabrics commonly radiate from a single point of the substrate from which they grew (Plate 3.8). They often consist of consecutive layers in one single cavity, where the boundary between the layers is usually sharp and marked by a thin black band under crossed-nicols. From the characteristics above, it is obvious that the radiating pattern of chalcedony typically occurs as a void-filling cement, since it is never as pseudomorphic skeletal grains and calcite cements, never interrupts carbonate fabrics, and never contains undigested carbonate inclusions.

Macroquartz is rare, but occurs as both a replacement of skeletal grains and a cement, either coexists with microquartz or with length-fast chalcedony. Macroquartz exhibits equant, anhedral crystals varying from 0.05 - 0.2 mm.

### **3.5.2 Source of Silica**

The source of silica nodules is often explained by the redistribution of biogenic silica, which is contained in carbonate sediments, during diagenesis. Sponge spicules are a widely quoted source of silica (e.g., Meyers, 1977). However, sponge spicules have not been seen in thin sections in the Turner Valley carbonates, or are very rare if any. Therefore, this source for silica is unlikely. One possible silica source was attributed to the post-Mississippian unconformity. The unconformity may act as a feeder for silica fluids. Knauth (1979) suggested that meteoric water percolated and leached a considerable thickness of unlithified source sediment which may be devoid of any silica. Moreover, the distribution of chert in the Turner Valley Formation shows an increase upward, and the overlying strata, including the Mount Head and Etherington Formations, have much more silica impurities in carbonates (Ng and Jones, 1989). Hence the Banff and Pekisko Formations could not be the source of silica, though they have silica-rich nodules. Another alternative source of silica from the dissolution of detrital silica is possible. Detrital silica is seen in the Turner Valley Formation. It usually occurs in fine grained packstones and mudstones, up to 5% locally, but is less prominent in grainstones. Detrital silica has been observed along late stylolites, probably as the evidence of pressure dissolution. Most detrital silica has etched outlines.

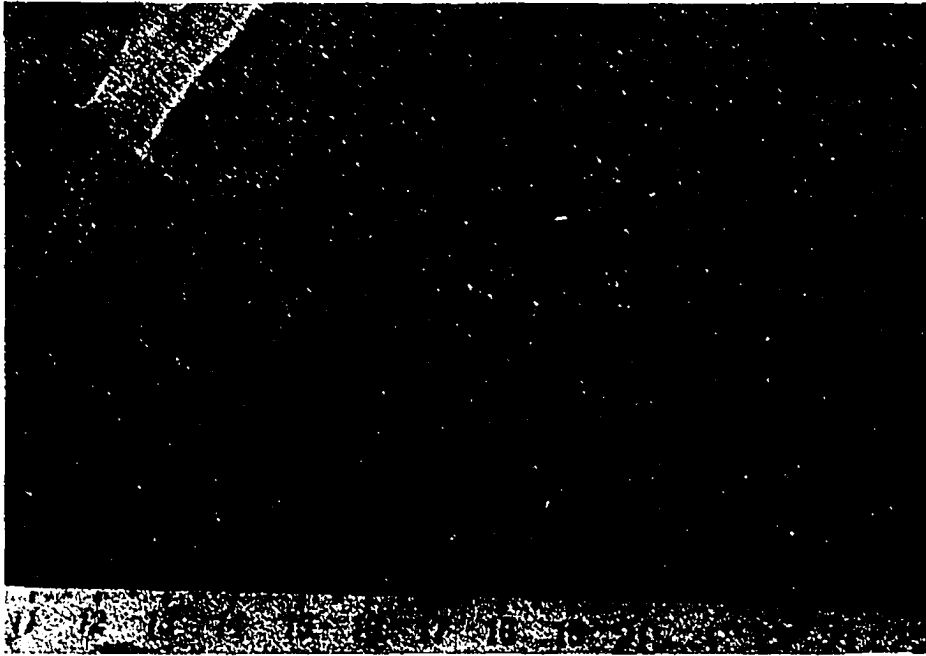


**Plate 3.9.** Core photography of dark microdolomite and white, primary anhydrite. scale in cm. Core 12-22, 1905 m.

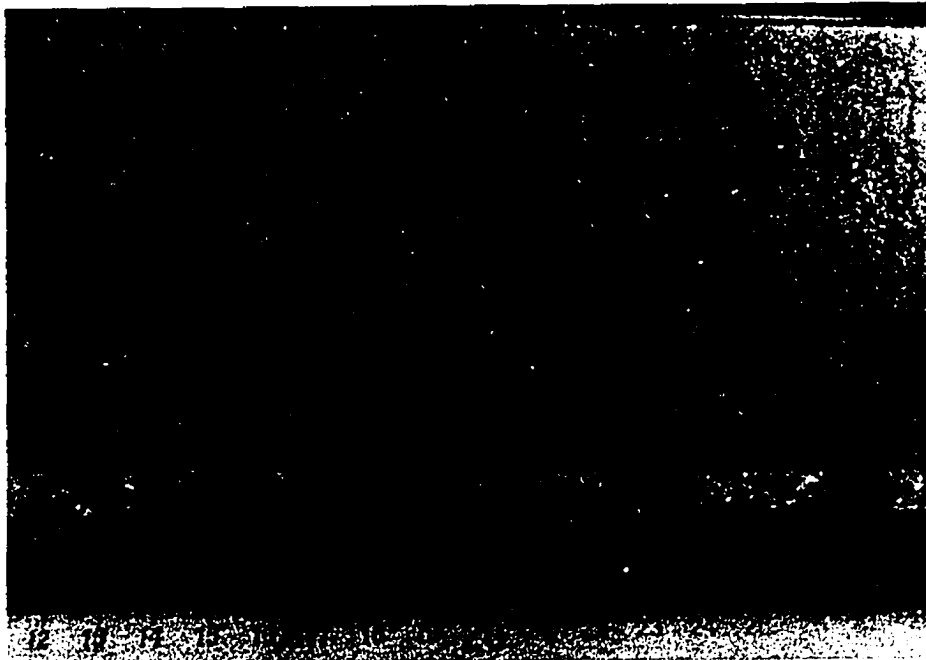


**Plate 3.10.** Core photography of burial anhydrite nodules are distributed along fractures. Scale in cm. Core 6-7, depth 2011 m.

### **3.5.3 Timing of Silicification**

It is difficult to date the silicification in the Turner Valley Formation with the limited information. However, a lot of petrographic evidence indicates that silicification occurred relatively early in the diagenetic history of the carbonate sediments. Megaquartz and length-slow chalcedony formed at an early stage of diagenesis, because they usually coexist with microdolomite in sabkha lithofacies, and replace primary anhydrite and early calcite cement. Megaquartz also acted as a nuclei for microquartz, microquartz grew around the crystals of megaquartz. In addition, both of these were replaced by pervasive matrix dolomite. Microquartz is usually present in skeletal carbonate as both a replacement and a cement. Careful observations indicate that microquartz does not obliterate preexisting carbonate depositional or diagenetic features. Chertification in fact freezes certain fabrics of carbonate depositional and diagenetic features, such as internal skeletal textures, calcite cementation and compaction, thereby preserving these features from further modification by late diagenetic events (Meyers, 1977). Mechanical compaction is a common phenomenon in the Turner Valley carbonates as discussed earlier in this chapter, but intense compaction is rarely seen in silicified skeletal carbonates. However, there is also some degree of compaction such as orientation of elongated skeletal grains and grain interpenetration. Furthermore, stylolites are common in the Turner Valley Formation, but were rarely developed within chertified skeletal carbonates, whereas they are relatively common outside chert nodules rather than crosscut the nodules. In addition, pervasive matrix dolomite crosscuts through and/or replaces microquartz. However, patchy dolomite, resulting from early compaction, often floats inside chert nodules or layers with etched rims (outlines), possibly was modified during selective silicification. Therefore, all these features prove that cherts occurred after early compaction, patchy dolomite before intense compaction, massive dolomite.

### **3.6 ANHYDRITIZATION**

Anhydritization is one of the important diagenetic processes in the Turner Valley Formation in spite of the fact that less attention has been devoted to it in previous studies. Anhydritization has been found in all carbonate lithofacies of the Turner Valley

Formation. There are two generations of anhydrite: primary anhydrite and secondary anhydrite. The primary anhydrite is small in volume and occurs locally, whereas secondary anhydrite has a much larger volume and a relatively wide distribution, and formed much later during burial diagenesis.

### **3.6.1 Primary Anhydritization**

Primary anhydrite here means that anhydrite precipitated in a sedimentary basin with carbonate sediments. Although it is possible that the primary sulfate was gypsum which was transformed to anhydrite during increasing burial, the origin of sulfate (gypsum or anhydrite) resulted from primary deposition. Primary anhydrite occurs in the "Middle Dense" member and the "Upper Porous" member of the formation. It often consists of fine, anhedral anhydrite, occurring as nodules, or filling the voids in microdolomite (Plate 3.9). Some anhydrite crystals are in the shape of laths, probably preserved the shape of the replaced gypsum, but most of them have a fine, elongate shape. Fine-grained anhydrite has a typical "chicken-wire" texture (Tucker et al., 1990). Megaquartz and/or poikilotopic calcite cement usually occupy the boundary between primary anhydrite and microdolomite, the former two replace and include the latter two.

### **3.6.2 Secondary Anhydrite**

Secondary anhydrite is a diagenetic product, precipitated after the sediments were buried, and is also called burial anhydrite in this study. Secondary anhydrite is much more important and occurs widely compared with primary anhydrite. It occurs as both nodules and scattered replacements (Plate 3.10). It appears milk-white in hand specimens. Crystals are of various sizes from fine lenses to coarse laths (up to 1 mm). Scattered anhydrite occludes voids, occupies the space between pervasive matrix dolomite, or replaces early calcite cements and skeletal fragments. Nodules usually distribute along fracture II (Plate 3.11). The boundaries between anhydrite nodules and carbonate hosts are either sharp or gradational. Anhydrite nodules have some similarities to sabkha nodules described by some workers (e.g., Buller, 1969). However, the burial anhydrite nodules of the Turner Valley Formation have much different characteristics

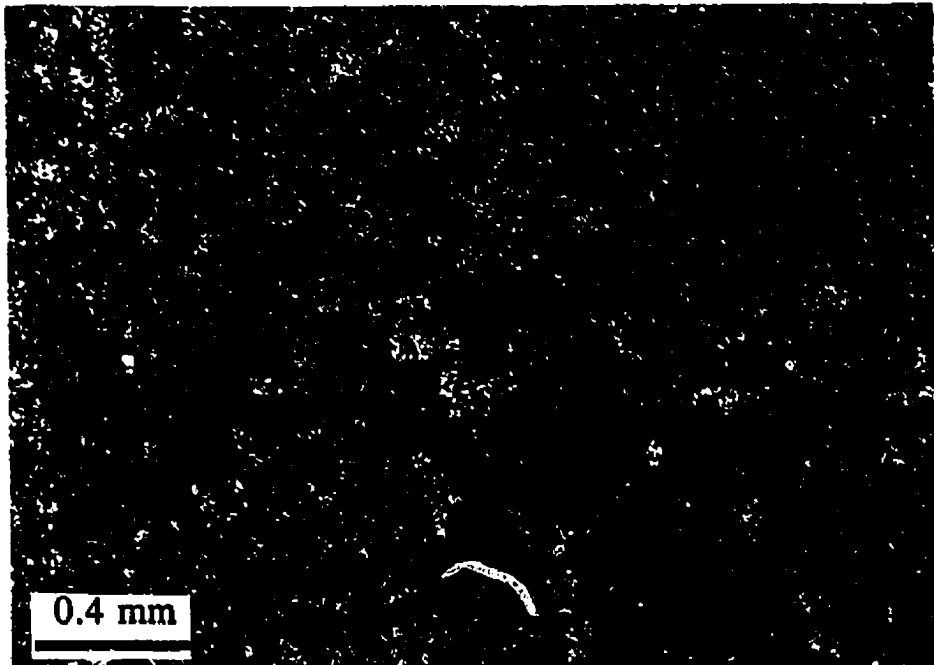


**Plate 3.11.** Crystals of burial anhydrite are distributed along fractures. Note massive dolomite replaces and crosscuts the anhydrite vein.



**Plate 3.12.** Back-scattered electron micrography shows euhedral crystals (rhombs) of microdolomite (right). The grey, coarse grained grains are detrital quartz (left).

which reflect a burial origin: (1) they occur in different carbonate facies from mudstone, wackestone to packstone and grainstone, (2) they replaced host limestone, calcite cements, and even patchy dolomite, (3) they often distribute along fractures and stylolites. From these features, secondary anhydrite could be distinguished from primary anhydrite.

### **3.6.3 Source and Timing of Secondary Anhydrite**

The Mississippian succession was deposited in shallowing-up marine environments varying from normal marine to restricted lagoon to sabkha facies as discussed in chapter II. Although primary anhydrite is very rare in the Turner Valley Formation, the overlying Mount Head Formation has abundant primary sulfate which provides the possibility for a lot of late-diagenetic brines to develop. This is evident especially along the post-Mississippian disconformity, where there was a recharge of meteoric water, which percolated and leached ancient rocks including evaporates of the Mount Head Formation, the fluids flowed down through fractures or other permeable channels.

Although it is not easy to date the time of burial anhydritization, the petrographic study can provide some useful information. Much anhydrite was observed to have not only replaced skeletal grains, and calcite cements, but also to crosscut early compactional features (e.g., fitted fabrics) and filled fracture II. In addition, burial anhydrite usually coexists with pervasive matrix dolomite, and there is a positive correlation of anhydrite abundance related to massive dolomite, either in partially dolomitized grainstones or in completely dolomitized mudstones. On the one hand, anhydrite was replaced or crosscut by massive dolomite; on the other hand, patchy dolomite and even pervasive matrix dolomite rims are found corroded and modified by anhydrite. Meanwhile, anhydrite filled stylolite II. Hence, burial anhydrite possibly formed in two major stages-predated and postdated massive dolomite, with the same crystal size and texture. In addition, anhydrite was also crosscut and replaced by megadolomite and moldic dolomite or as their inclusions. Moreover, burial anhydrite and matrix dolomite have similar  $^{87}\text{Sr}/^{86}\text{Sr}$  values. All these features prove that anhydrite precipitated in relatively late diagenetic stages, probably after patchy dolomite and before coarse dolomitization.

### **3.7 DOLOMITIZATION**

#### **3.7.1 Petrography**

Dolomitization is the most important diagenetic process during the diagenetic history of the Turner Valley Formation. Almost all limestones in three cores of the study area are partially to completely dolomitized. Since dolomitization has usually resulted in higher porosity and permeability than undolomitized limestone, prolific hydrocarbon reservoirs are related to dolomitized carbonates in the Turner Valley carbonates. Hence, an investigation of the cause and distribution of dolomitization has not only academic but also economic significance. This part presents a detailed petrographic description of dolomitization in the Turner Valley Formation. The classification of dolomite described here is based on the texture, abundance, distribution and geochemistry of dolomite. Four types (or generations) of dolomite have been identified: microdolomite, patchy dolomite, pervasive matrix dolomite, and megadolomite. Though all types of dolomite are described as having formed in different geological times, the replacement and formation of dolomite were probably more of a continuum and overlapping. Each type of dolomite has its own limestone replacive precursor, and early dolomites have been modified by relatively late dolomitization.

#### **Microdolomite**

Microdolomite consists of subhedral to euhedral crystals of mosaic texture. Its crystals are very small varying from 4 to 10  $\mu\text{m}$  in size (Plate 3.12). Microdolomite usually shows a grey, brown, and even dark colour, and exhibits dull colour under cathodoluminescence. Under SEM microdolomite crystals show euhedral rhombs, while some crystals have developed stepped crystal surfaces, whereas the relatively coarser dolomite grains (10-50  $\mu\text{m}$ ) disseminated in microdolomite are characterized by one or two fluorescence syntaxial overgrowth rims. They may have resulted from the recrystallization and overgrowth of microdolomite crystals, and they are called enlarged grains here (Plate 3.13). The rims and their host crystals are in optical continuity. Some enlarged grains are homogeneous under light microscopes, but their cloudy cores and clear rims were revealed under fluorescence. If two rims are present, the internal rim is



clear whereas the external rim is usually cloudy. The shape of enlarged grains depends on the shape of core crystals. If the core crystals are rhombs, the enlarged grains are also rhombs. Some rims are not symmetric in some cases, and even only partially developed. In addition, coarse burial calcite spar in microdolomite usually engulfs some microcrystals as inclusions, whereas the microdolomite with rims (enlarged grains) clearly replaces and crosscuts the calcite cement, suggesting the rims formed after calcite cementation. Microdolomite occurs only in sabkha lithofacies, where no skeletal grains were found, and only some algae were present. Microdolomite usually coexists with primary anhydrite, which has a typical chicken-wire texture. This lithofacies is very thin (usually < 2 m), interbedded with wackestones in the middle and upper parts of Turner Valley Formation, and absent at one of three wells in Quirk Creek (14-12). Both microdolomite and primary anhydrite have relatively low  $^{87}\text{Sr}/^{86}\text{Sr}$  (0.7077) values, which are similar to that of Mississippian seawater (0.7076) (Burke et al., 1982). Therefore, microdolomite may have formed penecontemporaneously in a sabkha environment.

### **Patchy Dolomite**

Patchy dolomite is widespread throughout the formation, but small in volume (5-15%). Patchy dolomite is easily observed in slightly dolomitized grainstone facies and packstone facies. It is often disseminated between skeletal grains and in the centers of grains as floating single-rhomb patches (Plate 2.2 and Plate 2.3), whereas local concentrations of dolomite crystals along fractures, compaction fabrics, and/ or in a fine matrix between grains also exhibit larger multiple-crystal patches with subhedral to euhedral mosaic texture. Dolomite crystals have a wide range in size from 20  $\mu\text{m}$  to 200  $\mu\text{m}$ , usually about 50  $\mu\text{m}$ . Patchy dolomite is clear, non-ferroan with a dull cathodoluminescence colour. It also exhibits two to three layers of syntaxial overgrowth in some crystals (Plate 3.14). Like microdolomite, if two rims are present on one crystal, the internal rim is clear, and the external rim is cloudy. If three rims are present, the innermost and outermost rims are clear, whereas the middle one is cloudy. Some patchy dolomite crystals exhibit only one clear-rim and cloud-center under fluorescent microscope. All

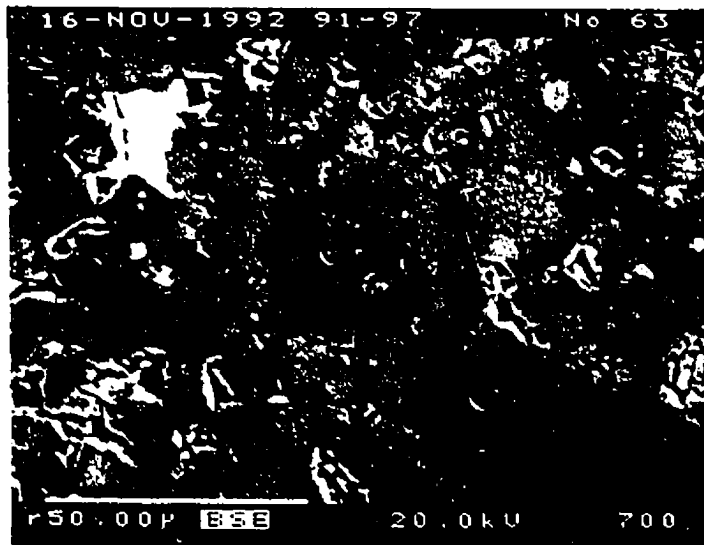


**Plate 3.13.** Back-scattered electron micrography displays that a enlarged-grain (center) has a cloudy center and a clear rim. Note microporosity has been developed inside crystals of microdolomite.

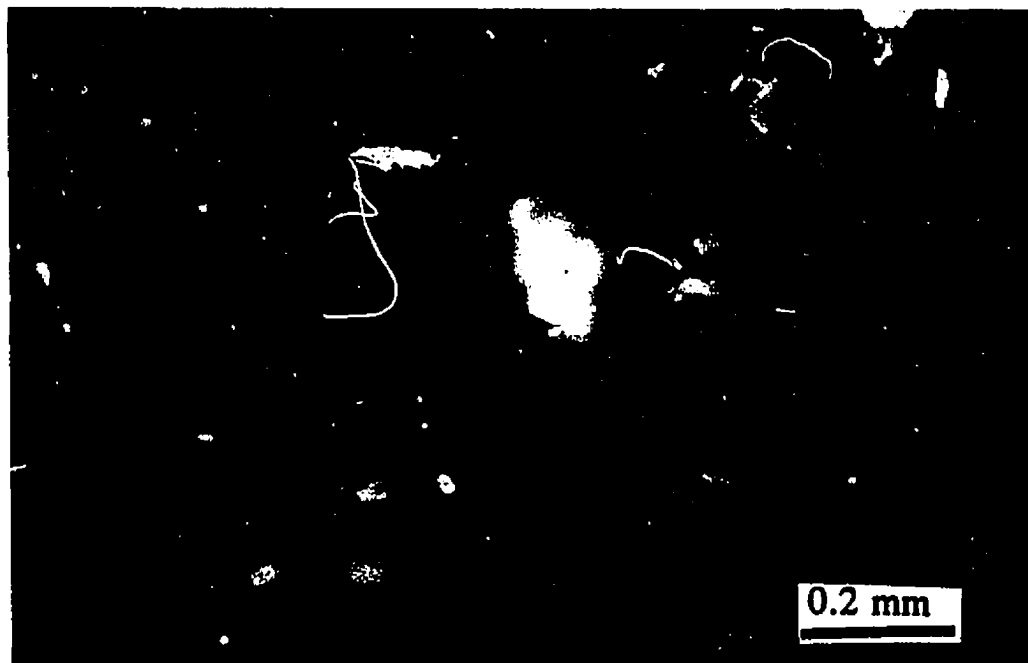


**Plate 3.14.** Overgrowth rims of patchy dolomite are seen under fluorescence.

these rims represent that patchy dolomite underwent the processes of crystal-enlargement during the later stages of dolomitization. Patchy dolomite is often observed to occur along fitted fabrics, dissolution seams and stylolite I, and also crosscuts stylolite I. In addition, patchy dolomite was engulfed and corroded by microquartz and burial anhydrite. Therefore, from the features discussed above, patchy dolomite could have been formed during relatively early chemical-compaction.

### **Pervasive Matrix (Massive) Dolomite**

Pervasive matrix dolomite is the most abundant type of dolomite (80% in volume). It consists of anhedral to euhedral, porous and dense mosaic textures (**Plate 2.6** and **Plate 3.15**). Porous, pervasive, massive dolomite has the highest intercrystalline and moldic porosity. Matrix dolomite is destructive and has strongly modified or obliterated earlier diagenetic fabrics, and dolomitized not only relatively fine matrix but also skeletal grains. Matrix dolomite has a wide range in size from 20 to 300  $\mu\text{m}$  enlarging from fine- to coarse-grained facies. Pervasive matrix dolomite is non-ferroan and has brown to dull cathodoluminescence colour without fine zonation. Some crystals have clear rims of fluorescence. Most crystals are clear, limpid rhombs. Pervasive dolomite occurs in every lithofacies, usually dolomitizing limestones with various proportion of dolomite from 20% to 100%. In mudstone and wackestone lithofacies, the proportion of dolomite is usually higher (80-100%). In packstones and grainstones, most limestones have been dolomitized from 20 to 80%, some have been 100% dolomitized, especially in well 14-12. In completely dolomitized limestones, the previous sedimentary and diagenetic fabrics have been obliterated. However, the ghosts of skeletal grains (e.g., crinoids) can still be observed in some thin sections under fluorescence microscope. Burial anhydrite usually coexists with massive dolomite, replaced calcite cements, skeletal grains; and even engulfed massive dolomite, while massive dolomite also crosscuts anhydrite. Pervasive matrix dolomite replaced all calcite cements and cherts, but was crosscut by stylolite II, which is partially filled by bitumen, anhydrite, and was also replaced by megadolomite.

### **Megadolomite**

Megadolomite consists of very coarse rhombic dolomite and anhedral, coarse crystals of dolomite (Plate 3.16). Coarse, euhedral rhombs have an average size of 1 mm, ranging from 0.3 to 3 mm. Coarse rhombs usually occur in voids and as patches in matrix dolomite similar to patchy dolomite occurs in skeletal limestones (see patchy dolomite). Anhedral crystals of dolomite are the completely dolomitized crinoids. Crinoids were dolomitized as single crystal dolomite, the shape and size of the crinoid is still preserved, but partially stepped crystal surfaces have been developed. Coarse rhombic dolomite and anhedral crystals of dolomite are usually present together with small volume (<5 %). Both of them have relatively small dolomite inclusions and crosscut stylolite II, and occur mainly in massive dolomitized packstones and grainstones. Megadolomite is non-ferroan and have a brown CL colour, and some coarse rhombs close to voids have a bright orange colour. Megadolomite obviously formed in the late burial stage because they replaced massive dolomite and crosscut stylolite II.

#### **3.7.2 Spatial Distribution of Dolomite**

The proportion of dolomite in Turner Valley carbonates changes vertically and laterally. An increase in dolomite proportion horizontally from west to east towards the paleocoast was noted by Stein (1977). A decrease in dolomite proportion with increasing depth is observed from the observation and evaluation of cores and of thin sections in this study.

### **3.8 FRACTURING**

Various fractures are observed in the Turner Valley carbonates. Three generations of fracture are identified. Fracture I is fine in scale with a width varying from 0.5 to 3 mm, and extends no longer than 30 mm. Fracture I is usually at a vertical orientation to bedding, completely sealed by calcite cement as calcite veins (Plate 3.2). Fracture I (or veins) has been transected by late stylolite and disappeared in pervasive matrix dolomite. Fracture II is relatively wider than fracture I. It is often oblique to bedding at some degrees. Fracture II is filled partially by burial anhydrite (Plate 3.11). Fracture III has various widths and lengths, in general, wider and much longer than fracture I and

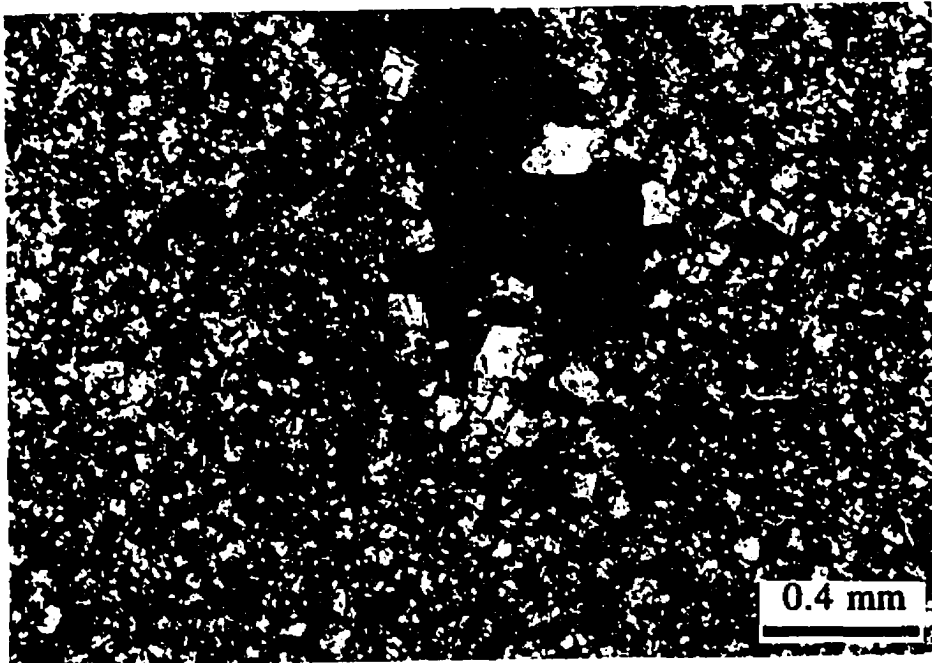


**Plate 3.15.** Massive dolomite with subhedral to euhedral crystals. Note crystals protruding into pores are cleaner and larger than the interlocking crystals of massground. Perfect vuggy and intercrystalline porosities are presented.

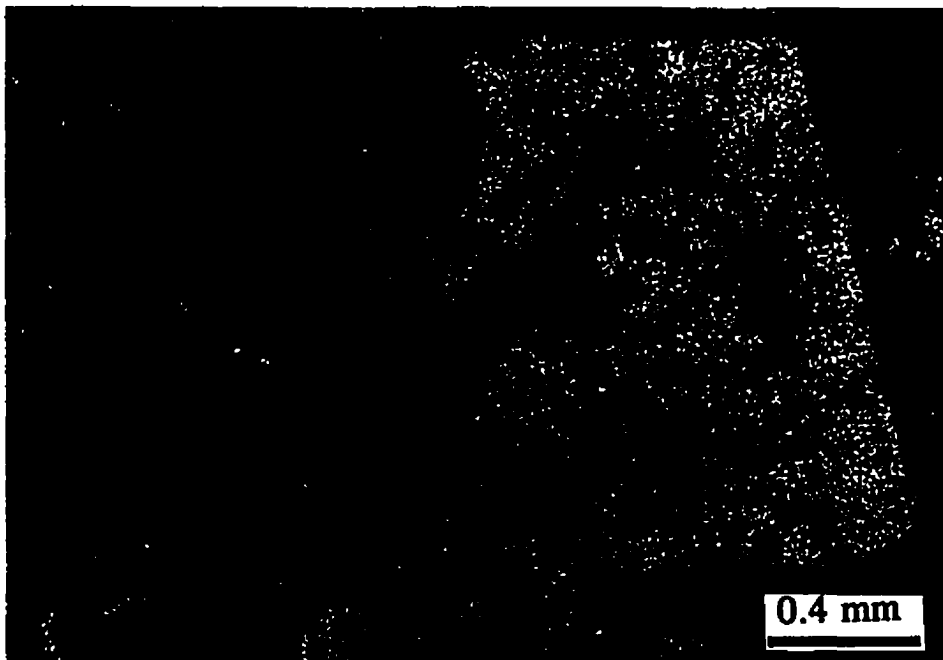


**Plate 3.16.** Megadolomite replaces burial anhydrite (red ones).

fracture II. It also has various relations with bedding from parallel, inclined to perpendicular. Fracture III has not been filled by anything. It transects stylolite II and megadolomite.

The development of fractures in the Turner Valley Formation occurred in different diagenetic stages. Based on petrographic relationships and paragenetic sequence, fracture I was probably caused by early compaction or basin tilting (Mundy et al., 1992). Fracture II might have resulted from later compaction or the basin tilting and rising, and probably formed with massive dolomite. Fracture III formed in a very late stage, probably with the formation of folding and faulting in late Cretaceous.

Although quantitatively unimportant in the Turner Valley Formation, fractures have possibly influenced the development of the reservoir in two ways. The first is to act as channels to transport various fluids, which increase the permeability considerably; and the second is to act directly as a trap for hydrocarbons (Stein, 1977).

### **3.9 DISSOLUTION**

Widespread dissolution is observed in the Turner Valley carbonates. The dissolved materials are usually CaCO<sub>3</sub> components. They were aragonite, high Mg calcite as skeletal grains, matrix and calcite cements in the Turner Valley carbonates. During late stages of diagenesis, Calcitic components became undersaturated relative to diagenetic fluids (e.g., dolomitization fluids) which are only saturated with dolomite or/and anhydrite. Dissolution probably occurred in three different stages. The first probably occurred in the early burial environment where some skeletal fragments consisting of metastable carbonate minerals were dissolved and then filled by calcite cements. The second probably occurred early or/and during pervasive matrix dolomitization due to the intervening of enormous amounts of dolomitization fluids (Pate 3.15). The last stage of dissolution occurred very late, not only were calcite components and burial anhydrite dissolved, but also some dolomites were partially dissolved.

### **3.10 GEOCHEMISTRY OF THE TURNER VALLEY FORMATION**

In conjunction with petrographic studies, geochemical techniques were utilized to

further constraint diagenetic environments of the Turner Valley carbonates. These techniques are: (1) all thin sections were stained as discussed in chapter I to distinguish dolomite from calcite, and identify rocks with or without ferroan dolomite and calcite; (2) selected thin sections were studied for fluid inclusions; (3) all thin sections were examined under cathodoluminescence (CL) and fluorescence devices to look for any fabric and compositional variations; (4) various types of dolomite and calcite cements were chemically analyzed for major, minor and trace elements and isotopes, and the electron microprobe was employed to selectively analyze major and minor elements of different types of dolomite. Stained thin sections show that colourless dolomite is easily distinguished from pink to red colour-stained calcite; however, neither ferroan dolomite nor ferroan calcite has been observed in any thin section. Perhaps, calcite and dolomite components were formed either in surface oxidizing conditions or in deep burial reducing environments, no abundant Fe component is present, perhaps the fluids for whole diagenesis of the Turner Valley Formation are Fe-depleted, and perhaps all diagenetic fluids have similar sources. They are discussed in details in following parts.

### **3.10.1 Fluid Inclusions**

Fluid inclusions have been widely used in geology, particularly in igneous, metamorphic and economic geologic studies, where temperature of formation and fluid composition are usually of importance, but have only recently been used in carbonate diagenetic studies. Calcite cements, dolomite cements and replacive dolomites often entrap inclusions of fluids (from which the crystals precipitated) at lattice defects or irregularities. This type of fluid inclusion is called a primary fluid inclusion. Secondary fluid inclusions are those formed as a result of fractures or crystal dislocation affecting the crystal after it has stopped growing (Roedder, 1979). Temperature and salinity of precipitating crystals can be measured from fluid inclusions. If fluid inclusions are trapped as a single phase (e.g., one liquid phase) at a relatively low temperature of less than 50°C (Roedder, 1979), the inclusions would remain as single-phase fluid inclusions; whereas if they are trapped as a single phase under elevated temperature (>50°C), as the host mineral and inclusion cool, they would separate into two phases: a liquid and

vapour. The homogenization temperature of formation of the crystal containing a two-phase fluid inclusion can be determined by heating up the sample until the vapour bubble disappears.

The temperatures of homogenization of inclusions in carbonates and their impurities of the Turner Valley Formation were measured and are listed in Table 3.1.

**Table 3.1.** Inclusions and homogenized temperatures of two-phase fluid-inclusion.

Mineral Phase	Inclusions	Temperature Range (°C)	Temperature Average (°C)
Primary anhydrite	None	----	
Calcite cements	One Phase, Rare	----	
Cherts	Very Rare	----	
Patchy Dolomite	Very Rare	----	
Massive Dolomite	One Phase	----	
Megadolomite	Single- and Two-phase	103-129 n=6	116
Secondary Anhydrite	Single- and Two-phase	159-260 n=5	221

From Table 3.1, two very different temperature groups can be observed. All calcite cements, all cherts, patchy dolomite and even pervasive matrix dolomite formed at relatively low temperatures ( $< 50^{\circ}\text{C}$ ), whereas burial anhydrite and megadolomite formed at higher temperatures. However, the petrographic and isotopic results demonstrate that burial anhydritization occurred with matrix dolomitization, although lasted longer; and megadolomite has slightly negative  $\delta^{18}\text{O}$  values relative to matrix dolomite. Hence it is possible for anhydrite and megadolomite to have formed at higher temperatures than massive dolomite (i.e.,  $> 50^{\circ}\text{C}$ ). However, no hydrothermal lead-zinc mineralization has been reported from the Turner Valley Formation. The temperatures of anhydrite and megadolomite from fluid inclusions could be higher than that they should be if the following possibilities exist: (1) Some secondary fluid inclusions were measured during



measuring, especially in anhydrite. (2) The volume of the cavity probably changed (e.g., dissolution) significantly. (3) The fluid inclusions stretched or leaked. (4) The fluids in the inclusions probably contain some impurities besides water (Moore et al. 1989). Anyway, some conclusions can still be achieved from the results of fluid inclusions. Microdolomite, calcite cements, cherts, and patchy dolomite formed at lower temperatures and probably in relatively early diagenetic stages. Pervasive matrix dolomite also formed at relatively low temperatures. Burial anhydrite and megadolomite probably formed at higher temperatures and later diagenetic stages.

In addition, if carbonates have hydrocarbon inclusions, the inclusions can be recognized by their fluorescence under fluorescence microscopes (Burruss et al., 1985). Megadolomite crystals of the Turner Valley Formation include hydrocarbon inclusions, suggesting that hydrocarbon production and migration could have occurred during the crystallization of megadolomite.

### **3.10.2 Cathodoluminescence (CL) Petrography**

Cathodoluminescence (CL) has been widely used to examine the various luminescent patterns and fabrics of carbonates, which are invisible in ordinary light microscopes. Luminescence involves adsorption of radiation followed by instantaneous emission of visible light. CL is produced by trace elements incorporated during mineral precipitation (Machel, 1985). With CL, the luminescence is mostly a function of  $\text{Fe}^{2+}$  and  $\text{Mn}^{2+}$  contents and also the Fe/Mn ratios, with  $\text{Mn}^{2+}$  being the activator and  $\text{Fe}^{2+}$  the inhibitor, but other elements are involved such as  $\text{Pb}^{2+}$  and rare earth (activators), and  $\text{Ni}^{2+}$  and  $\text{Co}^{2+}$  (quencher) (Machel, 1985). Dolomite requires higher Mn concentrations than calcite for similar luminescent intensities because some Mn ions enter Mg sites, thus decreasing their efficiency as activators.

The redox conditions, temperature and fluid chemistry during carbonate precipitation can be inferred from their luminescent patterns, because they are related to the relative abundance of activator and quencher elements in minerals. Therefore, the typical non-luminescent, dull luminescent, and bright luminescent in different zones or minerals are believed to reflect a continual decrease in Eh, varying gradually from oxidizing to

reducing conditions with increasing burial (Machel, 1985). In the Turner Valley carbonates and impurities (cherts and anhydrites), three CL features were observed: (1) Non-Luminescence. (2) Dull to brown orange. (3) Brown to slightly bright orange.

**Non-Luminescence:** All anhydrites, gypsums and various types of chert exhibit non-luminescence under CL, and all calcite cements and undolomitized calcite muds and skeletal grains show this type of colour, although they have different origins and formed in different stages.

**Dull to brown orange:** Most dolomites have this type of colour. Microdolomite, patchy dolomite and some pervasive matrix dolomite have a dull CL colour. Some pervasive matrix dolomite and most coarse and crinoid-moldic dolomite have a brown CL colour.

**Brown to slightly bright orange:** This colour is rare, and is only found in the rims of some megadolomite crystals abut to voids. The rims of megadolomite crystals probably formed as cements.

Although different CL colours of diagenetic component are identified, it is probably improper to use different CL colours to divide various environments which resulted in different Fe, Mn contents and their ratios in a whole iron- and manganese-depleted setting such as in the Turner Valley carbonates, and it is hard to detect any compositional variation. However, fluorescence in this study can distinguish the rims of dolomite, and the ghosts of primary skeletal grains which were replaced by pervasive matrix dolomite as discussed in detail as follows.

### **3.10.3 Fluorescence Stratigraphy**

Fluorescence has been introduced as a complementary technique to cathodoluminescence, first used in the studies of coal and fluid inclusions in carbonates. Fluorescence may show similar features as CL, but not necessarily, nor do they produce comparable results (Dravis and Yurewicz, 1985). The factors that cause fluorescence are not yet well understood. Organic components are believed to be the primary factor in carbonate rocks (Dravis and Yurewicz, 1985). Trace elements may be another possible factor.

In this study, a white card, inserted between the transmitted light and the thin section,

is used in the fluorescence microscope to detect microfibrils and organic matter, effectively sometimes, as suggested by Folk (1987). To reveal the diagenetic fabrics and porosity of the Turner Valley carbonates, fluorescence is more helpful than CL. Some important diagenetic phenomena were detected under fluorescence microscopy. (1) Diagenetic rims (or zones) on microdolomite, patchy dolomite and even pervasive matrix dolomite are identified, which probably resulted from compositional variations of dolomitization fluids during water-rock interaction, or multiple stages of dolomitization occurred. (2) Skeletal ghosts that have been overprinted by matrix dolomite are revealed. (3) Hydrocarbon inclusions are detected in dolomite crystals. (4) The distribution and evolution of macro- and micro-porosity are observed. All those mentioned above are discussed in detail in different parts of this chapter.

### **3.10.4 Major, Minor, and Trace Elements**

#### **3.10.4.1 Introduction**

Forty-four samples representing different calcite and dolomite components were analyzed for major, minor and trace elements. Analytical procedures are discussed in chapter I and the results are listed in Appendix (I). Minor and trace elements are found widely in natural calcite and dolomite. They can be incorporated into carbonate minerals in the following ways (Veizer, 1983): (1) substitute for  $\text{Ca}^{2+}$  in the crystal lattice; (2) occur interstitially between lattice planes; (3) occupy defect-lattice positions; (4) be absorbed due to remanent ionic charges; (5) be present as inclusions. At present, when trace element analysis is utilized as a diagenetic tool, only (1) is considered; the rest are usually less significant in volume, less understood and out of control.

The amount of a trace element to be incorporated into a  $\text{CaCO}_3$  lattice and dolomite is controlled by the distribution coefficient (D) between crystals and solution at complete equilibrium. When  $D > 1$ , the precipitated crystal will contain higher trace element concentrations than solutions from which the crystal precipitated. When  $D < 1$ , the crystal will have more depleted trace element concentration than the solutions. In general, Mg, Na and Sr have D values much less than 1, and Fe, Mn have D values larger than 1 (Veizer, 1983). Therefore, during diagenetic processes, trace elements of  $D > 1$

preferably incorporate into crystals, hence recrystallization will lead to Mg, Na, Sr ( $D < 1$ ) depletion, whereas Fe and Mn ( $D > 1$ ) enrichment will occur (Veizer, 1983). Similarly, during the processes of water-rock interaction, trace elements, such as Mg, Na and Sr with  $D$  values less than 1 must increase downflow of diagenetic fluids in rocks, whereas Mn and Fe must decrease if the diagenetic fluid composition is constant and the flow direction is linear. From this point, the direction of diagenetic fluids could be inferred based on the spatial distribution of trace elements in rocks (Veizer, 1983).

#### **3.10.4.2 Calcium and Magnesium**

The amount of the Calcium carbonate often changes relative to the of the Magnesium carbonate in natural dolomite. Dolomite with 50 mol % of  $\text{CaCO}_3$  and  $\text{MgCO}_3$  is thought as a stoichiometric and possible ordered dolomite mineral. Naturally, dolomites are often Mg-depleted (less than 50 mol %) to some degree. Strongly Mg-depleted and poorly-ordered dolomite is called protodolomite (Goldsmith and Graf, 1958a in Tucker and Wright, 1990), which is a metastable dolomite. In modern shallow marine environments, metastable carbonate minerals are dominated by Mg-calcite (Mg-rich), aragonite (Sr-rich), and protodolomite, if any, in evaporative environments. Stabilization of these metastable minerals to diagenetic calcite and dolomite involves a major reapportionment (partition) of these elements between the new diagenetic carbonates and the fluids.

In the Turner Valley Formation, undolomitized calcitic crinoids and all calcite cements usually have Mg lower than 1 mol percent, suggesting that they underwent stabilization or/and formed as diagenetic calcites. Various types of dolomite have different Mg contents (Table 3.2). Microdolomite is not stoichiometric with a  $\text{CaCO}_3$  mean of 55.2 mol%. Patchy dolomite is also not stoichiometric (56.9 mol%  $\text{CaCO}_3$ ). Massive dolomite has a  $\text{CaCO}_3$  mean of around 52.3 mol%, hence, massive dolomite is relatively stoichiometric and possibly ordered. Megadolomite is also slightly Ca-rich (53.7 mol%), suggesting that megadolomite is at least nonstoichiometric, even if it is still ordered.

**Table 3.2. Major- and Minor-elements in Dolomites. Results with stars were analyzed by Electron Microprobe.**

	Microdolomite n=7	Massive dolomite n=15	Megadolomite n=8	Patchy dolomite n=2
<b>CaCO<sub>3</sub>(mol%):</b>				
<b>Mean</b>		54.9*(n=1)		
<b>Range</b>	55.2    59.4*(n=8) 51.8-62.8 55.1-63.5*	52.3 49-54.9	53.7    52.2*(n=2) 50-56.4 55.5-55.9*	56.9* 56.7-56.8*
<b>Sr (ppm):</b>				
<b>Mean</b>	148	82	113	-
<b>Range</b>	90-260	40-174	92-175	-
<b>Na (ppm):</b>				
<b>Mean</b>	369	223	269	-
<b>Range</b>	290-476	180-270	200-305	-
<b>Fe (ppm):</b>				
<b>Mean</b>	257    435*(n=3)	134	303	125* n=1
<b>Range</b>	174-351 154-864*	69-259	184-423	
<b>Mn (ppm):</b>				
<b>Mean</b>	80    197*(n=2)	31	40	-
<b>Range</b>	35-128 184-210*	20-51	20-52	-

### 3.10.4.3 Sodium

Sodium is the most abundant cation in seawater. Sodium has been used as a palaeosalinity indicator (Veizer, 1978). In carbonate minerals, sodium can be present in the crystal lattice replacing Mg and Ca (Land and Hoops, 1973), and also in interstitial positions of crystal as inclusions. In the Turner Valley carbonates, calcitic crinoids have the highest Na concentration with a mean of 558 ppm, varying from 349 to 893 ppm. Calcite cements (equant and coarse spar) have somewhat lower Na concentrations than that of crinoids and averages about 340 ppm. Different types of dolomite have various

Na contents (Table 3.2). Microdolomite has the highest Na content with an average of 369 ppm varying from 290 to 476 ppm. Pervasive matrix dolomite has a much lower Na content, varying from 180 to 270 ppm, while megadolomite has a slightly higher Na content than matrix dolomite with a mean of 269 ppm, varying from 200 to 305 ppm. Na contents in various types of dolomite are higher than that of normal marine dolomite (110 to 160 ppm, Veizer, 1983). Dolomite crystals may have some Na-rich inclusions.

#### **3.10.4.4 Strontium**

Strontium concentrations are low in both calcite and dolomite components of the Turner Valley Formation. Calcite crinoids have a mean of 302 ppm, much lower than that of modern marine high-Mg calcite, 1000 ppm (Veizer, 1983). Hence crinoids may have undergone recrystallization and stabilization during diagenesis. Calcite cements (equant and coarse spar) have similar Sr concentrations to crinoids and average about 278 ppm. The diagenetic fluids for cementation may be either similar to the fluids of crinoid diagenesis or somewhat similar to seawater.

Dolomite has a much lower Sr concentration than calcite components due to the smaller Sr partition of dolomite than that of calcite. The distributions of Sr are similar to those of Na in various types of dolomite of the Turner Valley Formation (Fig. 3.1). Microdolomite has the highest Sr content (average 148 ppm), but still much lower than that (470 to 550 ppm) reported by Veizer (1983) or that (500 to 700 ppm) reported by Behrens and Land (1972) for marine dolomite.

Few ancient dolomites contain more than 200 ppm Sr, even when presumed to be initially of hypersaline origin (Land, 1985). Two distribution coefficients of dolomite have been experimentally obtained at high temperatures (250°C-300°C). One is 0.07 by Jacobson and Vsdowski (1976), the other is 0.025 by Katz and Matthews (1977). Veizer (1983) prefers 0.07. Land (1985) proposes that there are at least two distribution coefficients applied to dolomite, one for the formation of the original phase, and a second (lower) for the stabilization reaction to a more ordered, stoichiometric phase. In addition, Veizer (1978) suggested that the "precursor influence" of Sr concentration is of significance. Perhaps, this is why microdolomite has the highest Sr content since

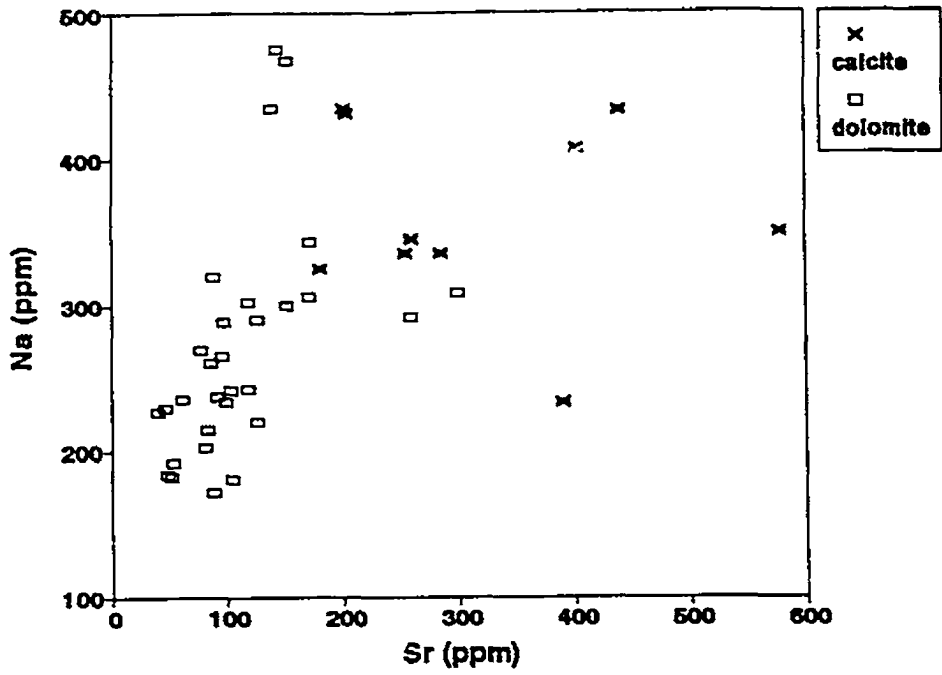


Fig. 3.1. Na vs. Sr for all calcite and dolomite components.

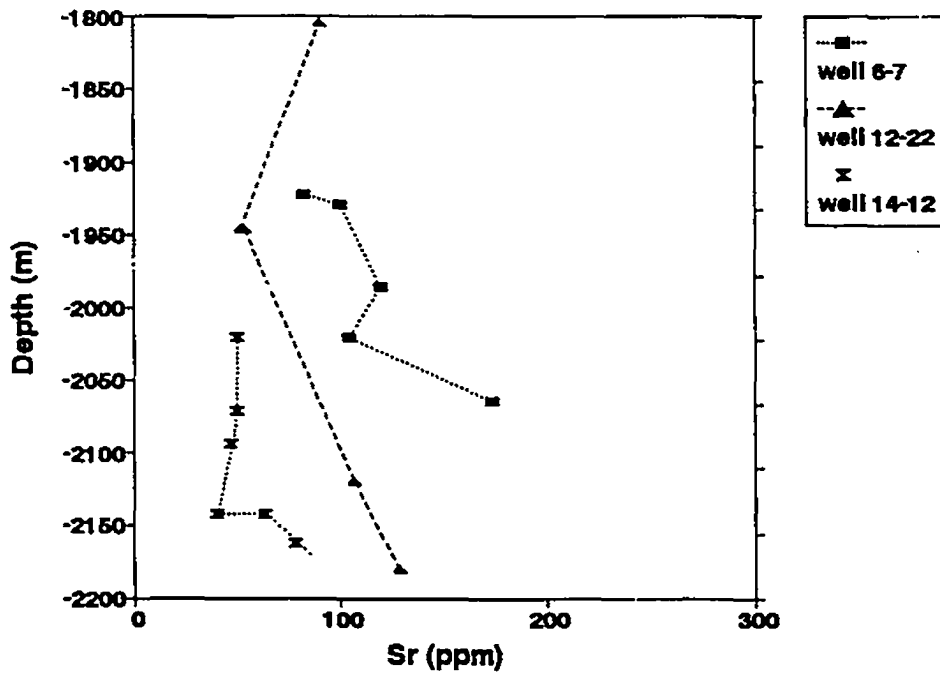


Fig. 3.2. Sr-Depth relationship for massive dolomite.

its precursor (lime mud) could be aragonite, which also has a higher Sr distribution coefficient and Sr content than calcite. Meanwhile, microdolomite could have formed first as a protodolomite (original phase) with high Sr contents.

However, in the Turner Valley Formation, pervasive matrix dolomite and megadolomite could have the same precursor (diagenetic calcite), but their Sr contents are different. The precursor of pervasive matrix dolomite should be limestone (calcite), whereas the precursor of megadolomite could be matrix dolomite as well as skeletal grains from the petrographic observation. In addition, megadolomite crystals are much coarser than matrix dolomite, hence more stable since the larger a crystal is, the more stable it will be (Durham and Olson, 1980). So, according to either Land or Veizer (also Durham and Olson), megadolomite should have a lower Sr concentration than pervasive dolomite. The opposite results obtained suggest that dolomitization is a very complex process(es), and the ordered state and precursor influence are not the only important factors; other factors such as dolomitization process and fluids should be considered, too. From the discussion above, megadolomite is not the recrystallization product of matrix dolomite at elevated temperature, nor have megadolomite and matrix dolomite resulted from the same dolomitization fluids and formed during the same geological time scale. The low Sr concentration of pervasive matrix dolomite could have resulted from the flushing of lower Sr content fluids (e.g., meteoric water) if megadolomite formed later in deeper burial environments.

In addition, Sr and Na contents have changed with burial depth in pervasive matrix dolomite (Fig. 3.2 and Fig. 3.3). Sr and Na concentrations increase as the depths increase. It is interesting that Sr and Na contents of crinoids have similar patterns of distribution to that of pervasive matrix dolomite with depth (Fig. 3.4). Hence, if both dolomitization fluid and stabilization fluid compositions are constant, and the flow direction is linear, then the diagenetic and dolomitization fluids for both crinoids and pervasive matrix dolomite could have a predominantly downward movement since both Na and Sr have  $D < 1$  as discussed in details in section 3.10.4.4, and the fluids came from upper parts or overlying strata, probably from the surface freshwater recharge during sedimentary basin exposure.



#### **3.10.4.5 Manganese**

Mn concentrations in all carbonates of the Turner Valley Formation are very low (Fig. 3.5). They usually vary from 20 to 40 ppm in both calcites and dolomites. Calitic crinoid and cements have lower Mn than dolomite, some of them have concentrations too low to detect. Microdolomite has a high Mn content relative to other dolomites. Massive dolomite and megadolomite have low Mn concentrations.

#### **3.10.4.6 Iron**

Fe like Mn has a low concentration in the Turner Valley carbonates (Fig. 3.5). Ferroan calcite and dolomite have not been seen from the stained thin sections. CL also exhibits dull to brown colour for calcite and dolomite. It is interesting that Fe concentrations show somewhat similar trends to that of Na and Sr for dolomites (Fig. 3.6). Microdolomite has higher Sr and Fe contents, whereas massive dolomite has the lowest Fe concentration. However, crinoid and calcite cements have relative higher Fe contents (Table 3.2).

Because the significance of iron and manganese in the 2+ valence state is that they require reducing conditions to exist, they are incorporated into the carbonate mineral lattice as bivalent cations in at least moderately reducing environments (Pierson, 1978; Frank et al., 1982). Near-surface meteoric groundwater is normally well oxygenated (Evamy, 1969), but distal parts of intermediate and deep carbonate aquifers, remote from recharge areas, can be anoxic (Meyers, 1978; Grover and Read, 1983). Fe and Mn are preferentially incorporated into carbonate minerals during diagenesis due to their distribution coefficients larger than 1. Hence,  $Mn^{2+}$  and  $Fe^{2+}$  concentrations are supposed to be low in marine water and meteoric water where at least partially oxidized environments are maintained related to completely subsurface reduced environment.

#### **3.10.4.7 Analytical Results of Microprobe**

Four thin sections containing four types of dolomite were analyzed for major and minor elements. Some results (with stars) are listed in Table 3.2. Trace element (Sr, Fe and Mn) contents were too low to detect. Although these results are somewhat different

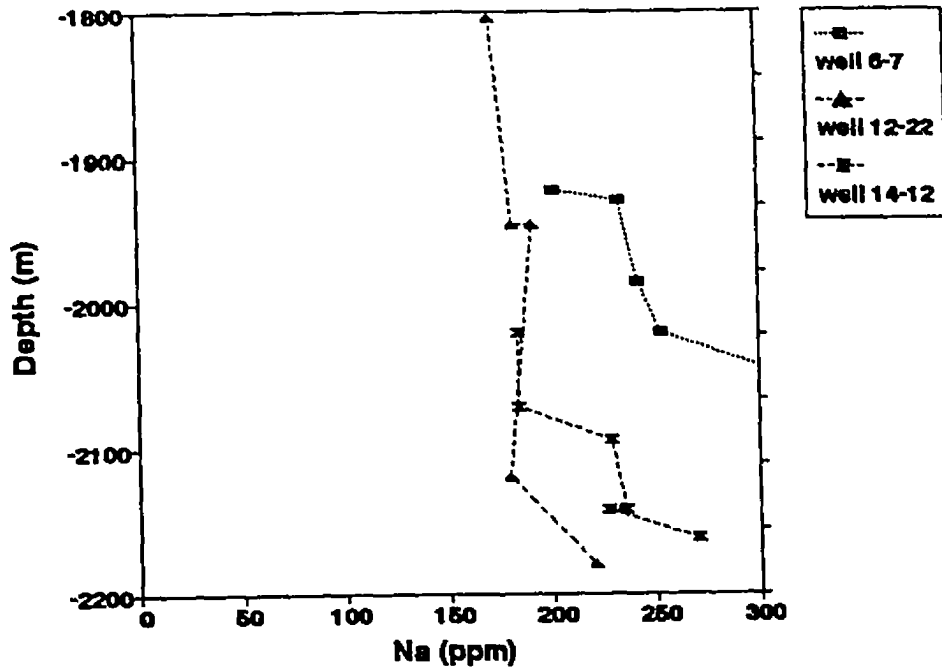


Fig. 3.3. Na-Depth relationship for massive dolomite.

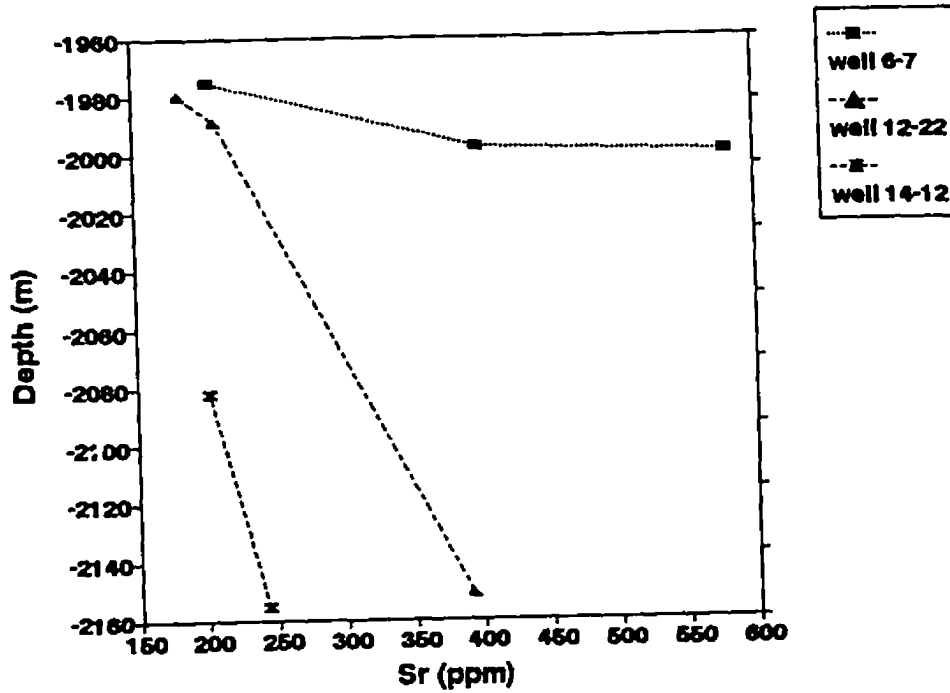


Fig. 3.4. Sr-Depth relationship for calcitic crinoid fragments.

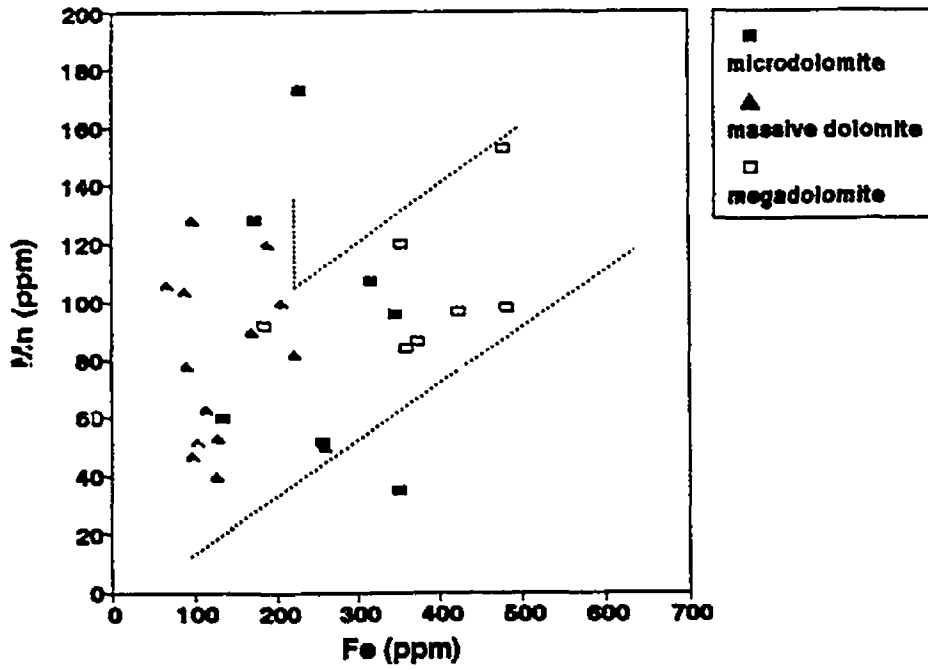


Fig. 3.5. Scatter diagram of Mn vs Fe for dolomites.

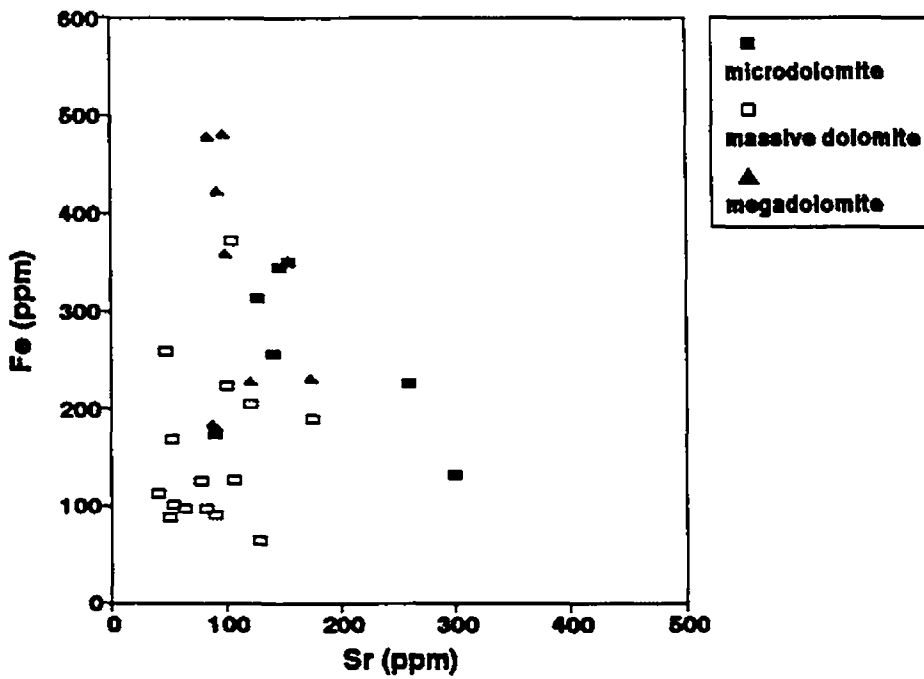


Fig. 3.6. Scatter diagram of Fe and Sr for dolomites.

from those of chemical analysis due to using different methods (the resolution of the microprobe is much higher) the trends of compositional variation of various dolomites are similar (Table 3.2). For instance, Microdolomite is the least stoichiometric, and massive dolomite is relatively stoichiometric, and microdolomite has relatively high Mn and Fe concentrations from the results of two analytical methods.

Furthermore, the electron microprobe analysis also illustrated some compositional variations in the microdolomite phase. Enlarged grains usually are more stoichiometric, and have higher Mn and Fe concentrations than smaller rhombs of microdolomite (Plate 3.13), suggesting that enlarged grains formed during late burial environments or recrystallized from crystals of microdolomite.

#### **3.10.4.8 Summary of Major, Minor and Trace Elements**

The study of major and minor elements is used to determine the precipitating and diagenetic environments of carbonates. Several conclusions were reached from the results of this study.

(1) Crinoids have undergone recrystallization (neomorphism) evidenced by their lower Mg contents and lower Sr concentrations than that of normal marine calcite. The diagenetic fluids had a downward movement and/or came from overlying strata.

(2) All calcite cements probably formed at the time of crinoid stabilization due to the similar major and minor element concentrations between crinoids and cements, or they had similar diagenetic fluids.

(3) Microdolomite formed in Na- and Sr-rich evaporative environments under reducing or weakly oxidizing conditions. It may have undergone recrystallization during burial environments.

(4) Dolomitization fluids for pervasive matrix dolomite and megadolomite are different, and the two types of dolomite formed under very different conditions. Dolomitization fluids for pervasive matrix dolomitization had a downward movement direction, possibly resulting from meteoric water recharge of the overlying strata.

(5) Relatively low Fe and Mn concentrations in all calcites and dolomites probably represent that Fe- and Mn-depleted diagenetic fluids were supplied during the whole

diagenetic history of the Turner Valley Formation.

### **3.10.5 Isotopes**

#### **3.10.5.1 Oxygen and Carbon Isotopes**

##### **3.10.5.1.1 Introduction**

For carbonate studies, the two most naturally abundant stable isotopes of O and C are commonly used, and have become increasingly important tools in diagenetic studies. The isotopic composition of calcite cement and dolomite is usually used to help characterize the diagenetic fluid that have reacted with the rocks (Land et al., 1975).  $\delta^{18}\text{O}$  and  $\delta^{13}\text{C}$  values of normal marine carbonates will increase when altered by evaporative water, and will decrease when altered by meteoric water. Carbonates precipitated from marine water generally have a  $\delta^{18}\text{O}$  ranging from -2 to +4 per mil PDB, and  $\delta^{13}\text{C}$  from +1 to +5 per mil PDB. Carbonates stabilized under meteoric water generally have  $\delta^{18}\text{O}$  from 0 to -5 per mil and  $\delta^{13}\text{C}$  from +2 to -10 per mil (Drunkman and Moore, 1985; Moore, 1989).

During burial diagenesis, there are several situations that affect the  $\delta^{18}\text{O}$  and  $\delta^{13}\text{C}$  values of carbonates at the time of precipitation or recrystallization, and lead to compositional trends far from the ideal presented. For  $\delta^{18}\text{O}$ , the most important is temperature fractionation, which can cause negative shifts in  $\delta^{18}\text{O}$  values at elevated temperatures (Anderson and Arthur, 1983). The relationship of oxygen isotopic fractionation and temperature between water and calcite as a function of temperature has been estimated before (e.g., Epstein et al., 1953; Craig, 1965; Friedman and O'Neil, 1977 in Land, 1985). Because the fractionation factor is poorly understood, dolomite has presented a special problem for many years. While extrapolating the results of high-temperature exchange experiments suggests that dolomite should concentrate  $^{18}\text{O}$  by approximately 6 per mil relative to contemporaneous calcite (Northrop and Clayton, 1966; O'Neil and Epstein, 1966b). However, Land (1980) believes that a 3-4 per mil of  $^{18}\text{O}$  higher than syngenetic calcite is more reasonable. For  $\delta^{13}\text{C}$ , the organic activity in carbonate diagenesis can result in a considerable negative shift in  $\delta^{13}\text{C}$  values. Organic carbon exhibits low values of  $\delta^{13}\text{C}$  (-24 per mil, PDB) relative to the oxidized forms of carbon found as  $\text{CO}_2$  (-7 per mil) and marine carbonates (0 to +4 per mil). Extremes in  $\delta^{13}\text{C}$

values generally involve methane generation either by biochemical fermentation in the near surface, or by thermochemical degradation of organic matter in the subsurface at temperature greater than 100°C (Anderson and Arthur, 1983). Soil weathering and carbonate mineral stabilization involving dissolution of marine limestones and sediments and subsequent precipitation of calcite cements in the vadose and the shallow phreatic zones will generally result in cements and limestones with moderately low  $\delta^{13}\text{C}$  composition (Allen and Matthews, 1982; James and Choquette, 1984). Both O and C isotopes for calcite and dolomite components of the Turner Valley Formation in Quirk Creek were analyzed. They can be divided into two groups with obviously different  $\delta^{18}\text{O}$  and  $\delta^{13}\text{C}$  values. The difference between dolomites and coexisting calcites is more than 3-4 per mil, as Land (1980) predicted.

#### **3.10.5.1.2 Analytical Results**

##### **Crinoids and calcite cements:**

Figure 3.7 shows the  $\delta^{18}\text{O}$  versus  $\delta^{13}\text{C}$  values of crinoids and calcite cements. Undolomitized crinoid grains have a mean  $\delta^{18}\text{O}$  of -5.1 per mil, varying from -6.77 to -3.29 per mil PDB; and a mean  $\delta^{13}\text{C}$  of +3.08 per mil varying from +2.59 to +3.55 per mil. Bladed prismatic calcite has a mean  $\delta^{18}\text{O}$  of -5.88 per mil ranging from -6.20 to -5.56 per mil, and a mean  $\delta^{13}\text{C}$  of -4.35 per mil varying from -8.40 to -0.31 per mil. Blocky calcite cement has a mean  $\delta^{18}\text{O}$  of -7.42 per mil, varying from -7.65 to -7.19 per mil PDB; and a mean  $\delta^{13}\text{C}$  of -2.55 per mil, varying from -3.02 to -2.07 per mil, PDB. Equant calcite spar and coarse mosaic spar have much more negative values in both  $\delta^{18}\text{O}$  and  $\delta^{13}\text{C}$ . They have  $\delta^{18}\text{O}$  averaging -11.45 and -10.94 per mil, varying from -12.48 to -9.33 per mil and from -12.33 to -9.31 per mil, PDB, respectively;  $\delta^{13}\text{C}$  values averaging -8.1 per mil and -8.56 per mil, PDB varying from -9.67 to -5.82 per mil and from -2.82 to -12.69 per mil, PDB, respectively.

Crinoid calcite has slightly negative  $\delta^{18}\text{O}$  values and a similar mean  $\delta^{13}\text{C}$  value relative to those precipitated in modern marine environments. Crinoid deposited in shallow marine usually consists of high-Mg calcite (Scholle, 1978). Unstable Mg-calcite will change into low-Mg calcite or diagenetic low-Mg calcite during diagenesis. Because the

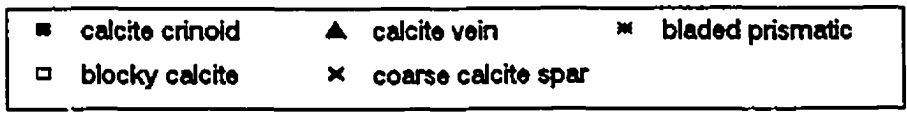
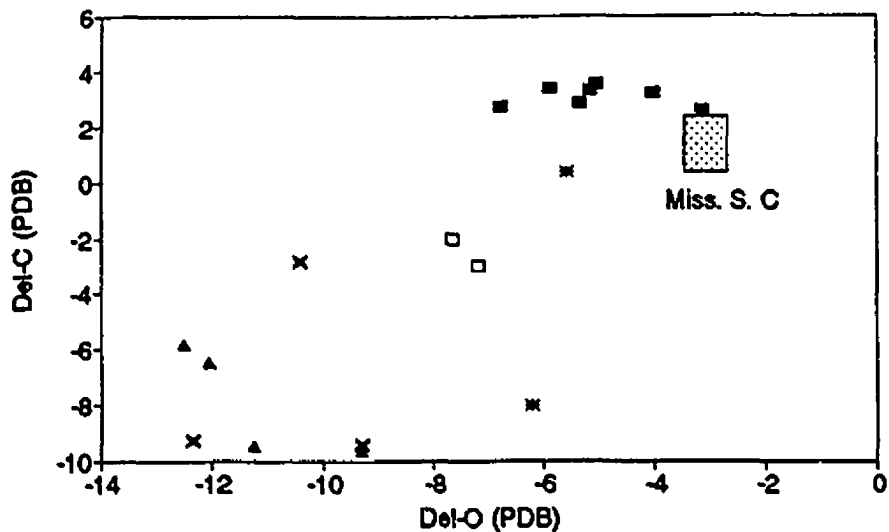


Fig. 3.7. Oxygen and Carbon isotopic composition of calcitic crinoids and cements.

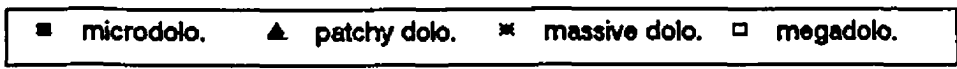
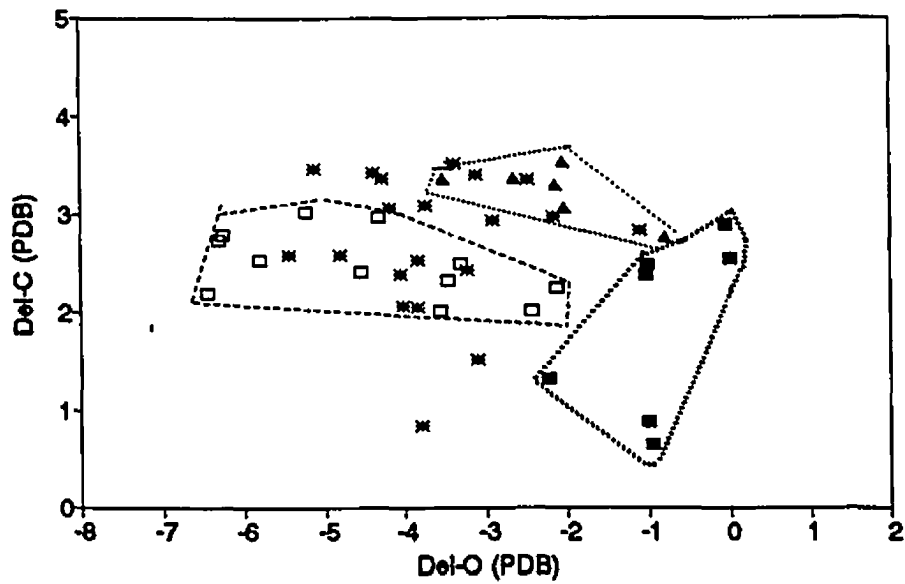


Fig. 3.8. Oxygen and Carbon isotopic composition of dolomites.

isotopic composition is a function of solution, mineralogy and temperature (Land, 1980; Arthur and Anderson, 1983), if one of the three was modified from its original value, then the stabilization of metastable minerals would also result in some change of isotopic composition. The stabilization of crinoids and limestones of the Turner Valley Formation possibly occurred during early burial as is indicated by their similar  $\delta^{13}\text{C}$  values to those of marine carbonates. The slightly negative  $\delta^{18}\text{O}$  is probably due to elevated temperatures or alteration by later meteoric fluids (Al-Aasm and Veizer, 1986; Moore, 1989).

Bladed prismatic calcite and blocky calcite cements probably formed during early burial due to their similar  $\delta^{18}\text{O}$  values to crinoids, and were associated with organic activity because of the negative  $\delta^{13}\text{C}$  values and also the presence of pyrite with blocky calcite cement. The association of authigenic pyrite with sediments is an indicator of an anaerobic environment (Berner, 1970), and indicates that bacterial sulfate reduction is the first major step in the process of sedimentary pyrite formation. Organic matter is needed as an energy for the sulfate reduction. Vein equant calcite and coarse mosaic spar formed later than bladed prismatic calcite and blocky calcite cements because vein equant calcite crosscuts blocky calcite, whereas coarse mosaic spar includes or/and succeeds to bladed prismatic calcite in voids. According to petrography, all calcite cements, especially calcite veins and blocky cement, are distributed in the middle and upper parts of the Turner Valley Formation. And from trace elements, crinoid stabilization and calcite cementation probably occurred at the same time or from the same fluids. The diagenetic fluids resulted from the overlying strata, possibly from meteoric water. Hence, their formations were also probably overlapped by meteoric fluids and probably associated with organic activity due to their strongly depleted  $\delta^{18}\text{O}$  and  $\delta^{13}\text{C}$  values.

### Dolomites

All types of dolomite have much higher  $\delta^{18}\text{O}$  and  $\delta^{13}\text{C}$  values than various calcite components in the Turner Valley carbonates (Fig. 3.8). Microdolomite has the heaviest  $\delta^{18}\text{O}$  varying from 0 to -2.22 per mil averaging -0.53 per mil, PDB. Patchy dolomite has lighter  $\delta^{18}\text{O}$  than microdolomite varying from -3.52 to -0.79 per mil with a mean of -2.19 per mil PDB. Pervasive matrix dolomite has lower  $\delta^{18}\text{O}$  than patchy dolomite varying



from -5.46 to -1.11 per mil with a mean of -3.43 per mil, PDB. Megadolomite has the lowest  $\delta^{18}\text{O}$  varying from -6.47 to -2.12 per mil with a mean of -4.49 per mil, PDB. Petrographic and trace element results show that microdolomite probably formed in a sabkha evaporative environment. Its slightly depleted  $\delta^{18}\text{O}$  relative to that of modern sabkha (0 to +3 per mil, PDB; McKenzie, 1981) may reflect that microdolomite has undergone some recrystallization during late stages of dolomitization. According to petrography, patchy dolomite formed in a relatively early burial environment. Assuming that the dolomitization fluids for patchy dolomite were of marine parentage, with  $\delta^{18}\text{O}$  values similar to the Mississippian seawater (about -1 per mil SMOW, e.g., Veizer, 1983), then the temperatures of the dolomitization fluids can be calculated using the following equation (Fritz and Smith, 1970):

$$10^3 \text{Ln} \alpha_{\text{dol-water}} = 2.78 \times 10^6 \text{T}^{-2} (\text{K}) + 0.11 \quad (1)$$

Assuming the starting temperature is 25°C (average annual temperature), then the patchy dolomite could have formed at a temperature of 34°C. If 25°C/km is used for the geothermal gradient in the Western Canada Basin, then the burial depth of patchy dolomite would be around 360 m. The overlying Mount Head Formation has a preserved thickness of 200-300 m (Macqueen et al., 1968), covered the Turner Valley carbonates.

From petrography, pervasive matrix dolomite formed later than patchy dolomite. If patchy dolomite formed during burial diagenesis, then massive dolomite could have formed at relatively greater depths due to its lower  $\delta^{18}\text{O}$  than patchy dolomite. Using the same assumptions and calculations as for patchy dolomite, pervasive matrix dolomite could have formed at a temperature of 40°C and a burial depth around 650 meters. While if the meteoric water was intervening the dolomitization fluids, the burial depth and temperature of pervasive matrix dolomite did not need to be that deep (650 m) and that high (40°C) due to the negative  $\delta^{18}\text{O}$  values of meteoric water. In addition, the results of fluid inclusions also show that matrix dolomite formed at a low temperature (<50°C). Furthermore, the burial-temperature curve in Fig. 3.9 by Packard (personal communication, 1991) shows that the Turner Valley Formation had a predominantly shallow burial history, mostly shallower than 500 m and temperatures around 30°C. Only in early Cretaceous were burial depths greater than 1000 m and

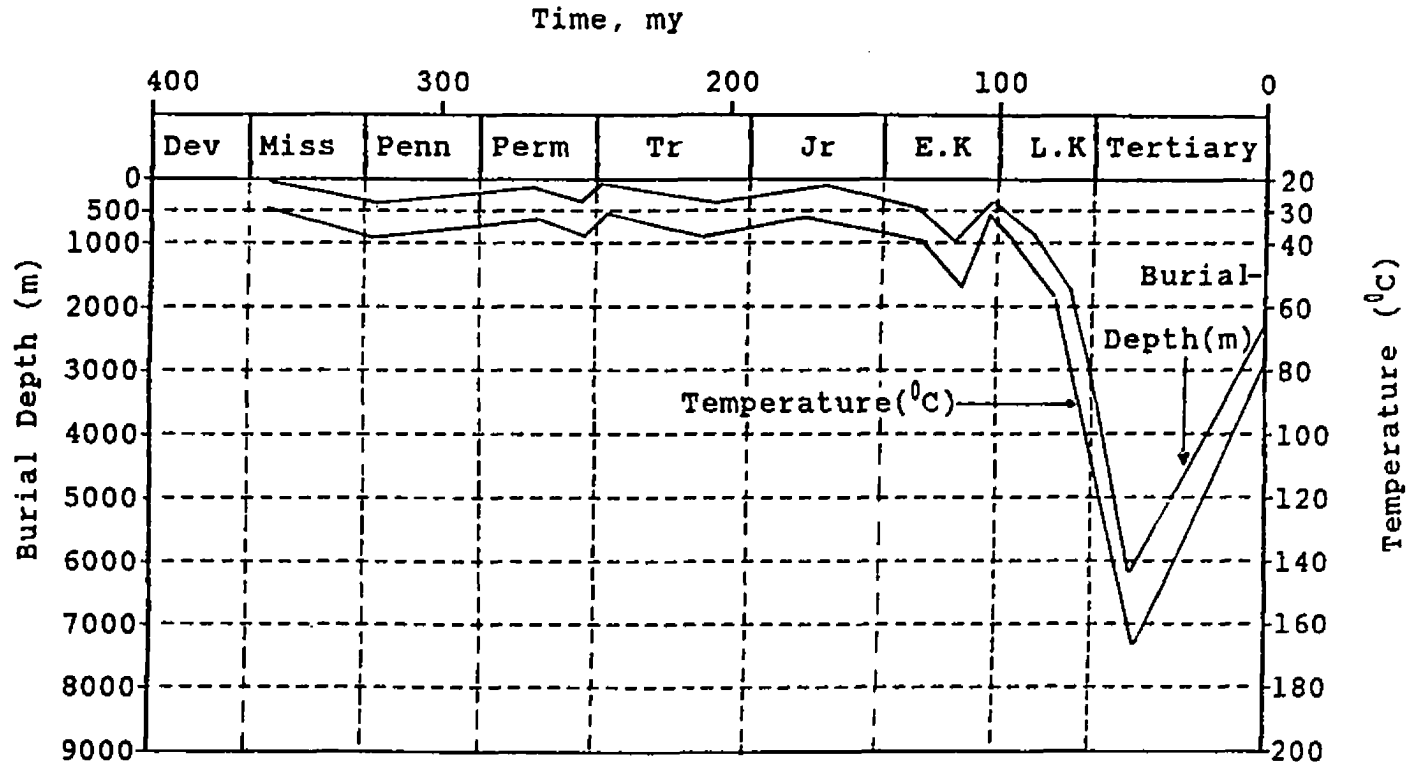


**Fig. 3.9.** Plot of the burial history curve of the Turner Valley Carbonates (modified from Packard, unpublished data).

temperatures were more than 40°C, and during Tertiary reached the deepest burial of 7000 m and the highest temperature of 170°C. Hence, the temperatures from burial curves of the Turner Valley Formation are coincident with that from O isotopic results, and show that massive dolomite probably formed before the Cretaceous at a relatively shallow burial, with freshwater possibly intervening. Megadolomite formed in the very late diagenetic stage, according to petrography. The lower  $\delta^{18}\text{O}$  of megadolomite related to massive dolomite could have resulted from elevated temperatures, and megadolomite probably formed in Cretaceous or later and deeper burial environment. The  $\delta^{13}\text{C}$  values of all dolomites have a narrow range and positive values relative to their  $\delta^{18}\text{O}$  values. The reason is probably because the calcite precursors of dolomites have buffered the  $\delta^{13}\text{C}$  values. According to the trace element results, massive dolomite may have formed in a mixing-zone, but if dolomitization occurred in the deep phreatic zone, then  $\delta^{13}\text{C}$  values of dolomite may have been negligibly effected by the soil zone (Lohmann, 1988).

### **3.10.5.2 Sulfur Isotopes**

Both primary and secondary anhydrites were analyzed for sulfur isotopes. Sulfate in modern marine water has a rather uniform  $\delta^{34}\text{S}$  values (about 20 per mil, CDT). Evaporative sulfates are deposited with negligible S isotope fractionation (Neilson, 1979), and thus preserve the  $\delta^{34}\text{S}$  of the sea water sulfate. Furthermore, sulfur isotopic composition has changed with time in oceanic reservoirs during geological history (Neilson, 1979). In sedimentary rocks and diagenetic processes, the redox reaction of S compounds usually influences S isotopic composition. As a general rule of kinetic fractionation, the reaction goes faster with the light isotope. The kinetic mechanism producing S isotope fractionation is involved in bacterial sulfate reduction. The Upper Mississippian seawater had a  $\delta^{34}\text{S}$  value around 14 per mil (Neilson, 1979), whereas primary anhydrite of the Turner Valley Formation has a  $\delta^{34}\text{S}$  of about 15 per mil, and secondary anhydrite has a  $\delta^{34}\text{S}$  about 14-16 per mil. There is no obvious difference between primary anhydrite and secondary anhydrite for S isotopes, and thus they may have the same sources. That is, secondary anhydrite resulted from the dissolution of primary anhydrite of both the Turner Valley Formation and other Upper Mississippian

strata (e.g., the Mount Head Formation). The presence of breccias in primary anhydrite-rich strata, and the evidence of widespread downward fluids in the Turner Valley Formation (trace element results) may prove this idea. The slightly higher values of S isotopes in primary and secondary anhydrites than that in the upper Mississippian seawater were possibly caused by the bacterial reduction of sulfate, as evidenced by the presence of pyrite in the Turner Valley Formation, although it is not abundant.

### 3.10.5.3 Strontium Isotopes

The utilization of strontium isotopes in carbonate diagenesis has become more significant in recent years.  $^{87}\text{Sr}$  is a radiogenic isotope that results from the decay of  $^{87}\text{Rb}$ .  $^{86}\text{Sr}$  is one of the stable strontium isotopes. Since carbonate minerals contain negligible Rb, once  $^{87}\text{Sr}$  is incorporated into a carbonate mineral, the relative ratio of  $^{87}\text{Sr}/^{86}\text{Sr}$  will remain constant (Faure et al., 1972).

The  $^{87}\text{Sr}/^{86}\text{Sr}$  value is constant in marine water at any one time, and has varied through geological time (Burke et al., 1982). Fresh meteoric water has a low Sr content and a high  $^{87}\text{Sr}/^{86}\text{Sr}$  value gained by interaction with terrestrial clays and feldspars, which usually have higher Rb. Hence,  $^{87}\text{Sr}$  will increase in clastic sediments with time. However, the  $^{87}\text{Sr}/^{86}\text{Sr}$  values in calcite and dolomite may reflect the age of a carbonate rock if they precipitate in seawater, and exhibit the intervening of enormous volumes of meteoric water which overcome the Sr-buffering of the marine limestones if calcite and dolomite have rich  $^{87}\text{Sr}/^{86}\text{Sr}$  above the marine value (Moore et al., 1988).

Upper Mississippian seawater has a  $^{87}\text{Sr}/^{86}\text{Sr}$  of 0.7076-0.7078 (Burke et al., 1982). Sr isotopes results show no strong radiogenic Sr was found in any component of the Turner Valley Formation. Primary anhydrite has a  $^{87}\text{Sr}/^{86}\text{Sr}$  of 0.7076, reflecting its precipitation in the Mississippian seawater and an unaltered Sr isotopic value. Burial anhydrite has  $^{87}\text{Sr}/^{86}\text{Sr}$  varying from 0.7081 to 0.7083.  $^{87}\text{Sr}/^{86}\text{Sr}$  for various types of dolomite are plotted versus  $\delta^{18}\text{O}$  (Fig. 3.10). Microdolomite has  $^{87}\text{Sr}/^{86}\text{Sr}$  values varying from 0.7077 to 0.7087 with a mean of 0.7080. Pervasive matrix dolomite has  $^{87}\text{Sr}/^{86}\text{Sr}$  values varying from 0.7083 to 0.7085 with a mean of 0.7084. Megadolomite has  $^{87}\text{Sr}/^{86}\text{Sr}$  values varying from 0.7083 to 0.7087 with a mean of 0.7085.

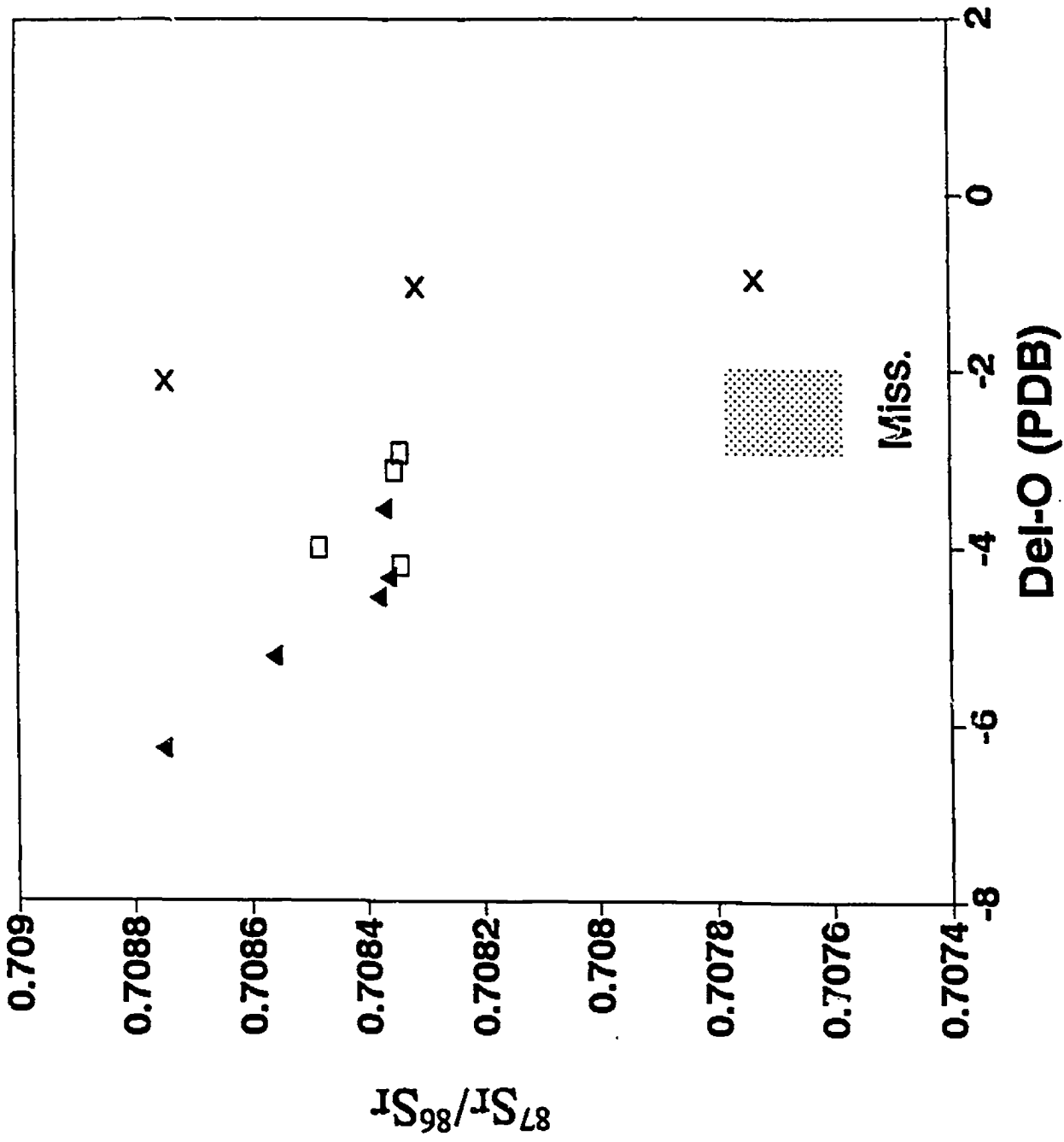
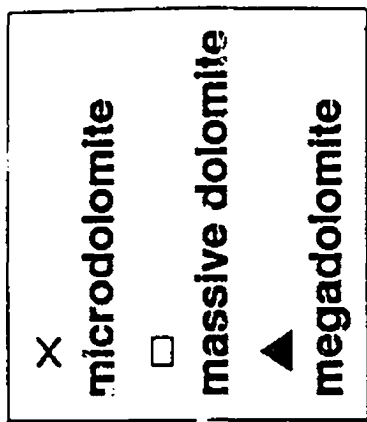


Fig. 3.10.  $^{87}\text{Sr}/^{86}\text{Sr}$  values of dolomites.

Microdolomite, as an evaporative dolomite, has a relatively wide range of  $^{87}\text{Sr}/^{86}\text{Sr}$  from primary Mississippian seawater value to the highest value in the Turner Valley Formation. The variations in  $^{87}\text{Sr}/^{86}\text{Sr}$  values possibly reflect the modifications (e.g., recrystallization) of microdolomite during later diagenesis (e.g., Gao and Land, 1990). The wider  $^{87}\text{Sr}/^{86}\text{Sr}$  values of microdolomite may have reflected that more radiogenic  $^{87}\text{Sr}$  was incorporated into microdolomite during water-rock interaction of later massive dolomite and megadolomite dolomitization. Pervasive matrix dolomite has higher  $^{87}\text{Sr}/^{86}\text{Sr}$  than the Mississippian seawater, suggesting that radiogenic  $^{87}\text{Sr}$  was incorporated into dolomite from relatively  $^{87}\text{Sr}$ -rich fluids during dolomitization. The Turner Valley Formation does not have shales or other Rb-bearing rocks, thus the radiogenic Sr must have come from extraformational fluids. One possibility is that the dolomitization fluids could have derived from the deeper basin, however this source of fluids could have resulted in much higher  $^{87}\text{Sr}/^{86}\text{Sr}$  in dolomite due to the availability of abundant radiogenic Sr and its older age. Hence, this source is unlikely, or less significant, because of low  $^{87}\text{Sr}/^{86}\text{Sr}$  in pervasive matrix dolomite. Another possibility is that dolomitization fluids came from meteoric water, especially with distal sources passed through old Sr-bearing rocks (e.g., shales). This meteoric water with high  $^{87}\text{Sr}/^{86}\text{Sr}$  and low Sr concentration could have resulted in moderate changes of  $^{87}\text{Sr}/^{86}\text{Sr}$  in dolomite during dolomitization (Moore, 1989; Banner et al., 1988; 1989). Megadolomite has similar  $^{87}\text{Sr}/^{86}\text{Sr}$  values to that of pervasive matrix dolomite. Hence, the dolomitization fluids for megadolomite were also relatively rich in  $^{87}\text{Sr}$ .

#### **3.10.5.4 Summary of Isotopic Studies**

From the results and discussion of isotopic values, the following conclusions have been reached:

1. Bladed prismatic calcite and blocky calcite cements formed in early burial environments associated with organic activity shown by depleted  $\delta^{13}\text{C}$ .
2. Equant vein calcite, coarse calcite spar and poikilotopic calcite cements also precipitated in early burial stages after bladed prismatic calcite and blocky calcite cements. All their precipitates were probably associated with meteoric water and organic

activity due to their strongly depleted  $\delta^{18}\text{O}$  and  $\delta^{13}\text{C}$  values.

3. Primary and secondary anhydrites have similar S isotopic composition, suggesting that secondary anhydrite resulted from the dissolution of primary anhydrite, probably by meteoric water. Sr isotopes show that secondary anhydrite formed at the time of pervasive matrix dolomitization.

4. Microdolomite formed in an evaporative marine environment, and underwent multiple modifications during late dolomitization.

5. Patchy dolomite probably formed at a shallow burial environment, about 360 m and at a temperature of  $35^{\circ}\text{C}$ .

6. From the  $\delta^{18}\text{O}$  values, pervasive matrix dolomite probably formed in a subsurface burial environment or/and affected by meteoric water. The consistent and narrow range of  $\delta^{13}\text{C}$  values of massive dolomite may be because the calcite precursors have buffered the  $\delta^{13}\text{C}$  values and/or dolomitization occurred in a deep phreatic zone.

7. Megadolomite formed during deeper burial, at higher temperatures than patchy and pervasive matrix dolomite.

### **3.11 SUMMARY OF DIAGENESIS**

In general, the carbonates of the Turner Valley Formation have undergone a complex diagenetic history. Various diagenetic events occurred during different geological times, and overlapped one another. A paragenetic sequence of the identified diagenetic features is summarized and listed in Table 3.3. The diagenesis of the Turner Valley Formation can be subdivided into 25 events or phases and five stages, although they grade into one another.

**Stage I:** After deposition, sediments underwent lithification and initial diagenesis such as seafloor cementation and evaporative dolomitization (Phase 1-3).

**Stage II:** Sediments were gradually buried at shallow depths (< 300 m) in the Mississippian. Stabilization of metastable minerals occurred; meanwhile, the basin began to be exposed due to crustal rising or sea level dropping. Then, freshwater began to flush the sediments followed by the dissolution of metastable minerals and skeletal grains, and major calcite cementation, and silicification (Phase 4-17).

**Stage III:** Basin was exposed during the early Pennsylvanian and flushed by meteoric water. Plaeokarst features were developed on the surface of the sedimentary basin. Sediments were undergoing vertical freshwater flushing and possible lateral seawater intervening, which resulted in wide burial anhydritization and pervasive dolomitization (Phase 18-20).

**Stage IV:** Basin subsided and burial increased (>1000 m) considerably in the early Cretaceous. Deep burial diagenesis began, such as the formation of stylolite II. Burial anhydritization continued from stage III, but became less significant in volume. Hydrocarbons were produced and migration ensued. Megadolomite might have also formed in this stage (Phases 21-23).

**Stage V:** Basin was uplifted again and underwent strong folding and faulting during the late Cretaceous, which resulted in fracturing, dissolution (Phase 24-25).



**Table 3.3. Paragenetic Sequence of the Turner Valley Carbonates**

Diagenetic Phase	Marine	Burial		
		shallow	intermediate --mixing-zone----	deep
1 Micritization	—			
2 Syntaxial Cement	—			
3 Microdolomite				
4 Fracture I		—		
5 Dissolution		—		
6 Bladed prismatic		—		
7 Blocky cement		—		
8 Vein cement		—		
9 Coarse Spar		—		
10 Poikilotopic cement		—		
11 Length-slow Chert		—		
12 Megaquartz		—		
13 Stylolite I		—		
14 Patchy Dolomite		—	—	
15 Micro-quartz			—	
16 Length-fast Chert			—	
17 Macroquartz			—	
18 Fracture II			—	
19 Burial Anhydrite			—	—
20 Massive Dolomite			—	
21 Stylolite II				—
22 Hydrocarbon Production and Recharge				
23 Megadolomite				—
24 Fracture III				—
25 Dissolution				—

## **CHAPTER IV**

### **ORIGINS AND MODELS OF DOLOMITIZATION**

#### **4.1 FACIES AND MASSIVE DOLOMITIZATION**

Lithofacies types in the Turner Valley Formation are discussed in detail in chapter II. There are five major sedimentary facies: grainstone, packstone, wackestone, mudstone and sabkha facies. Since sabkha facies has a local distribution and has been completely dolomitized to microdolomite, this facies and microdolomite will not be discussed in this part. Patchy dolomite and megadolomite make up a small proportion relative to massive dolomite. Hence, dolomitization here means pervasive matrix (massive) dolomitization if not mentioned specifically. Various characteristics of dolomite are different in different facies as mentioned in chapter III. The most obvious characteristics are the changes of the proportion and crystal size of dolomite in various facies. Though pervasive matrix dolomite is distributed widely from mudstone to grainstone facies, the crystal size changes considerably. In mudstone facies, dolomite crystals have a mean size of 40  $\mu\text{m}$  varying from 20 to 60  $\mu\text{m}$ . In wackestone facies, dolomite crystals have a similar size as mudstones with a mean of 70  $\mu\text{m}$  varying from 50 to 100  $\mu\text{m}$ . However, packstone and grainstone facies have much coarser dolomite crystals than mudstone and wackestone facies. In packstone facies, dolomite crystals have a mean of 120  $\mu\text{m}$  varying from 80 to 180  $\mu\text{m}$ , whereas in grainstone facies, dolomite crystals have a mean size of 150  $\mu\text{m}$  varying from 100 to 300  $\mu\text{m}$ . It is clear that dolomite crystal size increases from fine grained to coarse grained facies. This is possibly due to the surface area, because lime muds have a larger surface area than lime grains, thus for a unit volume, more dolomite crystals could nucleate in the muds (Murray and Lucia, 1967).

#### **4.2 PROPORTION AND DISTRIBUTION OF DOLOMITE IN LIMESTONES**

As mentioned often in this study, fine grained facies have usually been almost completely dolomitized (80-100%), and skeletal grains and matrix have rarely retained their calcite mineralogy in the Turner Valley Formation. On the one hand, coarser

grained-facies have usually been only partially dolomitized from 20 to 80 percent in volume. Some grainstones, though rare, have been dolomitized under 10% (patchy dolomite), in which dolomite crystals are usually present in bryozoans and corals, whereas crinoids remain unaltered. On the other hand, completely dolomitized packstones and grainstones are also observed in three wells of Quirk Creek.

The heterogeneous distribution of dolomite in various facies has been attributed to the selective dolomitization and was also noted by other researchers (Illing, 1959; Murray and Lucia, 1967). The preference of dolomitization in limestone has been controlled by several parameters: (1) permeability (Illing, 1959), (2) particle size (Murray and Luccia, 1967), (3) precursor mineralogy and other factors.

Permeability variations could have acted to control selective dolomitization because undolomitized packstones and grainstones have tight calcite cementation predating dolomitization, which hindered water-rock interaction and the passage of dolomitization fluids. However, massive dolomite occurred after major cementation and compaction, it is not clear whether the mud component still retained effective permeability after compaction and cementation since mud is sensitive to compaction. Compared to those undolomitized limestones, completely dolomitized coarse-grained limestones usually contain calcite veins. The pre-existing fractures probably provided access for diagenetic fluids through the limestones, resulting in more complete dolomitization.

Particle size involved in the selectivity is preferred by Murray and Luccia (1967). Because the mud component has a larger surface area than skeletal-grain components, for the given volume and kind of fluids, the mud component would have more sites for dolomite crystals to nucleate than skeletal grains. Therefore, mudstones have usually been completely dolomitized, with small crystal sizes, whereas grainstone usually has partially been dolomitized with coarser dolomite crystals (Fig. 4.1).

Limestone has various reactivities to transform into dolomite due to the variation of mineralogy. High-Mg calcite and aragonite are more soluble than low-Mg calcite or diagenetic low-Mg calcite. High-Mg calcite first changes to low-Mg calcite during early diagenesis (Friedman, 1964), hence more soluble aragonite is left at the time of dolomitization. Modern and recent muds consist predominantly of aragonite.

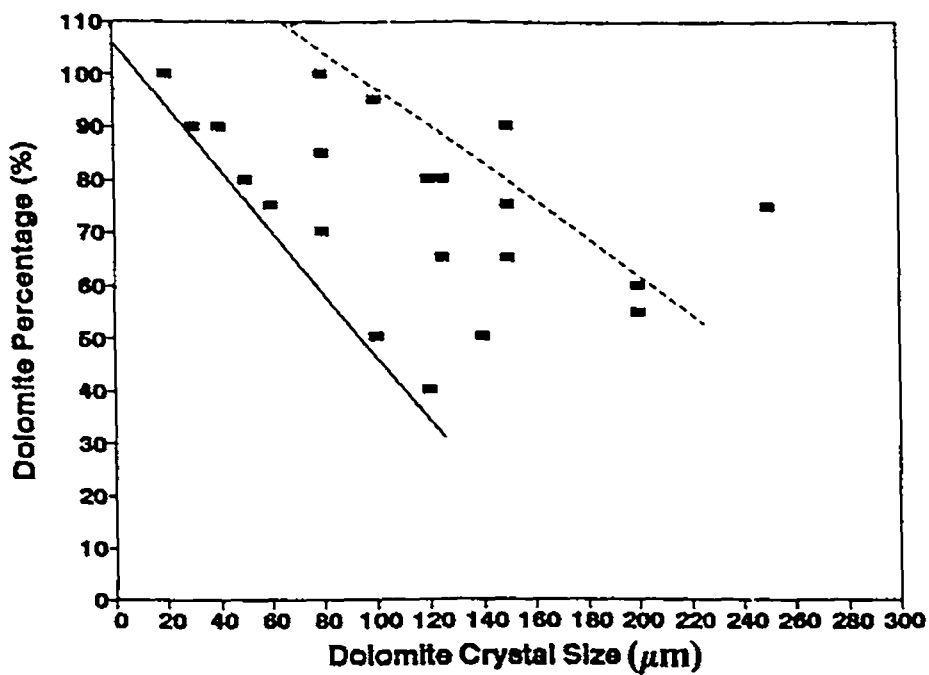


Fig. 4.1. Relationship between dolomite percentage and crystal size.

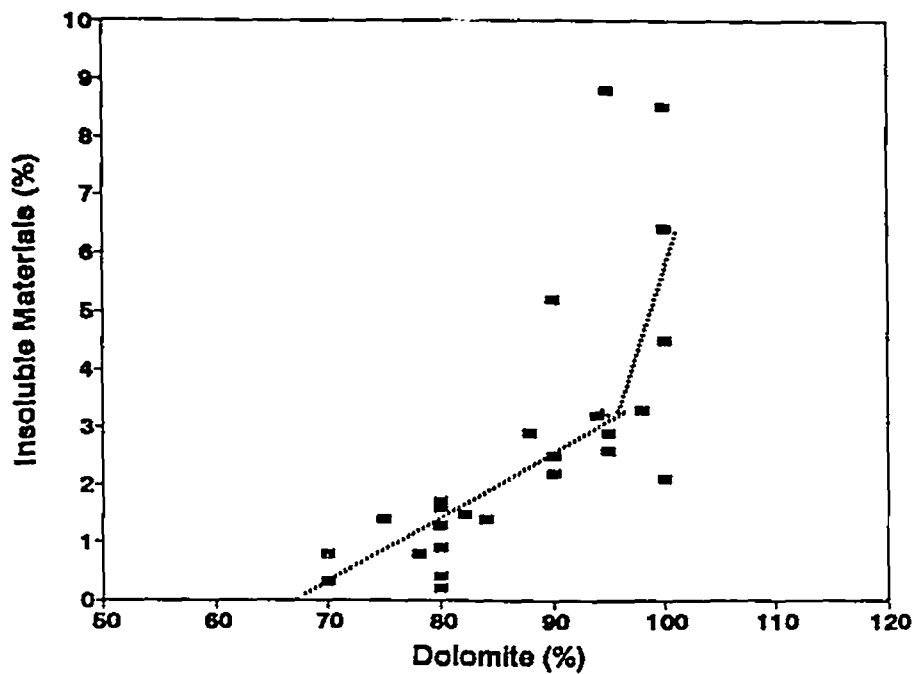


Fig. 4.2. Relationship between insoluble materials and dolomite percentage.

Mississippian seawater may have been aragonitic one (James and Choquette, 1983), and some fossils (e.g. molluscs, bryozoans) have a higher percentage of aragonite than crinoid (Scholle, 1978). Therefore, different soluble components (calcite and aragonite) in a limestone could be susceptible to selective dolomitization.

Experiments by Baker and Kastner (1981) show that the presence of some ions (e.g.,  $\text{SO}_4^{2-}$ ) inhibit dolomitization. Organic matter reduction usually results in the decrease of  $\text{SO}_4^{2-}$  in burial environments, therefore, the presence of organic matter could benefit dolomitization. In addition, anhydrite probably prevented dolomitization in some limestones since it filled pores of limestones and replaced parts in limestone, thus isolating calcite grains from alteration by dolomitization fluids. Furthermore, insoluble materials in carbonates may have been composed of clay minerals and/or organic matter, and may have acted to accelerate the reaction of dolomitization, because the correlative relationship between the percentage of insoluble materials and that of dolomite (Fig.4.2). This may be why mudstones (with more insoluble materials) have higher proportion of dolomite than other facies.

All these factors may have influenced dolomitization of the Turner Valley Formation, whereas permeability probably played a major role for selective dolomitization, especially for more completely dolomitized grainstones.

### **4.3 DOLOMITIZATION AND OTHER DIAGENETIC EVENTS**

Cementation, silicification and anhydritization are also important diagenetic events besides dolomitization in the Turner Valley Formation, and they either benefit or inhibit dolomitization. The study of these events could provide very helpful information for constraining dolomitization. Most importantly they can be utilized to evaluate the relative timing of dolomitization, based on their mutually crosscutting relationship with dolomite, and also to trace the dolomitization fluids according to their coexistence with dolomite.

Calcite cementation occurred before massive dolomite. Calcite veins are widely distributed in massive dolomite from mudstone facies to grainstone facies and in the middle and upper parts of the Turner Valley Formation. This suggests that the previous fractures probably acted as conduits, and provided potential dolomitization fluids as well

as fluids for calcite cementation. However, poikilotopic calcite tightly cemented some grainstone facies, where less dolomite crystals are present, suggesting this cement inhibited the access of dolomitization fluids.

Silica and silicification may have influenced the formation of dolomite due to their different environmental requirements of formation (e.g., pH, Eh). In the experiments by Baker and Kastner (1981) neither dolomite nor magnesite could form, especially during the transformation from opal-A to opal-CT, because the transformation requires the presence of Mg and high alkalinity, which are also the necessary conditions of dolomitization. However, as opal-CT transforms into chalcedony (or quartz), dolomitization is benefited since the Mg taken up by the opal-CT is eventually released during the transformation. It is certain that silicification in the Turner Valley Formation could not have played that much of a role to have hindered and/or favoured massive dolomitization due to the small amount of cherts, and at most, it worked locally. In fact, dolomitization rarely intervened into the chert nodules. Where some sedimentary and diagenetic fabrics are replaced partially by cherts, they could have been "freezed" by silicification and escaped dolomitization.

Knauth (1979) proposed a model associated with a meteoric-marine water mixing zone for shallow water origin, early replacive chert in limestone. Meteoric waters percolating through coastal carbonates will become saturated rapidly with respect to calcite due to the dissolution of aragonite and Mg calcite. The same waters may also become saturated with respect to silica following the dissolution of biogenic siliceous shells. When meteoric water is mixed with seawater, the mixing waters will become undersaturated with respect to opal-A due to the low silicon concentration in seawater and also undersaturated with respect to calcite, whereas opal-CT and quartz may be saturated. Therefore, calcite components could be silicified, but dolomite could retain because mixing waters may be supersaturated with respect to dolomite. This model is plausible for silicification of the Turner Valley Formation, which can explain why patchy dolomite rhombs are preserved whereas calcite components were silicified. It may also well explain the diagenetic order: at first, calcite cementation resulted from meteoric water percolating through aragonitic and Mg-calcitic components, then silicification occurred

when meteoric water mixed with seawater, finally followed by long and slow processes of massive dolomitization.

Anhydritization is a very important diagenetic process. Primary anhydrite is rare, but provides strong evidence for sabkha facies and the origin of microdolomite. Burial anhydrite usually coexists with pervasive matrix dolomite. They are possibly cogenetic. Pervasive matrix dolomite might form within a long geological period before deep burial due to its ordered crystal structure. Whereas burial anhydrite filled fracture II, both fracture II and filling-anhydrite were crosscut by pervasive matrix dolomite (Plate 3.7). Burial anhydrite also filled stylolite II, which crosscuts pervasive matrix dolomite. Hence it could be suggested that dolomite and anhydrite could have formed within the same geologic time scale, but anhydrite formed at multiple stages with a wider time scale. Meanwhile, the diagenetic fluids could have been the sources of dolomitization as well as anhydritization also due to their close  $^{87}\text{Sr}/^{86}\text{Sr}$  values.

According to the experiments by Baker and Kastner (1981) and Morrow et al. (1988), low contents of dissolved sulfate could inhibit the formation of dolomite. Hence, theoretically, dolomite could not have formed before anhydrite at relatively low temperatures. In addition, in some skeletal limestones, only anhydrite is present, whereas dolomite is rare or absent. The most possible explanation is that anhydrite formed first, which replaced the matrix and some skeletal fragments, occluded all channels and isolated limestones from dolomitization fluids.

Therefore, it could be concluded that sulfate precipitated first, which increased the Mg/Ca ratios as well as decreased the content of  $\text{SO}_4^{2-}$  considerably, then massive dolomitization followed. After major dolomitization, as the Mg/Ca ratios decreased again, some sulfates precipitated from the relicts of diagenetic fluids. From the point of  $\text{SO}_4^{2-}$  hindering dolomitization, it is unlikely that massive dolomite formed first, and increased Ca/Mg ratios of fluids for the relatively anhydritization as suggested by Machel (1988) for similar cases.

#### **4.4 ORIGINS AND MODELS OF DOLOMITIZATION**

Although dolomite rocks are important reservoirs for hydrocarbons and hosts for sulfide

mineralization, dolomite is still thought of as a problematic mineral to have bewildered geologists for several decades. There are a few reasons for that. The first is that dolomite has not yet been synthesized experimentally in sedimentary conditions, albeit a lot in high temperatures (e.g., Gaines, 1980). The second is that seawater is supersaturated with dolomite, but no widespread dolomite precipitation has been observed in modern normal marine environments. The third is that dolomite is a highly ordered and stoichiometric mineral and its formation probably needs strict conditions and enough time. Hence, a widely accepted theory regarding the chemistry of dolomitization is absent, which has prevented direct interpretation of the physico-chemical conditions of natural dolomitization. Therefore, people are used to proposing dolomitization models of inference based on field geology and chemical theory. There are four major models of dolomitization: Sabkha, seepage-reflux, meteoric-marine mixing zone, and burial compaction models (e.g., Morrow, 1982). Other models result from the modification of the four models and are less significant. Sabkha and seepage-reflux models are usually used for local and small volume dolomitization (Land, 1985; Morrow, 1982).

Two significant conditions must be satisfied for any model to act as an agent for dolomitization: (1) The amount of Mg is available to form a given mass of dolomitization. (2) A mechanism that can deliver the available ions (e.g.,  $Mg^{2+}$ ,  $CO_3^{2-}$ ,  $HCO_3^-$ ) and also to carry out some ions (e.g.,  $Ca^{2+}$ ).

In the following text, each type of dolomitization in the Turner Valley Formation will be provided a favourable model or models. All models will be examined in the light of the two preceding conditions and some criteria to test the proposition.

#### 4.4.1 Microdolomite

The petrography of microdolomite has provided much unequivocal evidence to indicate that microdolomite is distributed in a sabkha facies. The evidence includes: (1) Microdolomite is very fine, grey to dark crystals, suggesting that the precursor was composed of micrite. (2) No skeletal fossils have been observed except some algae. (3) Microdolomite coexists with primary anhydrite, which has a typical chicken-wire texture. (4) Solution seams and breccia are present in microdolomite facies, probably deriving



from the dissolution of primary sulfate. (5) Microdolomite is distributed locally, and only in the middle and top of the Turner Valley Formation with a thickness often less than 2 meters, and is absent in one (14-12) of three wells in Quirk Creek. In addition, geochemical results also show that microdolomite formed in an evaporative marine environment since microdolomite has the Mississippian marine  $^{87}\text{Sr}/^{86}\text{Sr}$  value of 0.7076 (Burke et al., 1982), relatively high Sr and Na concentrations and high  $\delta^{18}\text{O}$  (average - 0.5 per mil).

Detailed studies of a modern sabkha in the Arabian (Persian) Gulf (e.g., McKenzie, 1981; Patterson and Kinsman, 1981, 1982) have provided important information for the study of microdolomite in the Turner Valley Formation. Dolomite is formed by the evaporative flood waters which are periodically supplied by flood recharge of extra high tides and storms to the supratidal flats and along old channels. Dolomite is restricted to a narrow zone (a few km) within the old channels next to the strandline and in the top 1 to 3 m of sabkha sediments. McKenzie et al. (1981) found the Mg/Ca molar ratios in the areas of dolomite formation are between 2.5 and 7.0. Patterson and Kinsman (1982) determined the conditions with a Mg/Ca molar ratios  $> 6$ , pH 6.3-6.9 and a lower  $\text{SO}_4^{2-}$  content than seawater. The low  $\text{SO}_4^{2-}$  probably resulted from sulfate deposition and microbial reduction. The dolomite possibly forms by replacing aragonite according to:



Further sulfate precipitation can take up the released  $\text{Ca}^{2+}$ . The model for sabkha dolomitization is characterized by the process termed evaporative pumping (Hsü et al., 1969; McKenzie et al., 1980), or capillary concentration (Shinn et al., 1964; Friedman et al., 1967), which is the reverse of seepage-reflux. Morrow (1990) argued that the sabkha model may be regarded as a specific example of the reflux model. Whatever, evaporation is the key process.

The crystals of modern sabkha dolomite are usually Ca-rich (52-54.6 mol%  $\text{CaCO}_3$ ), poorly to moderately ordered and fine (1-5  $\mu\text{m}$ ), with  $\delta^{18}\text{O}$  values in the range of 1 to 3 per mil, PDB (McKenzie, 1981). However, the degree of order increases, the crystal shape is more perfect and crystal size gradually becomes coarser, from 1-2  $\mu\text{m}$  to 2-5  $\mu\text{m}$  to 20  $\mu\text{m}$  landward, as a result of progressive recrystallization through time.

From the many similarities between microdolomite of the Turner Valley Formation and sabkha dolomite of the Arabian Gulf, it can be concluded that microdolomite is a sabkha dolomite. Its perfect crystal shape, relatively coarse size, and lower  $\delta^{18}\text{O}$  may reflect recrystallization at late stages of dolomitization. Particularly, its rims and relatively wide  $^{87}\text{Sr}/^{86}\text{Sr}$  values covering those of unaltered crinoid, pervasive matrix dolomite and megadolomite suggest that microdolomite was altered by the later dolomitization fluids, which caused its syntaxial overgrowth and geochemical modification.

#### **4.4.2 Patchy Dolomite**

From petrographic results, patchy dolomite mostly formed during early chemical compaction since its distribution is closely associated with pressure solution fabrics such as fitted fabrics, dissolution seams, and early stylolite (I). Patchy dolomite is distributed along these fabrics, and is also crosscut by them. Hence, these compaction fabrics and patchy dolomite formed at the same time. According to  $\delta^{18}\text{O}$  values, patchy dolomite could have formed at burial of 360 m and at a temperature of  $35^{\circ}\text{C}$  (discussed in chapter III). Since patchy dolomite has a small volume (5-15%), the Mg required for dolomitization may have been derived from seawater (connate water) through compaction fabrics, which acted as channels to transport diagenetic fluids. Another source could be from the local stabilization of Mg-calcite, which released Mg. The timing for patchy dolomitization was possibly pre-Pennsylvanian since patchy dolomite was corroded by microquartz and burial anhydrite. Similar to microdolomite, patchy dolomite also has syntaxial overgrowth rims, suggesting that patchy dolomite underwent modification during later dolomitization.

#### **4.4.3 Pervasive Matrix Dolomite**

The origin of massive dolomitization is much more complex than the others. No single model has been widely accepted to date (Hardie, 1987). Sabkha and seepage-reflux models were proposed in the 1960's, however, both have narrow spatial distribution and sedimentary restriction, hence they can not explain the regional distribution and precursor sediments of massive dolomitization (Land, 1985). The mixing zone model was once

"popular" in the 1970's and 1980's since it "solves" the kinetic and Mg source problems, and can also explain limpid and ordered dolomite crystals due to slow crystallization from diluted solution. However, it has also been challenged since the late 1980's (e.g., Machel and Mountjoy, 1986; Hardie, 1987). The burial compaction model has been used to interpret massive dolomitization since the late 1950's (Illing, 1959). This model is also favoured by chemical theory and available time. Unfortunately, a sufficient supply of Mg and the mechanism for transporting Mg in massively dolomitized rocks, especially in deep burial environments, are hard questions for this model to answer.

Perhaps the processes and results of massive dolomitization are too complex for one single model to explain, perhaps the "right model" has not been found with our present knowledge. Anyhow, we are still used to choosing one from the available models to accommodate the petrographic and geochemical picture presented. For the study of the Turner Valley massive dolomitization, any interpretation has to account for the following facts: (1) the regional distribution and a large-scale Mg source; (2) the lowest trace element concentrations compared to other dolomites; (3) moderately depleted  $\delta^{18}\text{O}$  values and relatively consistent  $\delta^{13}\text{C}$  values; (4) widespread burial anhydrite coexisting with pervasive matrix dolomite and their slightly radiogenic Sr. Illing (1959) proposed that burial compaction resulted in massive dolomitization of the Turner Valley limestones, whereas Murray and Lucia (1967) preferred the reflux of brines. In this study, the author does not agree with either of them and presents a different interpretation associated with multiple agents and factors rather than a single model.

### Hypersaline Evaporative Models

The evaporation of seawater in areas of supratidal and restricted basins can produce dolomitization. The evaporation process is the mechanism of dolomite formation, which results in the precipitation of sulfate (gypsum), consequently increases the Mg/Ca ratios and the activity and density of seawater, providing the hydrodynamic potential necessary for Mg-bearing hypersaline floodwater to sink downward and flow seaward through the sediments by seepage-reflux. Sabkha and evaporative lagoons can provide the environment (Adams and Rhodes, 1960; Morrow, 1982). However, dolomitization of the

underlying intertidal and subtidal sediments only occurs up to a few meters beneath the sabkha surface (Patterson, 1972). Hence it is unlikely for massive dolomitization to happen due to the vertical and lateral restriction of sabkha environment.

Reflux of brines could have caused dolomitization in the Turner Valley Formation as Murray and Luccia (1967) suggested because the Mount Head Formation is a dominantly evaporative unit (Illing, 1959; Ng and Jones, 1989), and a likely source for dolomitization. In addition, from this study, dolomitization fluids of massive dolomite resulted from overlying strata (trace element results), and dolomite proportion also decreases downward and westward (away from paleocoast). However, many questions could not be answered by this model. Like the sabkha model, reflux-seepage of brines could not form regional dolomitization (Land, 1985). If massive dolomitization of the Turner Valley Formation did form by this model, then dolomitization should have occurred very early (e.g., during Mount Head precipitation), predated calcite cementation and silicification. Also, the values of  $\delta^{18}\text{O}$  and  $^{87}\text{Sr}/^{86}\text{Sr}$  should be similar to that of the Mississippian seawater. However, all conclusions of this study are contrary to those assumptions, hence this model is not reasonable.

#### **Burial Compaction Model**

This model was first proposed by Illing (1959) to interpret the Turner Valley dolomitization. In burial environments, there are no doubts concerning two important factors: kinetic inhibition and time availability due to the increase of temperature with depth and long burial. In the Turner Valley Formation, the  $\delta^{18}\text{O}$  of pervasive matrix dolomite provides a cloudy picture for pervasive matrix dolomitization fluids. A deeper burial compaction of pervasive matrix dolomite could have resulted in the lower  $\delta^{18}\text{O}$  relative to patchy dolomite. In addition, the crystal size of patchy dolomite and the texture of multiple-crystal patches are somewhat similar to those of pervasive matrix dolomite. Since patchy dolomite has an obvious compaction origin, it is logical to conclude that pervasive matrix dolomite resulted from the further and deeper compaction, at higher temperature, that followed patchy dolomite as calculated in chapter III.

However, many facts could not be explained simply by the burial dolomitization model.

Firstly, pervasive matrix dolomite actually has very different textural characteristics and distribution patterns from those of patchy dolomite. There is no clear relationship between pervasive matrix dolomite and compaction fabrics observed from petrography. Pervasive matrix dolomite crosscuts and obliterated most previous diagenetic fabrics including dissolution seams and early stylolite (I). While stylolite II crosscuts pervasive matrix dolomite, massive dolomite neither concentrates along stylolite II nor crosscuts stylolite II. Furthermore, it is difficult to explain the trace element data. If patchy dolomite, pervasive matrix dolomite and megadolomite formed cogenetically as continuous burial compaction (patchy dolomite and megadolomite have burial origins as discussed in this chapter) from similar dolomitization fluids, but at different depths, temperatures and stages, then in addition to that  $\delta^{18}\text{O}$  values would decrease gradually, another clear trend of trace element distribution could have been observed: Sr and Na would change from high to low concentrations, whereas Fe and Mn would increase gradually from patchy dolomite to pervasive matrix dolomite to megadolomite. Unfortunately, this trend does not exist, pervasive matrix dolomite has the lowest Sr and Na concentrations as well as Fe and Mn contents relative to the others.

In addition, one key problem for massive dolomitization is the source of Mg. No large-scale source of Mg is available for this model (Land, 1985). The proponents of the burial model, Illing (1959), Davis (1979), and Mattes and Mountjoy (1980), believe that Mg and pore waters can be supplied by burial-related clay mineralogical transformation (e.g., montmorillonitic clays to illite) in shales during deep basin compaction. However, the Turner Valley Formation does not contain any shale, and the low  $^{87}\text{Sr}/^{86}\text{Sr}$  value, low Mn and Fe concentrations, and dolomitization fluid flow direction of pervasive matrix dolomite can rule out the deeper basin dolomitization fluids. Meanwhile, the mechanism for delivering Mg is a problem. The deeper the rocks are, the harder it is for pore water and Mg to reach. Hence, the suggestion by Mundy and others (1992) that the Turner Valley massive dolomitization is due to the updip flow of basinal brines, resembling the formation of Devonian pervasive dolomitization in Alberta (Machel and Anderson, 1988) is also unlikely because massive dolomitization is absent in the underlying strata in addition to the evidence presented above.

### Mixing-zone Model

Chemically speaking, dolomite can precipitate in a dilute solution of meteoric water mixed with seawater because the solution still maintains a high Mg/Ca ratio of seawater but much less kinetic obstacles due to dilution (Folk and Land, 1975). Meanwhile, this model satisfies the two conditions of dolomitization: seawater supplies the Mg and the active groundwater movement pumps the dolomitization fluids through limestones (Fig. 4.3).

Mixing zone model is firstly cited for the Turner Valley dolomitization in this study because a lot evidence suggests that meteoric water, together with seawater, once intervened the Turner Valley sediments and possibly caused a series of diagenetic events. The top Mississippian strata underwent widespread exposure where a paleokarstic surface was developed in Alberta (Ng and Jones, 1989). This could have provided an extensive meteoric water recharge to the Turner Valley carbonates during the late Mississippian or early Pennsylvanian period. Microstalactitic cements were observed in the top Mississippian strata (Ng and Jones, 1989), which represent vadose environment. However, in spite of the absence of vadose cements in the Turner Valley Formation, vadose cements, such as pendant and meniscus, could have been destroyed by late cementation when pore space was completely filled by diagenetic fluids (James and Choquette, 1984). Furthermore, the Turner Valley Formation could have been in a phreatic environment during the meteoric water recharge (Fig. 4.3). Vein-filling cement and void-filling cement were widely observed in the middle and upper Turner Valley carbonates, both of which formed after microdolomite and before massive dolomitization. They have strongly depleted  $\delta^{18}\text{O}$  and  $\delta^{13}\text{C}$  values. In addition, almost all of those vein- and void-filling calcite cements are present in massive dolomitized limestones and in the upper Turner Valley Formation, are absent or/and rare in less dolomitized limestones, and at the bottom of the Turner Valley Formation. Therefore, the precursor fractures probably formed as the basin was rising or sea level was dropping, and voids resulted from the dissolution of limestones by the flushing of meteoric water. Both of them might act as conduits to deliver diagenetic fluids for calcite cementation as well as dolomitization. The lower  $\delta^{18}\text{O}$  of pervasive matrix dolomite relative to patchy dolomite

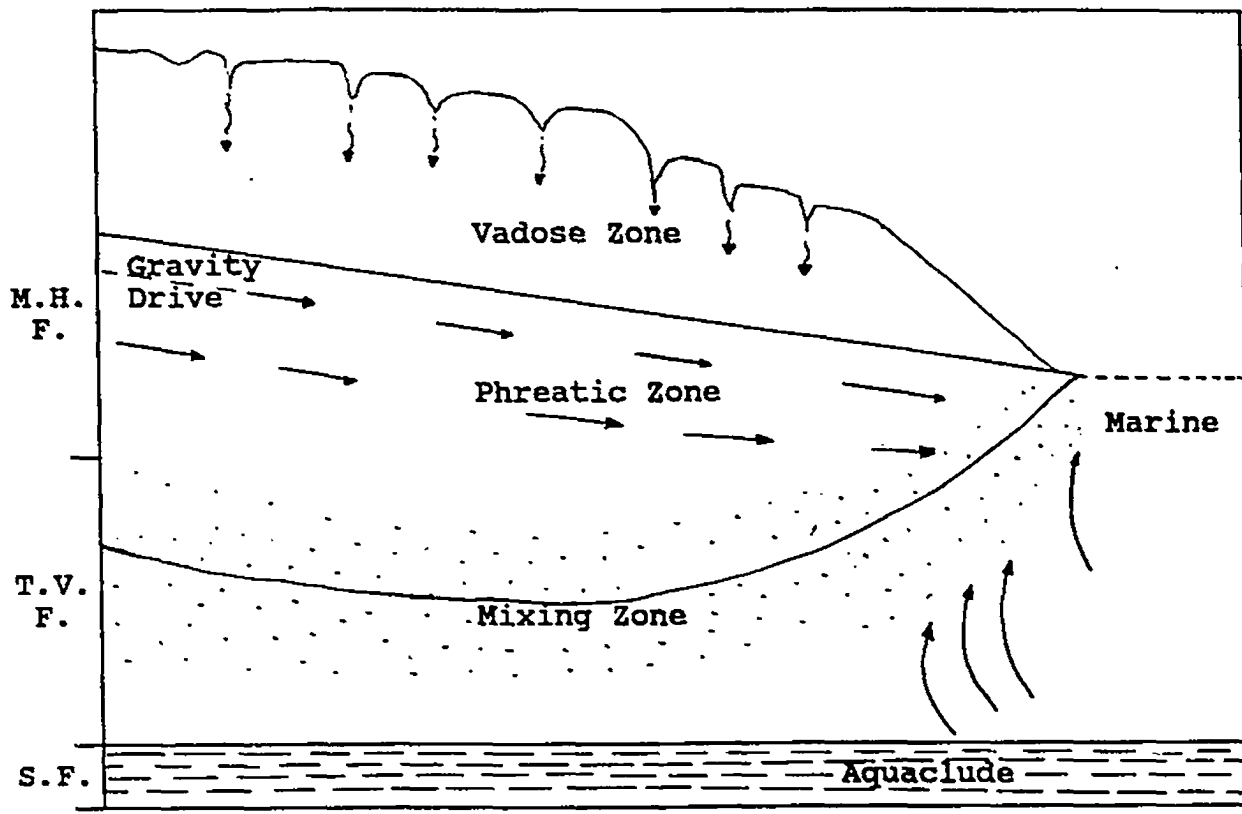


**Fig. 4.1.** Schematic diagram illustrating the inferred time and position of the Turner Valley massive dolomitization.

could be due to meteoric water in the dolomitization fluids. As discussed in chapter III, the temperature and burial depth of massive dolomitization would be lower and shallower when meteoric water was intervened relative to a simply burial environment. The flushing and dilution of freshwater can also account for the lowest trace element concentrations (Na and Sr) of pervasive matrix dolomite (in chapter III and Land, 1985). The downward flow of massive dolomitization fluids and diagenetic fluids for crinoids suggests that meteoric water recharge is very possible. Some calcite cements with similar trace element concentrations to that of crinoids suggest that their precipitation may be effected by seawater.

Moreover, the model of silicification (Knauth, 1979) associated with the meteoric-marine mixing zone well fits the situation of calcite cementation, silicification and dolomitization in the Turner Valley Formation as discussed earlier in this chapter. Furthermore, widespread burial anhydritization occurred in the Turner Valley Formation. The petrographic results show that it formed contemporaneously with massive dolomitization. The mechanism of anhydritization and dolomitization shows that is not impossible that meteoric water first flushed evaporative units in the overlying strata and then mixed with seawater. The mixing fluids were the sources of burial anhydritization as well as dolomitization. The sulfate possibly precipitated first, and was then followed by dolomitization as discussed before. The evidence from fluid inclusions also support low temperature dolomitization.

### **Summary of Massive Dolomitization**

In summary, the sabkha model is an unlikely model for massive dolomitization because of its spatial restrictions. Reflux of brines is not applicable since it conflicts with the petrographic and geochemical results. The burial dolomitization model, especially suggested by Illing (1959), Mattes and Mountjoy (1980) where dolomitizing fluids come from deep basinal compaction contradicts the facts. Meteoric water could have played an important role in diagenesis. However, it should be pointed out that the burial environment could exist during massive dolomitization. The Mount Head Formation has a thickness of several hundred meters, even if, the basin was in the exposure and erosion



during late Mississippian or early Pennsylvanian, most of the Turner Valley Formation was still covered by upper strata. Hence, the burial diagenesis of the Turner Valley Formation could have been a continuous process, which not only caused patchy dolomitization but also was maintained during massive dolomitization. This is how patchy dolomite would grade to massive dolomite. In other words, massive dolomitization formed in both burial (shallow to intermediate) and mixing zone environments. The freshwater recharged through younger Mississippian strata and percolated through the younger rocks, then mixed with seawater in the Turner Valley Formation. The mixed fluids supersaturated with respect to calcite, silica, sulfate and dolomite, and consequently calcite cementation, silicification, anhydritization and dolomitization occurred successively in the Turner Valley Formation. The supersaturated fluids stopped at the surface of the Shunda Formation, because it consists predominantly of micritic limestones and evaporites, and acted as an aquiclude. This is why replacive dolomite should be so largely confined to the Turner Valley Formation relative to other Mississippian strata.

#### **4.4.4 Megadolomite**

Megadolomite, including coarse dolomite rhombs and crinoid-moldic dolomite is very small in volume (<5%), and is the youngest generation of dolomite. Megadolomite crosscuts stylolite II. In turn, stylolite II crosscuts pervasive matrix dolomite, hence stylolite II is believed to have formed after pervasive matrix dolomite at deeper burial. Therefore, any other model except burial dolomitization is not reasonable for megadolomite. The results from fluid inclusions also provide evidence of the high temperature of megadolomite formation. Since megadolomite is small in volume and most coarse rhombs are replacements of pervasive matrix dolomite, dolomitization did not need much dolomitizing fluids and Mg ions. The moderate  $^{87}\text{Sr}/^{86}\text{Sr}$  values of megadolomite also rule out the possibility of fluids from deeper basin. The most possible source is that dolomitization for megadolomite fluids derived from the relicts of massive dolomitization and burial anhydritization fluids because megadolomite usually coexists with and replaces pervasive matrix dolomite and burial anhydrite. In addition, burial

anhydrite, massive dolomite, and megadolomite have close  $^{87}\text{Sr}/^{86}\text{Sr}$  values. However, fluids for megadolomite were already different from those for massive dolomitization and anhydritization, having higher Na and Sr concentrations released from the processes of massive dolomitization and higher  $\text{Fe}^{2+}$  and  $\text{Mn}^{2+}$  contents due to the increase of reducing condition with depth (chapter III). And the water-rock ratios were larger in megadolomitization. This is why megadolomite has higher Na, Sr, Fe, and Mn contents slightly higher  $^{87}\text{Sr}/^{86}\text{Sr}$  and more negative  $\delta^{18}\text{O}$  than pervasive matrix dolomite.

#### 4.5 SUMMARY

There are four types or generations of dolomite in the Turner Valley Formation. They formed at different stages and in different environments with distinguishable characteristics. The evolution of dolomitization fluids is exhibited in Fig. 4.4. The temperatures of formation and mean  $\delta^{18}\text{O}$  values of dolomites are listed in Table 4.1. The temperature of microdolomite was cited from modern sabkha environments (Mckenzie, 1981); the temperature of megadolomite was from 3.10.1; other results were discussed in 3.10.5.1. In Figure 4.4, it is clear that dolomitization fluids became more negative from microdolomite to patchy dolomite to massive dolomite. If megadolomite had formed at the similar temperatures (e.g.,  $< 50^{\circ}\text{C}$ ) as other dolomite, it would have the most negative  $\delta^{18}\text{O}$  values of dolomitization fluids. However, from the results of fluid inclusions, megadolomite formed at relatively higher temperatures ( $116^{\circ}\text{C}$ ). The higher it formed, the more positive its formation fluids could have been.

**Table 4.1.** Temperatures of formation and  $\delta^{18}\text{O}$  values of dolomites.

	$\delta^{18}\text{O}$ per mil PDB	Temperature ( $^{\circ}\text{C}$ )
Microdolomite	-0.9	35-40
Patchy	-2.19	35
Massive	-3.5	40
Megadolomite	-4.5	> 50 (116?)

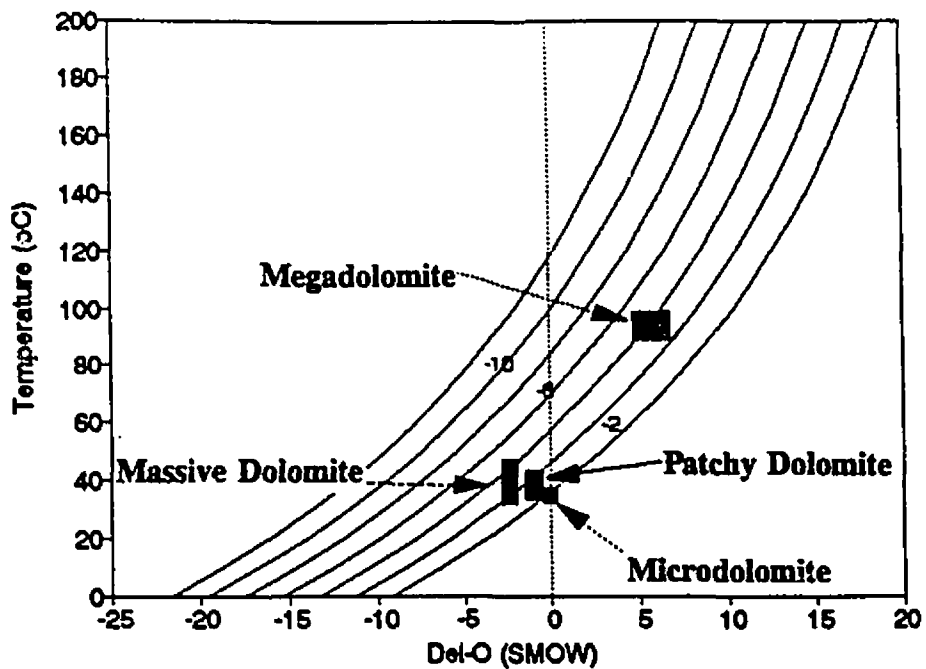


Fig. 4.2. Equilibrium relationship between  $\delta^{18}\text{O}$  of dolomite, temperature and  $\delta^{18}\text{O}$  of fluid. X-axis represents temperature  $\delta^{18}\text{O}$  value of diagenetic fluids; y-axis represents temperatures of dolomitization. The curved lines represent  $\delta^{18}\text{O}$  values (PDB) for dolomite calculated from equation (1) (section 3.10.5.1).

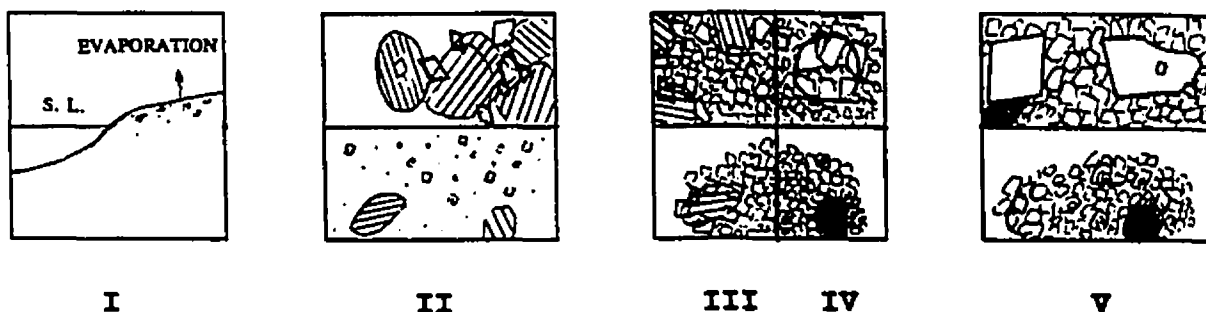


Fig. 4.3. The simplified origin and evolution of various types of dolomite.  
 ☉ calcitic skeletal fragments; ☐ lime mud; shadow-moldic porosity.

The simplified formation and evolution of dolomitization in the Turner Valley Formation are also demonstrated in **Figure 4.5**. As the Mississippian seawater was evaporated, microdolomite formed penecontemporaneously in a sabkha environment in the earliest stage (I). Then the sedimentary basin subsided or sea level rose, younger Mississippian strata (e.g., Mount Head Formation) were deposited and covered the Turner Valley sediments. As burial depth increased, some metastable minerals (Mg-calcite and aragonite) in skeletal limestones began to dissolve, and patchy dolomite formed at the site of Mg and fluid availability; meanwhile, in fine grained mudstones, large-scale physical compaction and thickness-reduction accompanied by the nucleation of micro-dolomite crystals. When the Mississippian marine deposition was over, the sedimentary basin at least locally rose, whereas burial diagenesis and patchy dolomitization in the Turner Valley still continued. As freshwater recharged and mixed with seawater in the Turner Valley Formation, then massive dolomitization occurred widely succeeding to patchy dolomitization. If enough Mg-bearing fluids and time were available, stage IV formed, otherwise the process stopped in stage III (this coincides with the mode in the development of dolomite-related porosity in chapter V): in grainstones, dolomite replaced skeletal grains forming ghost texture; in mudstones (and also microdolomite), strong dolomitization occurred and fine crystals recrystallized and developed syntaxial overgrowth rims. Then the basin subsided again and received younger sediments (post-Mississippian). Increased burial depths ( $> 1000$  m) caused deep burial diagenesis such as stylolite II. As temperature and pressure increased, the relicts of fluids became supersaturated with respect to dolomite again, and dolomitized crinoids, replaced matrix dolomite, and/or precipitated in some voids, forming megadolomite. At the same time, older generations of dolomite such as microdolomite, patchy dolomite, and even pervasive matrix dolomite might have recrystallized and developed one more syntaxial overgrowth rim provided there was the availability of diagenetic fluids.

## **CHAPTER V**

### **POROSITY AND POROSITY EVOLUTION**

#### **5.1 INTRODUCTION**

The Turner Valley Formation is an important hydrocarbon reservoir with abundant reservoir porosity in the Western Canadian Basin. The Turner Valley carbonates are characterized by a spatially heterogeneous distribution of porosity and permeability. The porosity range varies from 0.1 to 18 %, whereas permeability changes considerably from 0 to 270 millidarcys (ESSO). Porosity and permeability are usually influenced by sedimentation, diagenesis, and probably structural factors. The porosity and reservoir characteristics of the Turner Valley Formation are predominantly controlled by diagenetic processes, especially by dolomitization. Hence, it is significant to understand diagenetic processes and events for the porosity evolution in the Turner Valley Formation.

The classification of porosity used in this study is based on that of Choquette and Pray (1970) and Longman (1981). Seven primary and diagenetic (secondary) types of porosity are observed. The primary porosity includes intergranular porosity and intragranular porosity; while secondary porosity includes intercrystalline porosity, moldic porosity, vuggy, stylolitic and fracture porosities.

#### **5.2 PRIMARY POROSITY**

Primary porosity forms during sedimentary processes. In the Turner Valley Formation, significant primary porosity is rare, only being preserved in skeletal grainstones and packstones. Much of the porosity was either destroyed or/and occluded by cementation, compaction and other diagenetic processes.

##### **Intergranular Porosity**

This type of porosity is the pore between grains/particles. In the Turner Valley Formation, intergranular porosity is rarely preserved, usually occluded by syntaxial overgrowth cement of skeletal grains, poikilotopic cement and burial anhydrite and

dolomite.

### **Intragranular Porosity**

This type of porosity is the pore within individual grains/particles and is observed in some fossils such as corals, brachiopods, bryozoan and crinoid fragments. However, most of the porosity is filled by micrite spar and equant cements. Intragranular porosity is rarely preserved.

## **5.3 SECONDARY (DIAGENETIC) POROSITY**

Secondary porosity is formed during diagenetic processes and/or during structural events. This type of porosity is much more abundant and important than primary porosity in the Turner Valley Formation.

### **Intercrystalline Porosity**

Intercrystalline porosity occurs between crystals (dolomite) of relatively similar size. This type of porosity is usually present in partially to completely dolomitized limestones (Plates 3.11 and 3.15). Good permeability was also developed, especially in a sucrosic texture of dolomite with euhedral and subhedral crystals.

### **Moldic Porosity and Vuggy Porosity**

Moldic porosity is formed by selective removal (solution) of fossil fragments, particularly those grains consisting of metastable minerals (aragonite and Mg-calcite). Some moldic porosity is filled by calcite and burial anhydrite cements. The shape and size of moldic porosity depend on those of the dissolved grains (Plate 5.1).

Vuggy porosity is an irregular, large pore visible to the naked eye. It is formed by the dissolution of fossil fragments, calcite cements, and even burial anhydrite (Plate 5.2).

### **Stylolitic Porosity**

Porosity occurs along stylolites. Stylolites can contain porosity and serve as significant pathways for diagenetic fluids. Like fractures, stylolites may yield relatively high permeability.

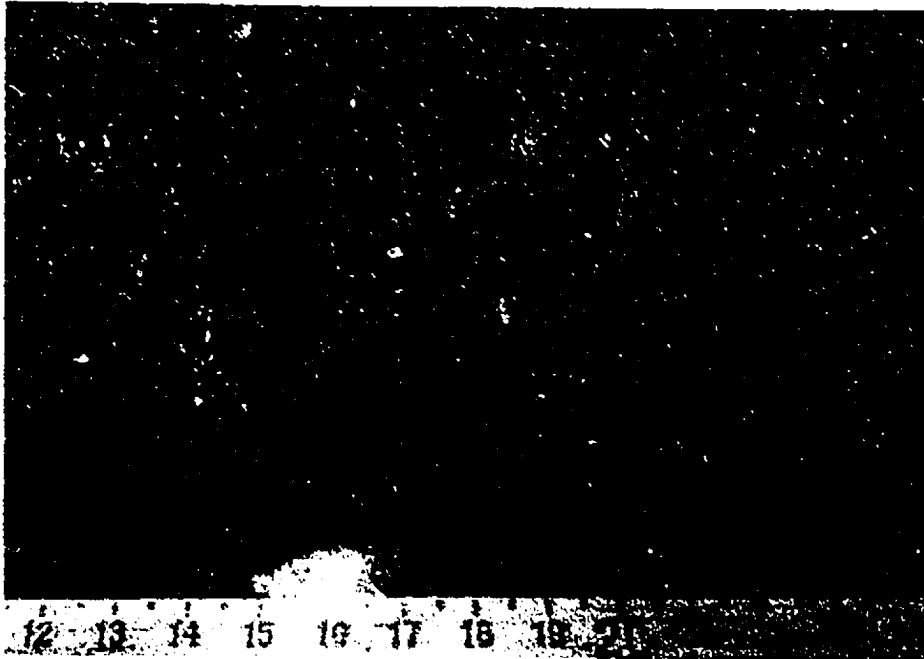


**Plate 5.1.** Core photography of moldic porosity. Scale in cm. Core 14-12, depth 2153 m.



**Plate 5.2.** Core photography of vuggy porosity. scale in cm. Core 14-12, depth 2156 m.

### **Fracture Porosity**

Fracturing is widely presented in the Turner Valley Formation. Early fractures are small in size and are usually filled by calcite cements. Later fractures are larger in size and are often partially filled or open, and acted as effective channels to deliver diagenetic fluids and connect isolated vugs, and increased permeability of rocks significantly.

### **5.4 POROSITY EVOLUTION DURING DIAGENESIS**

During diagenesis, porosity is predominantly controlled by diagenetic processes. Much of the primary porosity has been obliterated and/or enhanced; meanwhile, significant secondary porosity has been created. Various diagenetic events have acted differently for porosity evolution of the Turner Valley carbonate reservoir (Fig. 5.1).

### **Compaction**

Compaction is an important process of primary porosity reduction by increasing overburden stresses, especially on uncemented carbonate sediments. Early mechanical compaction can result in significant porosity reduction, especially in lime muds. The initial porosity could be reduced by compaction up to 30 % (Shinn and Robbin, 1983 in Tucker et al., 1989). Chemical compaction further reduces porosity by producing fabrics such as concavo-convex and fitted fabric contacts between skeletal grains. However, chemical compaction may also create porosity, such as in dissolution seams and stylolites. Though the porosity is rare, permeabilities could increase considerably.

### **Cementation**

Cementation is the precipitation of authigenic minerals in carbonate rocks. Hence cementation is another important process for reducing primary porosity. Syntaxial overgrowth cement, the earliest cement, and poikilotopic cement often fill some of the intergranular porosity between skeletal grains or oolites, whereas micritization occludes much intragranular porosity. Equant calcite cement usually fills fractures, and blocky cement, bladed prismatic cement and coarse calcite spar usually occupy moldic porosity



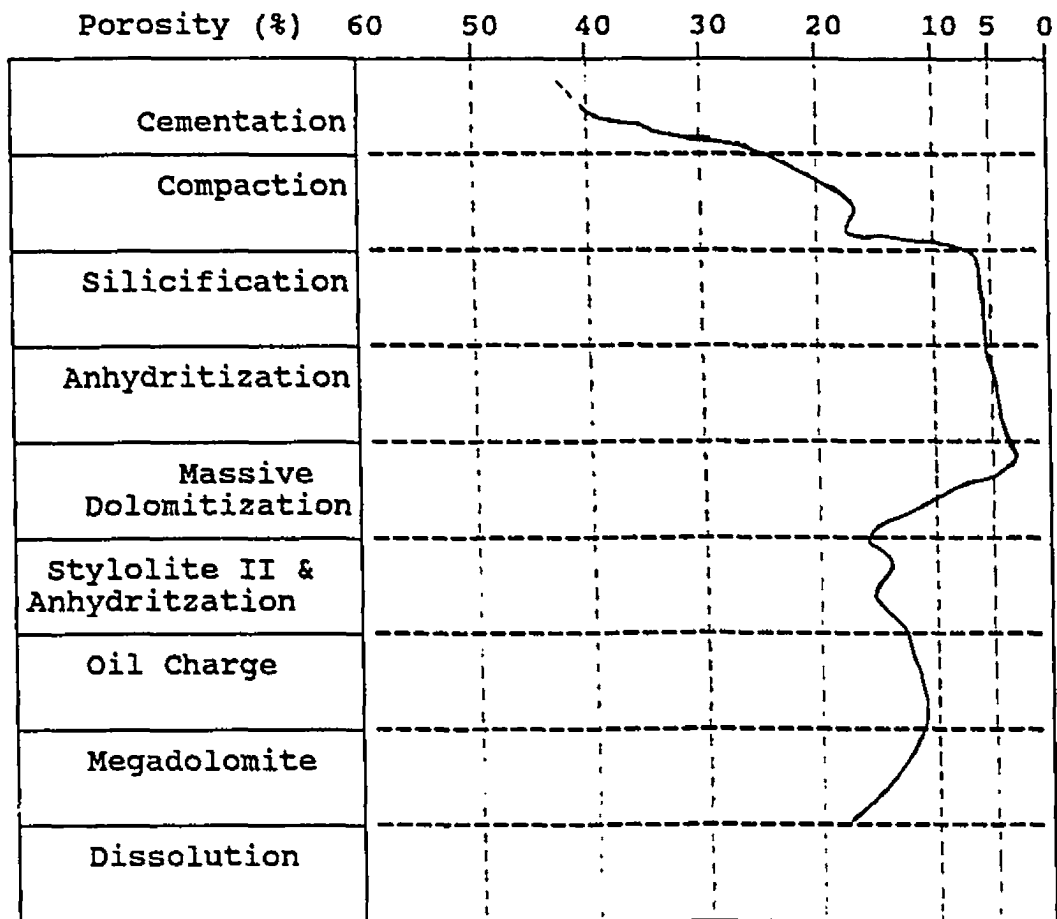


**Fig. 5.1. Porosity and various diagenetic events.**

and vuggy porosity.

### **Anhydritization**

Burial anhydritization has provided a significant influence on the reservoir and porosity development. Anhydrite is distributed in all facies and usually coexists with pervasive matrix dolomite, and is formed in multiple stages. Anhydrite formed as both a replacement and a cement. Pre-massive dolomite anhydritization replaced calcite skeletal grains, cements and also occluded some intergranular porosity; whereas post-massive dolomite anhydrite, although small in volume, occupies some porosity (e.g., moldic and vuggy) created by dolomitization. Where anhydrite is present there will often be lower porosity in dolomitized limestones of the Turner Valley Formation.

### **Other diagenetic events and Porosity**

Other diagenetic events such as silicification, fracturing and dissolution have some influence on the porosity evolution. Silicification is small in volume, but local silicification usually makes reservoirs poor due to its presence in pore space, and its more stable nature to resist dissolution. Fracturing usually increases porosity, but early fractures are filled by calcite cementation. Later fractures are often partially open, which increases permeability considerably as well as porosity. Dissolution always improves reservoir porosity. Like fracturing, early pores resulting from dissolution are filled by cements, late dissolution especially related to massive dolomitization, could have created reservoir-related porosities.

### **Dolomitization and Porosity Evolution**

After cementation and compaction, the primary porosity of the Turner Valley Formation decreased considerably, possibly to be under 5%, which was further reduced by burial anhydritization, probably ranging from 0 to 5%, because the porosity of the Turner Valley poorly dolomitized limestones is usually very low (<1%).

The influence of dolomite on porosity development is much more complex and significant (Moore, 1989). In dolomite rocks, three types of porosity are usually

observed, intercrystalline, moldic and vuggy porosity. Of these, intercrystalline porosity is the most common and important, whereas moldic porosity and vuggy porosity are concentrated in some parts, and locally enhance reservoirs in the Turner Valley Formation. **Figure 5.2** demonstrates the relationship between porosity and the proportion of dolomite in the Turner Valley carbonates. From the diagram (**Fig. 5.2**), porosity initially increases very slowly, or does not change or even decreases as dolomite proportion increases to 70 %, then porosity increases apparently with increasing dolomite proportion after that point. In order to explain the results above, we should understand the texture, arrangement, proportion and distribution of dolomite, and even the processes and mechanism of dolomitization in carbonates. In dolomite rocks, the euhedral form and uniformity in size of the dolomite rhombohedra (usually known as a "sucrosic" texture), are striking in comparison with calcite crystals of limestones, which are of less regular sizes and shapes. Hence, more porosity is supposed to exist between dolomite crystals than between calcite crystals of limestones. Naturally, if growth of euhedral dolomite crystals continues, the rhombohedral shape would become more complex polyhedral forms (anhedral) to form compromise boundaries, which probably happens at higher temperatures (Sibley and Gregg, 1987). This situation will decrease porosity and make the reservoir poor, however is not present in the Turner Valley Formation.

When the volume of dolomite crystals is small (e.g., <20%) in limestones, porosity of limestone would decrease rather than increase. This is because dolomite crystals are sparsely distributed, where they could occlude and fill primary porosity (e.g., intergranular porosity) and secondary porosity (e.g., porosity in dissolution seams). As dolomite percentage increases (still less than 70%), porosity would partially increase due to the concentration of dolomite crystals with a sucrosic texture. However, porosity in carbonate is still low because the concentrations of dolomite crystals are only locally distributed due to the small dolomite proportion, and much of the space between dolomite crystals is still occupied by calcite components. As the dolomite content further increases above 70 %, the rhombohedral crystals increasingly come into contact and provide a supporting framework, thus preventing compaction. Furthermore, intercrystalline porosity

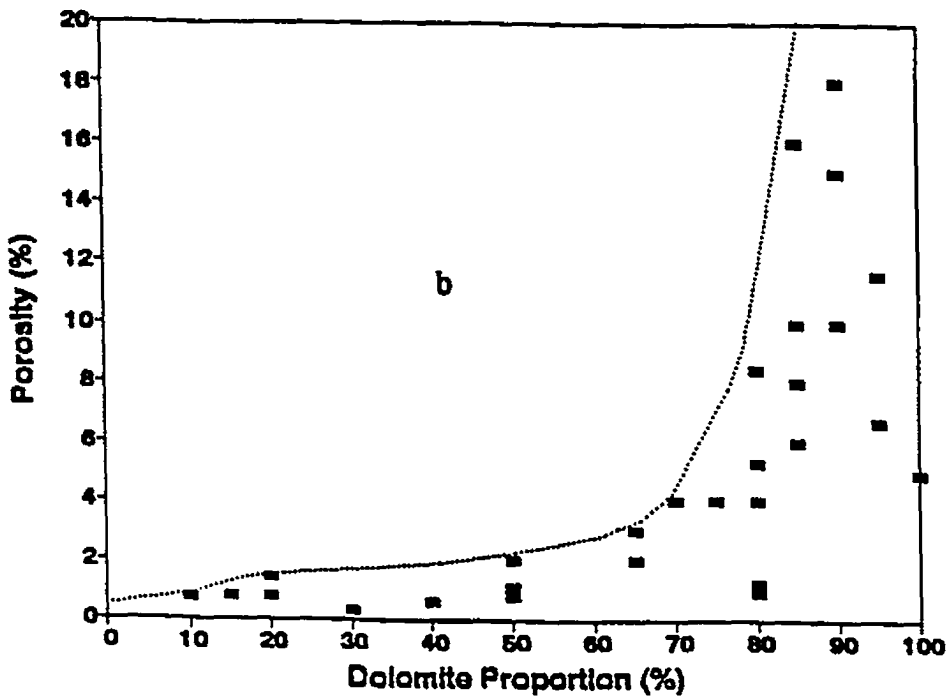
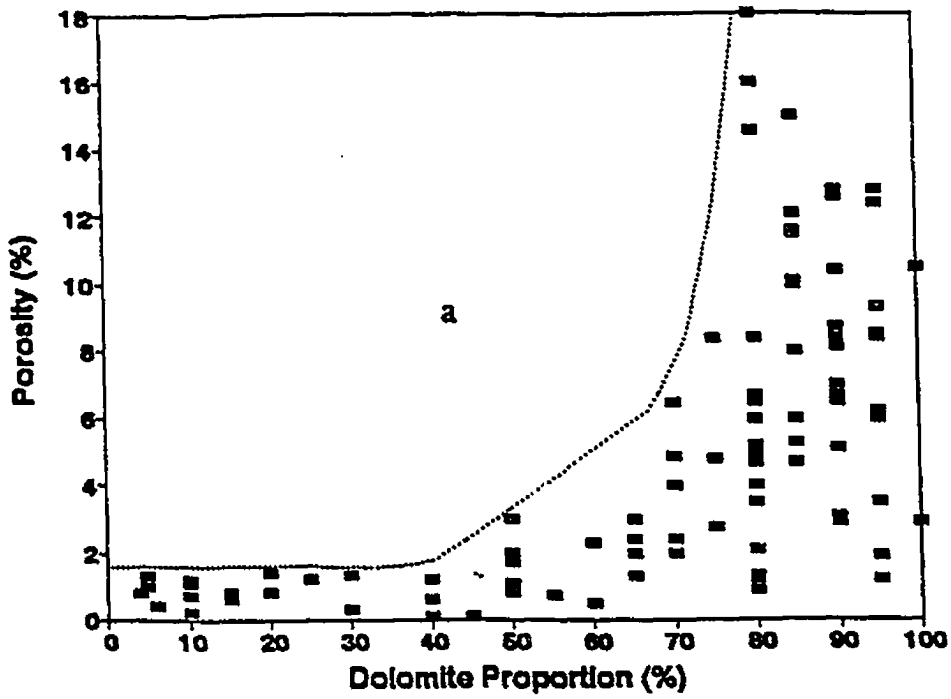


Fig. 5.2. Variation of porosity and dolomite percentage of the Turner Valley carbonates. (a) Showing three wells, and (b) one well (12-22) of the Quirk Creek field.

is produced by dissolution of calcite components or/and as a result of volume decrease accompanying dolomitization (Weyl, 1960).

The critical question for the understanding of dolomite-related porosity is the dissolution of calcite between dolomite rhombs. If the interrhomb calcite is lost by dissolution unrelated to dolomitization, then why does the increase of porosity only occur in carbonates with a high dolomite percentage (more than 70 %) rather than in those with less dolomite proportion? Therefore, concurrent dissolution of calcite has occurred during dolomitization. If dolomitization fluids are not abundant enough or/and less accessible to limestones, the dolomitization fluids are only enough for selective replacement of limestones, dolomitization would occur less completely (< 70 %). However, if enough dolomitization fluids are available and accessible, they have not only massively replaced the dominant calcite phases but have also been able to dissolve the calcite components between those dolomitized calcitic components, then dolomitization would proceed more completely (> 70 %). In other words, only more complete dolomitization in limestone could result in truly "sucrosic" dolomite texture, thus causing high porosity and permeability. This interpretation not only fits fairly well the porosity data presented for the Turner Valley carbonates, but also agrees with the conclusion in chapter IV that the percentage of dolomite is related to the accessibility and the amount of dolomitization fluids.

Further widespread dolomitization after massive dolomitization could destroy the dolomite-related porosity, because, on the one hand, massive dolomite would undergo strong recrystallization, and the euhedral crystals could continue to grow to anhedral crystals, especially at higher temperatures (Sibley and Gregg, 1987), a discussion of this is beyond this thesis. On the other hand, a later generation of dolomitization could fill the pores as a cement or/and destroy intercrystalline porosity as a replacement of massive dolomite. Although megadolomite is small in volume, because it usually replaces massive dolomite and fills some voids, it may have reduced some reservoir porosity in the Turner Valley Formation. Perhaps this is why the points of highest porosity are not concentrated around 100 % dolomite (Fig. 5.2).

Furthermore, in spite of the presence of burial anhydrite, the trend of porosity

distribution in dolomitized limestones and dolomite rocks has been little affected. The best reason is that major burial anhydritization formed before massive dolomitization, and replaced calcite components. Hence, its amount and presence are equal to those of skeletal grains and calcite cements preserved in those completely dolomitized carbonates.

**Figure. 5.3** shows the relationship between porosity and depth. This relation has been investigated by many researchers (e.g., Scholle, 1977; Garrison, 1981). The relationship shows that porosity decreases with increasing depth. However, because significant porosity is dolomitization-related in the Turner Valley Formation, thus the relationship becomes complex. On the one hand, because higher dolomite percentage has higher porosity as discussed above, and while the proportion of dolomite decreases downward as discussed in chapter IV, dolomitization enhances the trend of porosity decrease with increasing depth. On the other hand, some more completely dolomitized limestones are present in the bottom and the lower parts of the Turner Valley Formation, and some limestones in the upper parts of the Turner Valley Formation have been less dolomitized. Therefore, some points in the diagram (**Fig. 5.3**) do not fall on the general trend.

## **5.5 SUMMARY**

Most primary porosities were destroyed and/or occluded during the complex processes of diagenesis of the Turner Valley Formation. Some diagenetic events benefit reservoirs and some make reservoirs poor in the Turner Valley Formation (**Fig. 5.1**). The relatively well preserved primary pores including intergranular porosity and intragranular porosity but are rare. Secondary porosity is much higher and more important, including intercrystalline porosity, moldic porosity, vuggy, stylolitic and fracture porosities. Intercrystalline porosity is the most abundant and widespread, moldic porosity is also important for reservoirs in the Turner Valley Formation.

Compaction is an important process for reducing porosity, although chemical compaction can also create some local porosity and increase permeability. Calcite cementation also reduces porosity. Early cementation usually filled primary porosity, whereas late cements often occupied both primary and secondary porosities. Silicification locally reduced primary and secondary porosities. Burial anhydrite acted as late cements

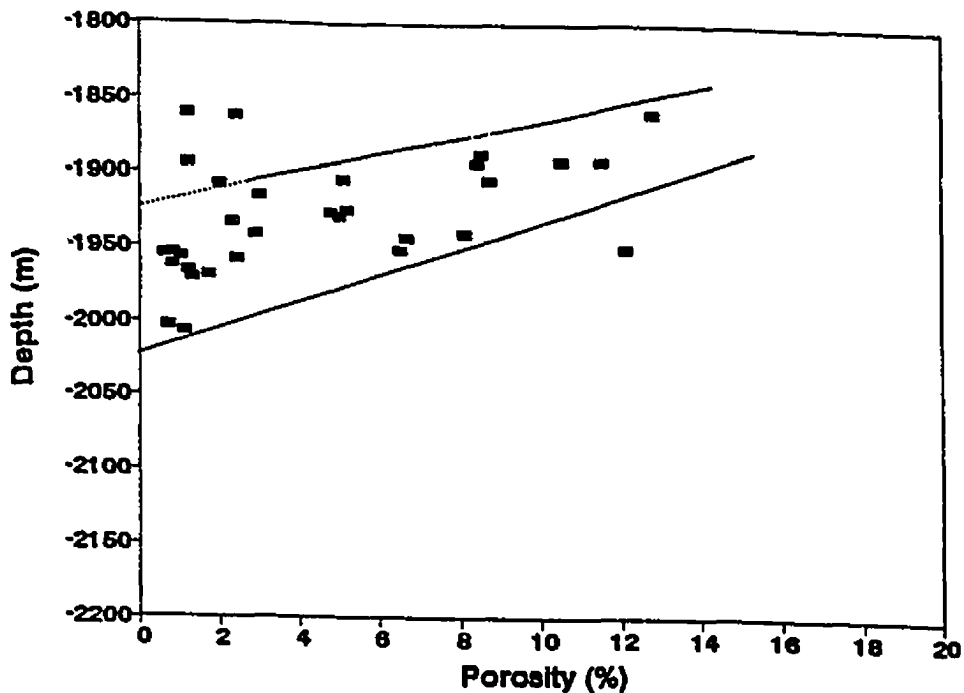


Fig. 5.3. Plot of porosity and depth of the Turner Valley carbonates.

for porosity development in the Turner Valley Formation, reducing primary and secondary porosities. Fracturing and dissolution usually increase porosity.

Dolomitization is a complex and significant process for porosity evolution in the Turner Valley Formation. Porosity increases very slowly, even decreases (dolomite < 20 %), until dolomite percentage reaches around 70%. After that point, porosity increases apparently with increasing dolomite percentage. Hence, the reservoir porosity is believed to be dolomite-related, where the amount and accessibility of dolomitization fluids are critical for the abundance of reservoir porosity as well as dolomite proportion in the Turner Valley carbonates.

## **CHAPTER VI**

### **CONCLUSIONS AND REMARKS**

#### **6.1 CONCLUSIONS**

This study has first documented, based on previous work, the presence of a sabkha facies, and has been the first to identify four types or generations of dolomite which have been developed associated with various diagenetic fluids and environments. Significant conclusions have been reached concerning sedimentology and diagenesis of the Turner Valley Formation based on the study of petrography and geochemistry.

1. The Turner Valley carbonate sequence consists of a shallowing-upward sequence deposited in a marginal, shallow shelf (bank) from an open marine shoal grading to lagoon and sabkha environments.
2. The Turner Valley sediments consist predominantly of five lithofacies: grainstone, packstone, wackestone, mudstone, and sabkha facies.
3. Twenty-five diagenetic phases (fabrics) were observed. These phases and their relative temporal relationships are listed in Table (3.3).
4. Initial diagenesis of the Turner Valley sediments occurred in the marine environment where micritization (micrite envelope) and syntaxial overgrowth rims developed on skeletal grains.
5. Bladed prismatic cement, blocky calcite cement, vein cement, coarse mosaic calcite spar and poikilotopic cement were all formed during early, shallow burial and were probably associated with meteoric water and organic activity. They are composed of non-ferroan low-Mg calcite with strongly negative  $\delta^{18}\text{O}$  and  $\delta^{13}\text{C}$  and similar trace element concentrations to crinoids.
6. Physical and chemical compaction fabrics were observed in the Turner Valley Formation. They are accompanied by other diagenetic events (e.g., patchy dolomite with fitted fabrics, anhydrite with stylolite II).
7. Diagenetic silicification is present as nodules, irregular masses, nodule bands parallel to bedding with various thicknesses, and occurred in multiple stages in the Turner Valley



Formation: length-slow chalcedony, megaquartz, microquartz, length-fast chalcedony and macroquartz. All types of silica are interpreted to have formed in relatively early stages after calcite cements, and patchy dolomite, and before massive dolomite, possibly associated with a mixing zone.

8. Burial anhydritization has a wide distribution and mainly formed in two stages in the Turner Valley Formation. Early anhydrite (stage I) formed before massive dolomitization, replacing calcite skeletal grains and cements, and filling fracture II; late anhydrite (stage II) formed after massive dolomitization and filled stylolite II. Both stages of burial anhydritization may have resulted from the dissolution of primary sulfates in the Turner Valley Formation and its overlying strata by the percolating of meteoric water.

9. Fracturing was widely observed in the Turner Valley Formation, occurring in several stages. Fractures may have acted as conduits for various diagenetic fluids and even as a trap of hydrocarbons, though fractures are quantitatively unimportant.

10. Dissolution has created significant porosity for the reservoirs of the Turner Valley Formation. Of all dissolution processes, that one related to massive dolomitization is the most important.

11. Dolomitization is the most important diagenetic event in the Turner Valley Formation. Four types or generations of dolomite are identified: microdolomite, patchy dolomite, pervasive matrix dolomite and megadolomite. All of them are non-ferroan dolomite with dull CL.

12. Microdolomite is interpreted to have formed in an evaporative marine environment (sabkha) with unequivocal petrographic evidence and geochemical results. It underwent recrystallization during later stages of dolomitization.

13. Patchy dolomite could have formed at shallow burial, based on its petrographic and geochemical results and also underwent later modification.

14. Massive dolomite is the most abundant and reservoir-related type of dolomite. A mixing-zone model and subsurface burial environment have been suggested for massive dolomitization.

15. Megadolomite is the last generation and the coarsest type of dolomite, and formed

in deeper burial environment with elevated temperatures.

16. Primary porosity and secondary porosity are observed in the Turner Valley Formation. Where secondary porosity is more important and controls the reservoir properties. Of all secondary porosities, intercrystalline and moldic porosities are the most significant. The abundance and development of reservoir porosity are controlled by the intensity or degree of dolomitization, in turn, the degree of dolomitization depends on the amount and accessibility of dolomitization fluids. Therefore, the further search for potential reservoirs in the Turner Valley Formation should concentrate on more completely dolomitized carbonates (> 70% and < 95%).

## **6.2 REMARKS**

Dolomite is still a key problem in carbonate studies, although its study has been improved tremendously since more models, such as mixing-zone and subsurface compaction, have been proposed in recent decades. Meanwhile, people have become more and more confused by various views and conclusions of dolomitization. It is necessary to offer some hypotheses for people to understand and solve the "dolomite problem". However, the facts and assumptions should first be distinguished; only to emphasize one model or suggestion and ignore other possibilities and facts would mislead the further study of dolomite and dolomitization.

In general, I have a lot of beautiful memories related to my stay in Windsor, although I also had a very hard time. My study here not only gave me a new starting for my professional career, but also let me believe more in what a great man said, "no matter how hard the problem is, I only wish I have a confidence to conquer it!"

I enjoyed my study here! A lot of fun!

## REFERENCES

- Adams, J.E. and Rhodes, M.L. 1960. Dolomitization by seepage-refluxion. *Am. Assoc. Petrol. Geol. Bull.*, 44: 1912-1920.
- Al-Aasm, I.S., Taylor, B.E. and South, B. 1990. Stable isotope analysis of multiple carbonate samples using selective acid extraction. *Chem. Geol. (Isot. Geosci.Sect.)*, 80: 119-125.
- Al-Aasm, I.S and Veizer, J. 1986. Diagenetic stabilization of aragonite and low-Mg calcite, 2. Stable isotopes in rudists. *J. Sediment. Petrol.*, 56: 138-152.
- Allen, J.R. and Matthews, R.K. 1982. Isotope signatures associated with early meteoric diagenesis. *Sedimentary*, 29: 797-817.
- Anderson, T.F. and Arthur, M.A. 1983. Stable isotopes of oxygen and carbon and their application to sedimentologic and paleoenvironmental problems. In: M.A. Arthur (Ed.), *Stable Isotopes in Sedimentary Geology. SEPM SHORT COURSE NO. 10*, pp. 1.1-1. 151.
- Baker, P.A. and Kastner, M. 1981. Constraints on the formation of sedimentary dolomites. *Science*, 213: 213-216.
- Bamber, E.W., Macqueen, R.W., and Ollerenshaw, N.C. 1981. Mississippian stratigraphy and sedimentology, Canyon Creek (Moose mountain), Alberta. pp177-194: In Thompson, R.I. and Cook, D.G. (Eds.) *Field guides to geology and mineral deposits. Calgary, 1981 Annual Meeting. Geol. Ass. Can., Min. Ass. Can., Geophy. Union.*
- Banner, J.L., Hanson, G.N. and Meyers, W.J. 1988. Water-rock interaction history of regionally extensive dolomites of the Burlington-Keokuk Formation (Mississippian). In: P.A. Baker and V.Shukla (Eds), *Sedimentology and Geochemistry of Dolostones. SEPM Spec. Pub, No. 43.*
- Bathurst, R.G.C. 1975. *Carbonate sediments and their diagenesis*, Elsevier, Amsterdam.
- Behrens, E.W. & Land, L.S. 1972. Subtidal Holocene dolomite, Baffin Bay, Texas. *J. Sediment. Petrol.*, 42: 155-161.

- Brand, U. and Veizer, J. 1980. Chemical diagenesis of a multicomponent carbonate system-1. Trace elements. *J. Sediment. Petrol.*, 50: 1219-1236.
- Burke, W.H., Denison, R.E., Hetherington, E.A., Koepnick, B., Nelson, H.F. and Otto, J.B. 1982. Variation of seawater  $^{87}\text{Sr}/^{86}\text{Sr}$  throughout Phanerozoic time. *Geology*, 10: 516-519.
- Buxton, T.M. and Sibley, D.F. 1981. Pressure solution features in a shallow buried limestone. *J. Sediment. Petrol.*, 51: 19-26.
- Choquette, P.W. and Pray, L.C. 1970. Geologic nomenclature and classification of porosity in sedimentary carbonates. *Am. Assoc. Petrol. Geol. Bull.*, 54: 207-250.
- Choquette, P.W. and James, N.P. 1987. Diagenesis #12: Diagenesis in limestones-3. The deep burial environment. *Geosci. Can.*, 14: 3-35.
- Conn, R.F. and Christie, J.A. 1988. Conventional oil resources of Western Canada. GSC., Paper 87-26, part 2, 127-149.
- Dickson, J.A.D. 1965. A modified staining Technique for carbonates in thin section. *Nature* 205, 587.
- Druckman, Y. and Moore, C.H. 1985. Late subsurface porosity in Jurassic grainstone reservoir Formation, Mt. Vernon field, southern Arkansas. In: P.O. Roehl and P.W. Choquette (Eds), *Carbonate Petroleum Reservoirs*, Springer-Verlag/New York, pp. 371-383.
- Dunham, R.J. 1962. Classification of carbonate rocks according to depositional texture. In: W.E. Ham. (Ed.), *Classification of Carbonate Rocks*. AAPG Mem.1, pp. 108-121.
- Dunham, J.B & Olson, E.R. 1980. Shallow subsurface dolomitization of subtidally deposited carbonate sediments in Hanson Creek Formation of central Nevada. *Spec. Publ. Soc. econ. Paleont. Miner.*, 28, 139-161.
- ESSO, core description, unpublished data.
- Faure, G. & Powell, J.L. 1972. *Strontium isotopes Geology*. Springer-Verlag.
- Folk, R.L. and Land, L.S. 1975. Mg/Ca ratio and salinity; two control over crystallization of dolomite. *Am. Assoc. Petrol. Geol. Bull.*, 59: 60-68.
- Folk, R.L. and Pittman, J.S. 1971. Length-slow chalcedony: a new testament for vanished evaporates: *J. Sediment. Petrol.*, v. 41, pp. 1045-1058.

- Folk, R.L. 1987. Detection of organic matter in thin sections of carbonate rocks using a white card: *Sedimentary Geology*, 54: 193-200.
- Frank, J.R., Carpenter, A.B. and Oglesby, T.W. 1982. Cathodoluminescence and composition of calcite cement in the Taum Sauk Limestone (Upper Cambrian), southeast Missouri. *J. Sediment. Petrol.*, 52: 631-638.
- Friedman, G.M., 1964. Early diagenesis and lithification in carbonate sediments. *J. Sediment. Petrol.*, 34: 777-813.
- Fritz, P. and Smith, D.G.W. 1970. The isotopic composition of secondary dolomites. *Geochim. Cosmochim. Acta.* 34:1161-1173.
- Gaines, A. 1977. Protodolomite redefined. *J. Sediment. Petrol.*, 47: 543-546.
- Gaines, A. 1980. Dolomitization kinetics: recent experimental studies. In: *Concepts and Models of Dolomitization* (Ed. by D.H. Zenger, J.B. Dunham and R.L. Ethington) Spec. Publ. Soc. Econ. Paleont. Miner., 28, 139-161.
- Gao, G. and Land, L.S. 1991. Early Ordovician Cool Creek dolomite, middle Arbuckle Group, Slick Hills, SW Oklahoma, USA: origin and modification, *J. Sediment. Petrol.*, 61: 161-173.
- Garrison, R.E. 1981. Diagenesis of oceanic carbonate sediments: a review of DSDP perspective. *SEPM Spec. Pub. No. 32*: 181-207.
- Gavish, E. & Friedman, G.M. 1969. Progressive diagenesis in Quaternary to Late Tertiary carbonate sediments. *J. Sediment. Petrol.*, 39, 980-1006.
- Grover, G. and Read, J.F. 1983. Fenestral and associated vadose diagenetic fabrics of tidal flat carbonates. Middle Ordovician, New Market Limestone, southwest Virginia. *Bull. Am. Ass. Petrol. Geol.* 67: 1275-1303.
- Hardie, L.A. 1987. Dolomitization: a critical view of some current views. *J. Sediment. Petrol.*, 57: 166-183.
- Hesse, R. 1987. Selective and reversible carbonate-silica replacements in lower Cretaceous carbonate-bearing turbidites of the Eastern Alps: *Sedimentology*, v. 34, pp. 1055-1077.
- Illing, L.V. 1959. Deposition and diagenesis of some Upper Paleozoic carbonate sediments in western Canada. 5th World Petrol. Cong., New York Proc., pp. 23-52.

- Hsü, K.J. and Siegenthaler, C. 1969. Preliminary experiments on hydrodynamic movement induced by evaporation and their bearing on the dolomite problem. *Sedimentology*, 12: 11-25.
- Jacobson, R.L. and Usdowski, H.E. 1976. Partitioning of strontium between calcite, dolomite and liquids: an experimental study under higher temperature diagenetic conditions and the model for the prediction of mineral pairs for geothermometry. *Contrib. Min. Pet.*, 59: 171-185.
- James, N.P. and Choquette, P.W. 1984. Diagenesis 9: Limestones-The meteoric diagenetic environment. *Geosci. Can.*, 11: 161-194.
- Jodry, R.L. 1969. Growth and dolomitization of Silurian reefs, St. Clair County, Michigan: *Am. Ass. Petrol. Geol., Bull.*, 52: 959-981.
- Katz, A. & Matthews, A. 1977. The dolomitization of carbonate: an experimental study at 252-295. *Geochim. Cosmochim. Acta*, 41, 297-308.
- Katz, A., Sass, E., Starinsky, A. and Holland, H.D., 1972. Strontium behaviour in the aragonite-calcite transformation: an experimental study at 40-98. *Geochim. Cosmochim. Acta*, 36, 81-496.
- Knauth, L.P., 1979. A model for origin of chert in limestone: *Geology*, 7: 274-277.
- Land, L.S. 1967. Diagenesis of skeletal carbonates. *J. Sedim. Petrol.* 37, 914-930.
- Land, L.S. 1980. The isotopic and trace element geochemistry of dolomite: the state of the art. In: D.H. Zenger, J.B. Dunham, and R.L. Ethington (Eds.), *Concepts and Models of dolomitization*. SEPM Spec. Pub. No. 28, pp. 87-110.
- Land, L.S. 1985. The origin of massive dolomite. *J. Geol. Educ.*, 33: 112-125.
- Land, L.S. and Hoops, G.K. 1973. Sodium in carbonate sediments and rocks: a possible index to the salinity of diagenetic solution. *J. Sediment. Petrol.*, 43: 614-617.
- Lohmann, K.C. 1988. Geochemical patterns of meteoric diagenetic systems and their application to studies of paleokarst. In: N.P. James and P.W. Choquette (Eds.), *Paleokarst*. Springer-Verlag/New York, pp. 58-80.
- Longman, M.W. 1981. Carbonate diagenetic textures from nearsurface diagenetic environments. *Am. Assoc. Petrol., Geol. Bull.*, 64: 461-487.
- Machel, H.G. 1985. Cathodoluminescence in calcite and dolomite and its chemical

- interpretation. *Geosci Can.*, 12: 139-147.
- Machel, H.G. and Mountjoy, E. W. 1986. Chemistry and environments of dolomitization-a reappraisal. *Earth-Sci. Rev.*, 23: 175-222.
- Machel, H.G. and Anderson, J.H. 1987. Pervasive subsurface dolomitization of the Nisku Formation in central Alberta. *J. Sediment. Petrol.*, 59: 891-911.
- Macqueen, R.W. and Bamber, E.W. 1967. Stratigraphy of the Banff Formation and Lower Rundle Group (Mississippian), southwestern Alberta. Geological Survey of Canada Paper 67-47, 37pp.
- Macqueen, R.W. 1968. Stratigraphy and facies relationships of the Upper Mississippian Mount Head Formation, Rocky Mountains and Foothills, southwestern Alberta; *Bull. Can. Soc. Petrol. Geol.*, 16: 225-287.
- Mattes, B.W. and Mountjoy, E.W. 1980. Burial dolomitization of the Upper Devonian Miette buildup, Jasper National Park, Alberta. In: D.H. Zenger, J.B. Dunham and R.L. Ethington (Eds.), *Concepts and Models of Dolomitization*. SEPM Spec. Pub. No. 28, pp. 259-297.
- McKenzie, J.A. 1981. Holocene dolomitization of calcium carbonate sediments from the coastal sabkhas of Abu Dhabi, U.A.E.: a stable isotope study. *J. Geol.*, 89: 185-198.
- Meyers, W.J. 1974. Carbonate cement stratigraphy of the Lake Valley Formation (Mississippian) Sacramento Mountains, New Mexico. *J. Sediment. Petrol.*, 44: 837-861.
- Meyers, W.J. 1977. Chertification in the Mississippian Lake Valley Formation, Sacramento Mountains, New Mexico. *Sedimentology*, v. 24, p. 75-105.
- Meyers, W.J. 1978. Carbonate cements: their regional distribution and interpretation in Mississippian limestones of southwestern New Mexico. *Sedimentology*, 25: 371-400.
- Moore, C.H. 1989. Carbonate diagenesis and porosity; *Development in sedimentology* 46, Elsevier 338.
- Moore, C.H., Chowdhury, A. and Chan, L. 1988. Upper Jurassic Smackover platform dolomitization northwestern Gulf of Mexico: a tale of two waters. in: V. Shukla and P.A. Baker (Eds), *sedimentology and Geochemistry of Dolostones*. SEPM Spec. Pub. No. 43.

- Morrow, D.W. 1982a. Diagenesis 1. Dolomite-part 1: the chemistry of dolomitization and dolomite precipitation. *Geosci. Can.*, 9: 5-13.
- Morrow, D.W. 1982b. Diagenesis 2. Dolomite-part 2: dolomitization models and ancient dolostones. *Geosci. Can.*, 9: 95-107.
- Morrow, D.W. and Ricketts, B.D. 1988. Experimental investigation of sulfate inhibition of dolomite and its mineral analogues. In: Shukla, V. and Baker, P.A. (Eds.): *Sedimentology and Geochemistry of Dolostones. SEPM Spec. Pub. No. 43.*
- Murray, R.C. and Lucia, F.J. 1967. Cause and control of dolomite distribution by rock selectivity. *Am. Assoc. Geol. Bull.*, 78: 21-35.
- Mundy, D.J.C., Widdowson, R.G. and Sabo, D.J. 1992. Field trip guidebook. AAPG Annual Convention.
- Ng, K. and Jones, B. 1989. Sedimentology and diagenesis of Upper Mississippian to Lower Permian strata, Talbot Lake area, Jasper National Park, Alberta. *Can. J. Earth Sci.*, 26: 275-295
- Nielsen, H. 1979. Sulfur isotopes. In E. Jäger and J.C. Hunziker (eds.): *Lectures in Isotope Geology*, 283-312. Springer-Verlag, Berlin, 329p.
- Northrop, D.A. and Clayton, R.N. 1966. Oxygen isotope fractionation in systems containing dolomite. *J. Geol.* 74: 174-196.
- O'Neil, J.R. and Epstein, S. 1966. Oxygen isotope fractionation in the system dolomite-calcite-carbon dioxide. *Science* 152: 198-201.
- Patterson, R.G. and Kinsman, D.J.J. 1981. Hydrologic framework of a sabkha along the Persian Gulf. *Bull. Am. Ass. Petrol. Geol.*, 65: 1457-1475.
- Patterson, R.G. and Kinsman, D.J.J. 1982. Formation of diagenetic dolomite in coastal sabkhas along the Arabian (Persian) Gulf. *Bull. Am. Ass. Petrol. Geol.*, 66: 28-43.
- Roedder, E. 1979. Fluid inclusions evidence on the environments of sedimentary diagenesis, a review. In: P.A. Scholle and P.R. Schluger (Eds.), *Aspects of Diagenesis. SEPM Spec. Pub. No. 26*, pp. 89-107.
- Rupp, A.W. 1969. Turner Valley Formation of the Jumping Pound area, foothills, southern Alberta. *Can. Petrol. Geol. Bull.*, 17: 461-485.
- Scholle, P.A. 1977. Chalk diagenesis and its relation to petroleum exploration: oil from



- chalks, a modern miracle? *Am. Ass. Petrol. Geol. Bull.*, 61: 982-1009.
- Shinn, E.A. and Robbin, D.M. 1983. Mechanical and chemical compaction in fine-grained shallow-water limestones. *J. Sediment. Petrol.*, 53: 595-618.
- Sibley, D.F. 1980. Climatic control of dolomitization, Seroc Domi Formation (Pliocene), Bonare, N.A. In: D.H. Zenger, J.B. Dunham and R.L. Ethington (Eds.), *Concepts and Models of Dolomitization*. SEPM Spec. Pub. No. 28, pp. 247-258.
- Sibley, D.F. 1982. The origin of common dolomite textures: Clues from the Pliocene: *J. Sediment. Petrol.*, 52: 1087-1100.
- Sibley, D.F. and Gregg, J. 1987. Classification of dolomite rock texture. *J. Sed. Petrol.*, 57: 967-975.
- Stein, E.M. 1977. The Turner Valley Formation at Whisky Creek. A Mississippian carbonate reservoir rock. pp 109-124: In: McIlreath, I.A. and Harrison, R.D. (Eds.): *The Geology of Selected carbonate Oil, Gas and Lead-zinc Reservoirs in western Canada*. core Conference, Canadian Society of Petrol. Geol.
- Tucker, M.E. & Wright, V. P. 1990. *Carbonate sedimentology*. Blackwell Scientific Publications, 482p.
- Veizer, J. 1983a. Chemical diagenesis of carbonates: theory and application of trace element technique. In M.A. Arthur (Ed), *Stable Isotopes in Sedimentary Geology*. SEPM Short Course Notes No. 10, pp. 3.1-3.100.
- Veizer, J. 1983b. Trace elements and isotopes in carbonate minerals. *Mineral. Soc. Am. Rev. in Mineral.*, 11: 265-299.
- Wanless, H.R. 1979. Limestones response to stress: pressure solution and dolomitization. *J. Sediment. Petrol.*, 51: 445-454.
- Weyl, P.K. 1960. Porosity through dolomitization: conservation-of-mass requirements. *J. Sediment. Petrol.*, 30: 85-90.
- Wilson, J.L. 1975. *Carbonate Facies in Geological History* Springer-Verlag/New York, 471pp.
- Yanguas, G.E. and Dravis, J.J. 1985. Blue fluorescent dye technique for recognition of microporosity in sedimentary rocks. *J. Sediment. Petrol.*, 55: 600-602.

## **APPENDIX I**

### **Chemical and Isotopic Results**

**Abbreviations:**

**Lith:** lithology

**Cri.Cal:** Calcitic Crinoids

**Cem.Cal:** Calcitic Cement

**Mic.Dol:** Microdolomite

**Ptc.Dol:** Patchy Dolomite

**Ms.Dol:** massive Dolomite

**Meg.Dol:** Megadolomite

Sample Number	Lith. Type	Depth (m)	I.R. %	MgCO3 (mol%)	CaCO3 (mol%)	Sr (ppm)	Na (ppm)	Mn (ppm)	Fe (ppm)	O Del	C Del
6-7-762	Cri.Cal	-2000	0	0.8	97.8	579	349	4	123	-3.29	2.59
6-7-105	Cri.Cal	-1998	1.7	1.6	94.8	400	432	2	140	-5.14	3.31
6-7-99	Cri.Cal	-1975	-	0.1	99.8	205	431	0	229	-5.03	3.55
6-7-98	Cri.Cal	-1970	-	-	-	-	-	-	-	-	-
12-22-31	Cri.Cal	-1969	0	1.7	95.4	210	434	24	199	-4.02	3.19
12-22-28	Cri.Cal	-1971	0	0.8	97	185	893	18	179	-5.57	3.39
12-22-26	Cri.Cal	-2155	0	1.4	94.8	243	815	0	174	-5.33	2.85
14-12-6	Cri.Cal	-2082	0	1.9	93.3	203	880	0	368	-6.77	2.68
12-22-34	Cri.Cem	-2008	-	-	-	-	-	-	-	-10.13	2.23
6-7-101	Cem.Ca	-2136	-	-	-	-	-	-	-	-12.48	-5.82
6-7-100	Cem.Ca	-2075	-	-	-	-	-	-	-	-12.04	-6.46
14-12-9	Cem.Ca	-2098	-	-	-	-	-	-	-	-12.18	-9.05
14-12-18	Cem.Ca	-2136	17.9	0.4	98.5	286	335	11	100	-11.24	-9.5
14-12-4	Cem.Ca	-2074	0	0.4	99	262	345	0	300	-9.33	-9.67
12-22-30	Cem.Ca	-1967	-	-	-	-	-	-	-	-5.56	-0.31
12-22-12	Cem.Ca	-1906	-	-	-	-	-	-	-	-6.2	-8.4
6-7-770	Cem.Ca	-1970	-	-	-	-	-	-	-	-7.19	-3.2
6-7-97	Cem.Ca	-1969	2.9	0.9	97.3	256	335	13	99	-7.65	-2.07
12-22-20	Cem.Ca	-2112	14.6	1.7	96.8	182	325	12	35	-11.67	-2.82
14-12-23	Cem.Ca	-2140	-	-	-	-	-	-	-	-10.44	-9.44
14-12-13	Cem.Ca	-2114	-	-	-	-	-	-	-	-9.31	-9.29
14-12-12	Cem.Ca	-2112	0.8	1.2	96.8	505	303	11	165	-12.33	-12.69
6-7-97	Mic.Dol	-1969	8.5	37.1	62.8	140	434	104	256	0	2.55
6-7-93	Mic.Dol	-1938	1.3	49.6	51.4	121	308	52	133	-1	0.88
6-7-91	Mic.Dol	-1934	4.4	47.7	52.3	127	290	60	314	-0.05	2.9

Sample	Lith.	Depth	I.R	MgCO3	CaCO3	Sr	Na	Mn	Fe	O	C
12-22-20	Mic.Dol	-1942	6.4	43.2	56.8	153	467	97	351	-1.02	2.48
12-22-11	Mic.Dol	-1905	0.9	48.2	51.8	90	319	35	174	-1.03	2.38
12-22-6	Mic.Dol	-1889	14.7	47.8	52.2	145	476	128	344	-0.96	0.65
12-22-2	Mic.Dol	-1850	3.2	40.9	59.1	260	292	96	228	-2.22	1.32
6-7-775	Ptc.Dol	-2072	-	-	-	-	-	-	-	-3.52	3.68
6-7-99	Ptc.Dol	-1975	-	-	-	-	-	-	-	-2.02	3.07
12-22-34	Ptc.Dol	-2008	-	-	-	-	-	-	-	-2.64	3.36
12-22-28	Ptc.Dol	-1971	-	-	-	-	-	-	-	-2.04	3.53
12-22-24	Ptc.Dol	-1955	-	43	56.9	-	-	-	-	-0.79	1.76
14-12-29	Ptc.Dol	-2162	-	-	-	-	-	-	-	-2.14	3.29
6-7-771	Mas.Dol	-2064	5.17	50.9	49.1	174	270	27	190	-1.11	2.83
6-7-102	Mas.Dol	-1985	0.89	47.3	52.7	120	241	51	205	-3.79	0.85
6-7-90	Mas.Dol	-1930	1.08	48.1	51.9	100	240	26	223	-5.46	2.59
6-7-781	Mas.Dol	-1922	2.56	48.3	51.6	82	223	34	97	-2.17	2.97
12-22-21	Mas.Dol	-1945	1.29	48.7	51.2	128	220	28	75	-3.74	3.09
12-22-17	Mas.Dol	-1932	0.28	47.6	52.4	106	200	23	127	-4.39	3.43
12-22-16	Mas.Dol	-1928	-	-	-	-	-	-	-	-2.49	3.35
12-22-8	Mas.Dol	-1893	2.57	46.3	53.6	53	192	38	102	-4.19	3.07
12-22-8	Mas.Dol	-1893	1.2	47.1	52.8	52	182	38	169	-3.12	3.4
12-22-3	Mas.Dol	-1861	8.84	47.5	52.5	90	180	20	91	-3.38	3.52
14-12-28	Mas.Dol	-2162	0.43	49.2	50.8	78	270	25	127	-3.83	2.53
14-12-22	Mas.Dol	-2143	0.18	47.9	52.1	40	237	27	113	-5.13	3.47
14-12-21	Mas.Dol	-2142	0.84	46.5	53.4	63	235	32	97	-3.23	2.43
14-12-17	Mas.Dol	-2133	-	-	-	-	-	-	-	-2.91	2.93
14-12-8	Mas.Dol	-2094	0.06	47.1	52.8	47	230	23	259	-4.29	3.37
14-12-3	Mas.Dol	-2071	1.56	45.1	54.9	50	185	73	75	-4.81	2.58
6-7-770	Mas.Dol	-2020	1.09	47.8	52.2	104	253	23	69	-4.01	2.07

Sample	Lith.	Depth	I.R	MgCO <sub>3</sub>	CaCO <sub>3</sub>	Sr	Na	Mn	Fe	O	C
12-22-20	Mic.Dol	-1942	6.4	43.2	56.8	153	467	97	351	-1.02	2.48
12-22-11	Mic.Dol	-1905	0.9	48.2	51.8	90	319	35	174	-1.03	2.38
12-22-6	Mic.Dol	-1889	14.7	47.8	52.2	145	476	128	344	-0.96	0.65
12-22-2	Mic.Dol	-1850	3.2	40.9	59.1	260	292	96	228	-2.22	1.32
6-7-775	Ptc.Dol	-2072	-	-	-	-	-	-	-	-3.52	3.68
6-7-99	Ptc.Dol	-1975	-	-	-	-	-	-	-	-2.02	3.07
12-22-34	Ptc.Dol	-2008	-	-	-	-	-	-	-	-2.64	3.36
12-22-28	Ptc.Dol	-1971	-	-	-	-	-	-	-	-2.04	3.53
12-22-24	Ptc.Dol	-1955	-	43	56.9	-	-	-	-	-0.79	1.76
14-12-29	Ptc.Dol	-2162	-	-	-	-	-	-	-	-2.14	3.29
6-7-771	Mas.Dol	-2064	5.17	50.9	49.1	174	270	27	190	-1.11	2.83
6-7-102	Mas.Dol	-1985	0.89	47.3	52.7	120	241	51	205	-3.79	0.85
6-7-90	Mas.Dol	-1930	1.08	48.1	51.9	100	240	26	223	-5.46	2.59
6-7-781	Mas.Dol	-1922	2.56	48.3	51.6	82	223	34	97	-2.17	2.97
12-22-21	Mas.Dol	-1945	1.29	48.7	51.2	128	220	28	75	-3.74	3.09
12-22-17	Mas.Dol	-1932	0.28	47.6	52.4	106	200	23	127	-4.39	3.43
12-22-16	Mas.Dol	-1928	-	-	-	-	-	-	-	-2.49	3.35
12-22-8	Mas.Dol	-1893	2.57	46.3	53.6	53	192	38	102	-4.19	3.07
12-22-8	Mas.Dol	-1893	1.2	47.1	52.8	52	182	38	169	-3.12	3.4
12-22-3	Mas.Dol	-1861	8.84	47.5	52.5	90	180	20	91	-3.38	3.52
14-12-28	Mas.Dol	-2162	0.43	49.2	50.8	78	270	25	127	-3.83	2.53
14-12-22	Mas.Dol	-2143	0.18	47.9	52.1	40	237	27	113	-5.13	3.47
14-12-21	Mas.Dol	-2142	0.84	46.5	53.4	63	235	32	97	-3.23	2.43
14-12-17	Mas.Dol	-2133	-	-	-	-	-	-	-	-2.91	2.93
14-12-8	Mas.Dol	-2094	0.06	47.1	52.8	47	230	23	259	-4.29	3.37
14-12-3	Mas.Dol	-2071	1.56	45.1	54.9	50	185	23	75	-4.81	2.58
6-7-770	Mas.Dol	-2020	1.09	47.8	52.2	104	253	23	69	-4.01	2.07

Sample	Lith.	Depth	I.R.	MgCO <sub>3</sub>	CaCO <sub>3</sub>	Sr	Na	Mn	Fe	O	C
12-22-12	Mas.Dol	-1906	-	-	-	-	-	-	-	-4.05	2.39
6-7-770	Mas.Dol	-2020	-	-	-	-	-	-	-	-3.84	2.05
6-7-764	Mas.Dol	-2006	-	-	-	-	-	-	-	-3.31	1.52
6-7-773	Meg.Do	-2068	1.31	54.8	87	260	36	184	-	-	-
6-7-772	Meg.Do	-2066	1.68	50.5	92	238	52	423	-	-6.33	2.73
12-22-16	Meg.Do	-1928	-	-	-	-	-	-	-	-6.47	2.19
14-12-28	Meg.Do	-2162	-	-	-	-	-	-	-	-4.55	2.41
14-12-22	Meg.Do	-2143	1.39	53.9	97	265	29	232	-	-2.12	2.25
14-12-17	Meg.Do	-2133	-	-	-	-	-	-	-	-3.55	2.02
14-12-13	Meg.Do	-2114	4.83	56.1	98	278	27	358	-	-6.28	2.19
14-12-1	Meg.Do	-2060	-	-	-	-	-	-	-	-3.3	2.5
6-7-772	Meg.Do	-2066	1.57	52.8	84	200	28	418	-	-	-
12-22-16	Meg.Do	-1928	1.38	56.4	153	300	92	353	-	-5.81	2.53
14-12-28	Meg.Do	-2162	2.9	51.5	120	303	32	230	-	-4.33	2.97
14-12-17	Meg.Do	-2133	-	-	-	-	-	-	-	-3.47	2.32
14-12-15	Meg.Do	-1927	1.54	52.7	175	305	20	231	-	-5.24	3.02
14-12-1	Meg.Do	-2060	-	-	-	-	-	-	-	-2.44	2.01

## **APPENDIX II**

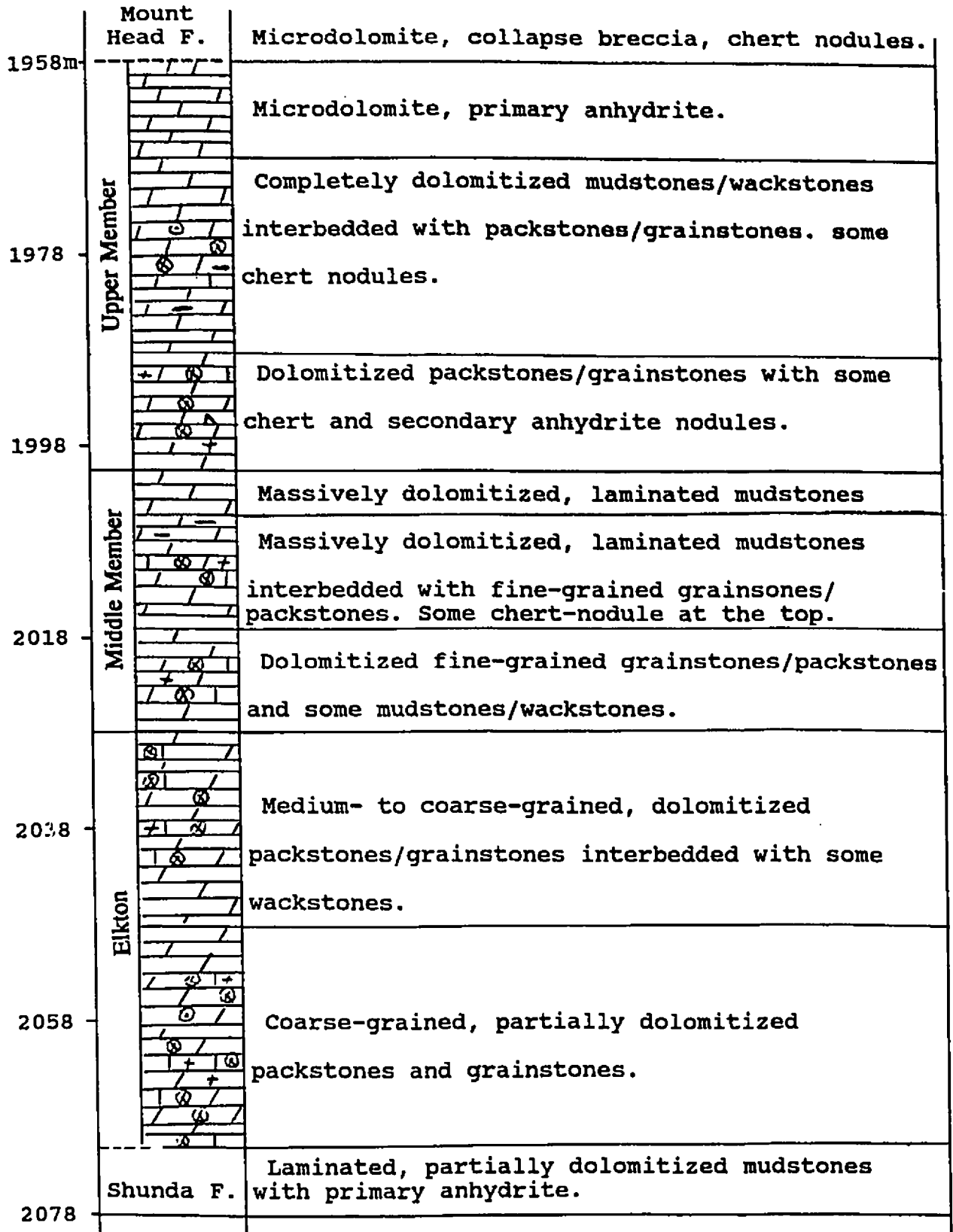
**Description of Studied Cores (6-7, 12-22 and 14-12).**

Well 14-12

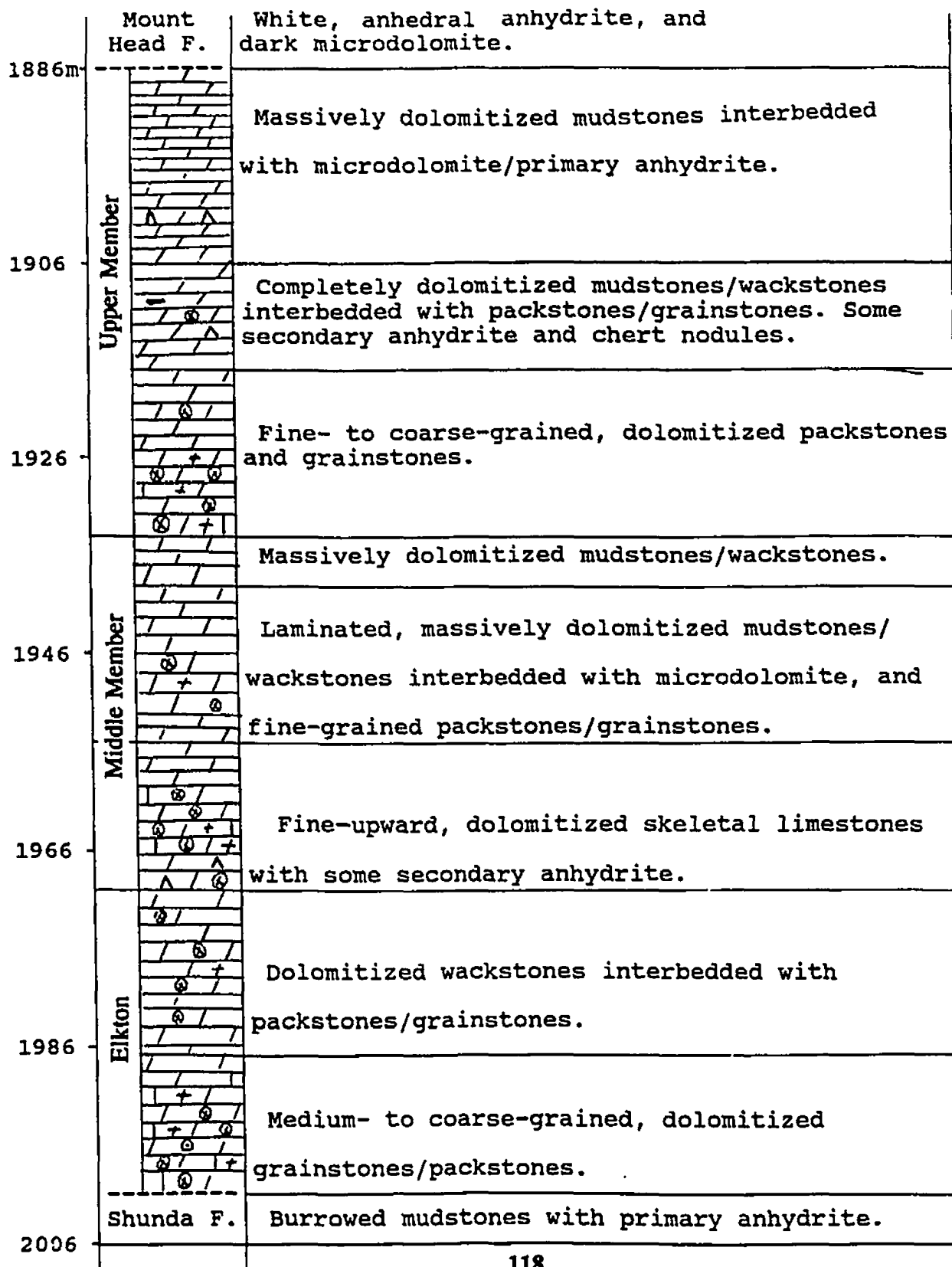
		Mount Head Formation
		Massively dolomitized grainstones/packstones.
2061m	Upper Member	Dolomitized mudstones interbedded with grainstones/packstones.
		Several cycles of dolomitized coarse- to fine-skeletal limestones.
2081		
	Middle Member	Laminated, dolomitized mudstones.
		Fine grained, dolomitized grainstones/packstones with anhydrite nodules.
2101		
		Dolomitized packstones/grainstones interbedded with mudstones/wackstones.
		Dolomitized grainstones/packstones. Some cherts
	Elkion	Coarse- to fine-grained, dolomitized skeletal limestones with anhydrite nodules.
2121		
		Several cycles of coarse- to fine-grained upward, dolomitized skeletal limestones with anhydrite nodules.
2141		
2161	Shunda F.	Very sharp, abrupt contact from mudstones of Shunda to coarse, dolomitized skeletal limestone of Turner Valley Formation.



Well 6-7



Well 12-22



## Legend

 Limestone

 Dolomite

 Mudstone

 Anhydrite

 Chert

 Crinoid

 Oolite

 Bryozoan

## VITA AUCTORIS

**Name:** Feng-Hu Lu  
**Place of Birth:** Hubei, China  
**Date of Birth:** February 1, 1963  
**Education:** China University of Geosciences  
B.Sc. Geology 1981-1985  
China University of Geosciences  
M.Sc. Geological Engineering 1987-1990  
University of Windsor  
M.Sc. Sedimentology and Geochemistry 1991-1992